Politecnico di Torino

Politecnico di Torino

Master in Mining Engineering

A/Y 2021/2022

Characterization of muck from TBM excavation aimed to its sustainable reuse

Master thesis

Supervisors:

Prof. Marilena Cardu

Prof. Paola Marini

Dr. Daniele Martinelli

Dr. Lorena Zichella

Candidate:

Gyslain Ngadi Sakatadi

21 March 2022

Abstract

Tunnel boring Machines (TBM) are widely used for the construction of long tunnel infrastructures; a large volume of muck is frequently generated during the excavation process. The muck can be considered as valuable resource if its properties are well understood to be able to detect and forecast its reuse in several construction applications.

In this regard, several investigations were carried out on the muck from TBM excavation aiming to find out all useful descriptions/data linked to the geometrical, mineralogical and petrographic properties in order to characterise the muck. Furthermore the TBM excavation process and its performance were studied in this thesis to connect its influence on the geometrical characterisation and properties of the excavated materials for a sustainable reuse of the muck as construction aggregates in order to bring up some environment and economic benefits.

The muck investigated is made up by the debris coming from an exploratory Tunnel located in the Susa valley, which is part of the Lyon-Turin high-speed railway; owned by The Euralpin Lyon Turin (TELT) Company.

Acknowledgements

I would like to express my immense gratitude to my supervisor Prof. Marilena Cardu for her availability and special guidance during the entire period of my thesis and also for all the valuable advices and teachings provided throughout my educational path at the Politecnico. Great appreciation to her passion, as well as her dedication to the mining field and underground work; that was very distinctive and inspiring.

Extremely grateful to Prof. Paola Marini for the valuable guidance and help during the entire period of my thesis work. I also thank her for all the exceptional advices and teachings provided throughout my educational path at the Politecnico.

Special thanks to Dr. Daniele Martinelli for his availability and important advices during my thesis work and also my journey at the Politecnico.

Enormous gratitude to Dr. Lorena Zichella for her availability, help and the time dedicated during my thesis and lab. work.

I dedicate this work to my parents and forever grateful to them. I thank them for their infinite love, support and trust during my studies and throughout my whole life.

Lastly, I would like to also extend my graduate to everyone who has positively contributed and help me in one way or another during my educational journey and life here in Italy, especially during the toughest moment of this global pandemic.

Table of Contents

List of tables

List of figures

Introduction

Nowadays, excavation by tunnel boring machines (TBM) are considered to be the most common technology adopted for the construction of large tunnel projects; they can provide good performance if all requirements are met .However a large amount of raw materials are needed during the construction of such big infrastructures .Taking into consideration a substantial rise in the shortage of construction raw materials like aggregates and environmental concerns, the muck from the tunnel excavation can be a good source of raw materials for concrete, refilling materials, railway embankments or highways construction.

This thesis is aiming on a sustainable goal for the reuse of the TBM excavated materials. This approach of the reuse of muck can be achieved if all the necessary requirements are satisfied depending on the intended reuse. A study of the excavation method and several tests/ investigations are performed in this thesis to hand us results for an appropriate reuse of the muck.

Furthermore, as known circular economy and environmental factors are always major concerns, particularly in large tunnel infrastructures. The need of re-mucking can respond to such concerns. The concrete needed in different stages during the construction of tunnels represents a significant value in the cost of most of the construction projects. For these reasons in this work the reuse of the muck are mainly study for its reuse as concrete aggregates.

The thesis is divided in 5 chapters, each one covering important aspects to reach the sustainable goal targeted.

The first chapter deals with the aspects about the production of muck in hard rock excavation with full face TBMs.it covers all the important aspects about TBM excavation in hard rock, the rock breaking mechanism/chipping theories and also the performance of the TBM with a special attention devoted to all the parameters affecting both the TBM's performance and the production of muck.

In the second chapter, laboratory tests are described: they were performed on the muck to determine its geometrical, petrographic and mineralogical properties according to dedicated UNI EN standards. Moreover, 2D evaluations with the help of cameras and sensors using software are performed for determining the grain size properties of a larger quantity of the muck.

The third chapter is devoted to understanding and discussing the relationships among the muck geometry (shape and the size of chips), the TBM parameters and the rockmass characteristics and properties. Moreover, a preliminary evaluation of the penetration rate is proposed following the NTNU approach. In order to establish a comparison, the muck is represented using some parameters like the coarseness index, and the absolute grain size from the Rosin-Rammler diagram.

The fourth chapter is devoted to the sustainable reuse of the muck; the main focus is on the important aspects of TBM re-mucking; and also on the physical, mechanical and chemical requirements of concrete aggregates in accordance with the EN 12920 standard for a possible reuse of the muck as aggregates in structural concrete. The aggregates requirements are also evaluated with reference to the investigations and laboratory tests carried out in the previous chapters.

The last Chapter (conclusion and recommendations), summarizes the main results and investigations obtained, and also suggested further work to be carried out in the future for the characterisation of the muck.

1. Production of TBM muck in hard rock

1.1. TBM excavation in hard rock

1.1.1. Overview

Different types of TBM can be used for the excavation of a tunnel, and the selection of a TBM mainly depends on structural settings and rockmass conditions. Regardless of the type and application, TBM are mainly composed of four system groups: Boring system, thrust and clamping system, muck removal and support & lining system (Maidl et al., 2008).

Hard rock TBM, also called full face TBM, can be identified as grippers (or open TBM) and shield TBM; the shield TBM can be classified as a single or double TBM. The single shield TBM and the Open TBM are relatively inexpensive compare to the double shield.

The grippers TBM operate in very competent rock with low geological discontinuities and good stand time to allow the installation of the primary supports safely. On the other hand, Excavation with shielded TBM are performed in poor to medium rock mass quality.

The single shield is commonly used in poor rock quality or geological formations with significant fractures. The double shield, which is a combination of the grippers and single shield TBM, can be used from poor to medium rock quality and also where faults or shear zones may be present.

In addition, the shielded TBM are equipped with protective shields to cover the main body of the TBM behind the cutter head, to ensure the safety of the workers and operations during the excavation process of the tunnel. Moreover, due to the limited stand time, these machines are also equipped with a segment erector for the installation of segment lining.

1.1.2. Open TBM

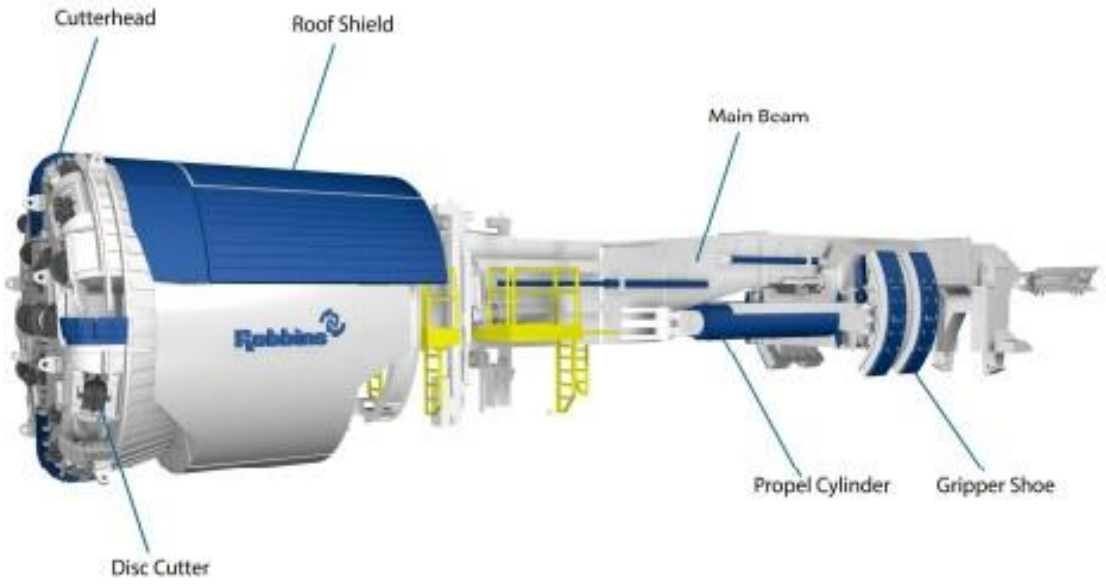

Figure 1.Representation of an open TBM with an indication of the main components of the machine (Robbins Company).

In the open TBM, the cutting process and the mucking operation are carried by the machine itself.

- **The cutter head** is equipped with disk cutters on its face, the disk cutters break the rock by applying a given pressure while the cutter is rotating. Pieces of rock detached are called chips. The cutters are mounted on the face of the cutter head; these cutters are usually of ring shaped type with a diameter ranging between 14" and 20".
- **The muck ring** put up the excavated materials that falls in the bucket into the conveyor belt system for its transfer to the rear of the machine for its disposal.
- **The roof shield** provides a temporary support to the rock and safety to the workers during installations.

- **The gripper shoes**, brace the grippers system against the walls using thrust cylinders for the boring phase and advancement.
- **The main beam** grants access to the personnel into the machine, just behind the cutter head to install the supports safely (shortcrete, ring beams, bolting, and steel mesh) and perform maintenance when required.

For the boring cycle of an open TBM: the gripper systems are locked by pushing them on the sidewalls to allow the propel cylinder to extend, then the rears of the machine are lifted.

The propel cylinders push the disk cutters against the rock, then the cutter disks break the rock while the cutter head is rotating. In this way, the detachment of the rock is obtained by the cracking effect due to the pressure applied on the rock mass from the thrust force to the cutters. When the boring stroke is completed, cutterhead rotation is stopped then, the rear legs are extended.

Finally there's the re-gripping, consisting in the last phase of the boring cycle. The rear legs of the machine are lowered, then the grippers and the propel cylinders are drawn back into the position for the next boring cycle.

1.1.3 Single shield TBM

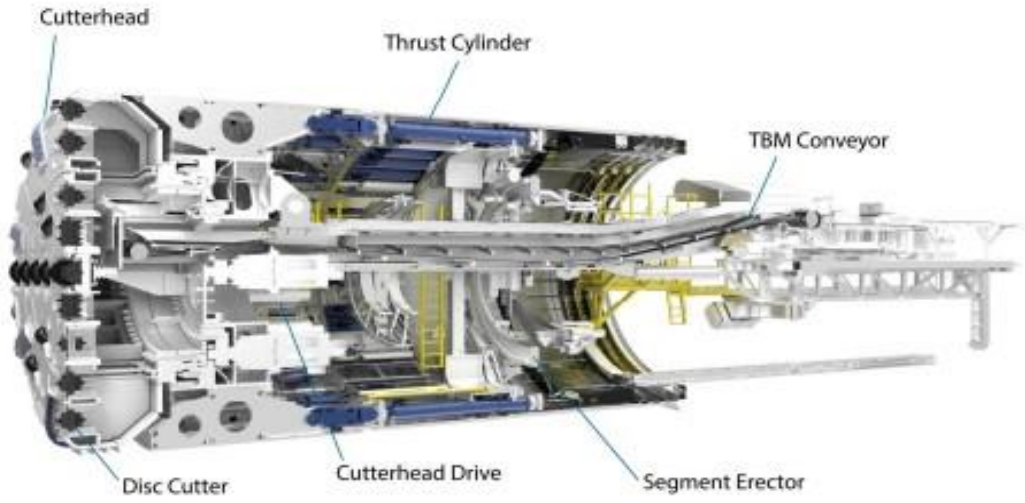

Figure 2. Picture of a section of single shield TBM with an indication of the main components of the machine (Robbins Company).

In the shield TBM also, the boring process and the haulage are carried by the machine itself. The haulage and boring process are similar to the open TBM.

- This machine has a shield that provides protection, and it is also equipped with a segment erector for the installation of precast segments lining during the advancement of the machine. There's also an annular gap between the excavated rock and the tunnel lining for the backfilling.

Moreover, this type of TBM can be equipped with probe drilling to study the rock mass conditions ahead of the TBM, with an automatic monitoring system for the collection of data and an advanced emergency thrust system to ensure efficient back up in poor ground condition, to prevent any case of entrapment.

1.1.4. Double shield TBM

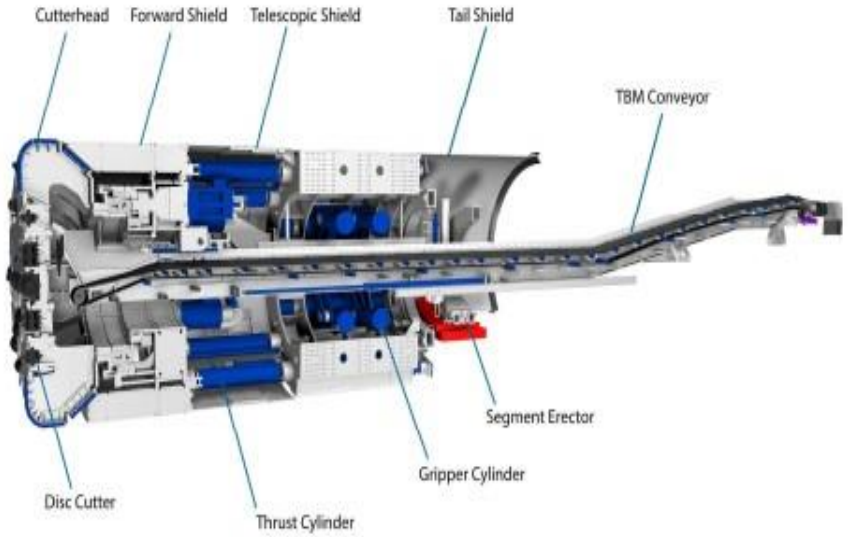

Figure 3. Picture of a section of double shield TBM with an indication of the main component of the machine (Robbins Company).

The double shield TBM is a combination of Grippers TBM and Single shield TBM. It can be used in poor, medium and good rock mass quality, therefore the double shield can be technically considered as the most sophisticated type of TBM in hard rock. The double shield TBM can also guarantee a very good overall performance of the machine during the excavation process, as it works in a continuous way.

- **Tail or grippers shield** covers the auxiliary trust cylinders, the gripping unit and tail skin. It remains static during the boring process. A segment erector is fixed to the gripping system for the installation of the precast segment lining during advancement after each boring process is completed. The gripper shoes are loosened once the boring stroke is completed, then the gripper shield pushes behind the forward shield thanks to the auxiliary thrust cylinders.
- **The forward shield** includes the cutter head and the main drives unit. The forward shield can independently advances while a stable ground condition is

present , thanks to the grippers shoes and also due to the fact that the machine is able to brace against the tunnel sidewalls; whereas, in case of unstable condition, the advancement can be obtain by pushing against the segment lining or tunnel walls .

- **The telescopic shield** extends during the advancement to ensure protection of the machine by keeping the whole machine under cover.

1.2 Rock breaking mechanism and cutting tools.

The rock breaking process in the TBM are performed by the disk cutters mounted on the face of the cutter head. The disc on the cutter head are frequently of ring shaped type in hard rock TBM. When the disk cutters are push against the rock mass by normal thrust forces, high pressure is built up under the contact area, thanks to this effect around the rock mass while the cutter head is rotating a cracking zone is created; as the stress grows, there's a propagation of cracks around the rock mass. A contribution of disks cutters on the axis creates the detachment of the rock '(Ozdemir, 1992; Bilgin et al., 2014).

Many authors agree on this fragmentation theory and to reach each stroke (excavation pull), the same chipping process for the rock fragmentation is required.

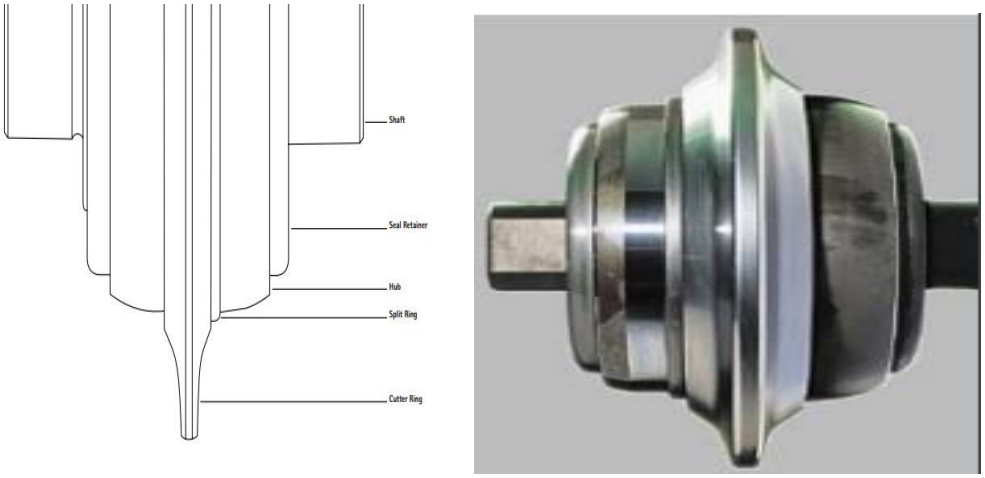

Figure 4. Picture of a TBM cutter disk with an indication of the main parts (Herrenknecht Company).

The detachment of chips is obtained by the rotation of the disk cutters along their axis and the rotation proceed on each axis thanks to the cutter head.

However, three acting forces can be distinguished during this process, as shown on figure 5. A normal force: this force is applied by the cutterhead to the disk cutters vertically and it progressively varies during the cutting process. A rolling force in the direction of the cut: this force is applied thanks to the cutterhead torque .When required, this force can be used to estimate the specific energy needed during the excavation of a unit volume of rock (Balci et al., 2009); and finally there's a side force acting on the disk edge.

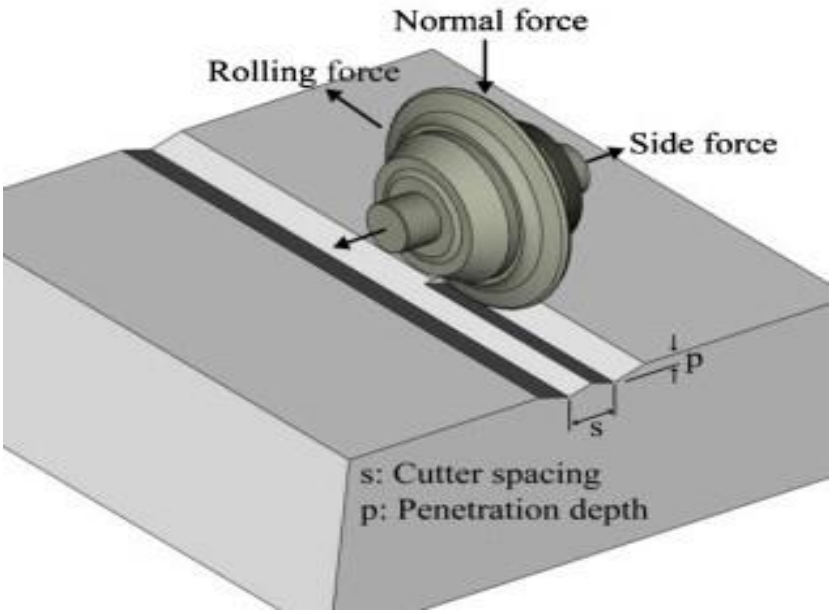

Figure 5. Representation of the three forces acting on a disc during the cutting process (Cho et al., 2010).

The cutter disk tools are selected based on the most significant geo-mechanical and geological properties of the intact rock. The market offers a wide range of cutter diameters in hard rock for different type of tunnels from micro tunnels to larger tunnels. Most frequently, the diameters are: 19"(483 mm) 15" (381 mm) and 17 "(432mm). For hard rocks, the minimum recommended diameter is about 432 mm (19") with a thrust between 267 and 311 kN (Zou, 2017) and with the linear speed limit of 165 and 200 mm/min

respectively. Cutter tools geometry can somehow affect the boring process, as the increase in diameter could bring up an increase in velocity and load.

Cutter rings can be of type standard or heavy duty. The heavy duty can last for long time and provide a better resistance to wear compare to the standard type, however due to the fact that they are expensive, they are usually selected only in case of high abrasive rock.

According to Xia et, al. (*2018)* the rock rupture process induced by the contribution of disk cutters based on the interaction of the cracks between adjacent cutting paths can be obtained by under break, overbreak and relieved cutting model. The breaking of the rock can be strongly influenced by the discontinuities i.e. fractures present in the rock mass. The performance of the tools primarily depends on the type of tools selected for a particular rock mass, as the efficiency of the cutting process can be reduced if the cutter tools aren't appropriately selected because they will fail to efficiently perform their goals; the problem of wear usually occurs depending on the abrasivity of rock; usually, in hard rock excavation, V type are preferable as they can provide a good cutting efficiency.

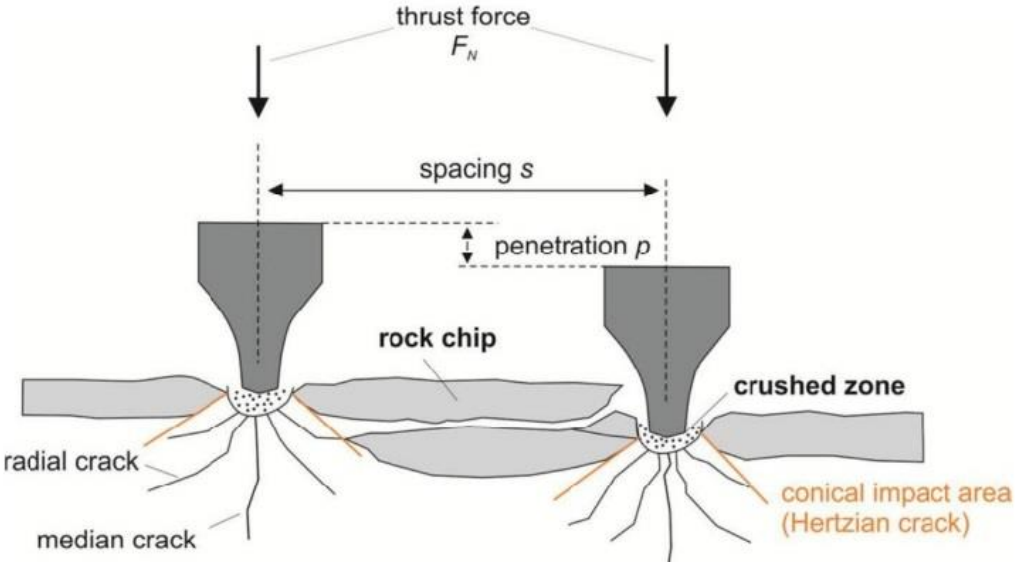

2

Figure 6. Cooperation between cutter tools for the detachment of the chip (Rostami, 1997).

For chip formation to occur, the cracks generated by a cutting path must coincide with those developed by the adjacent cut on the excavation face.

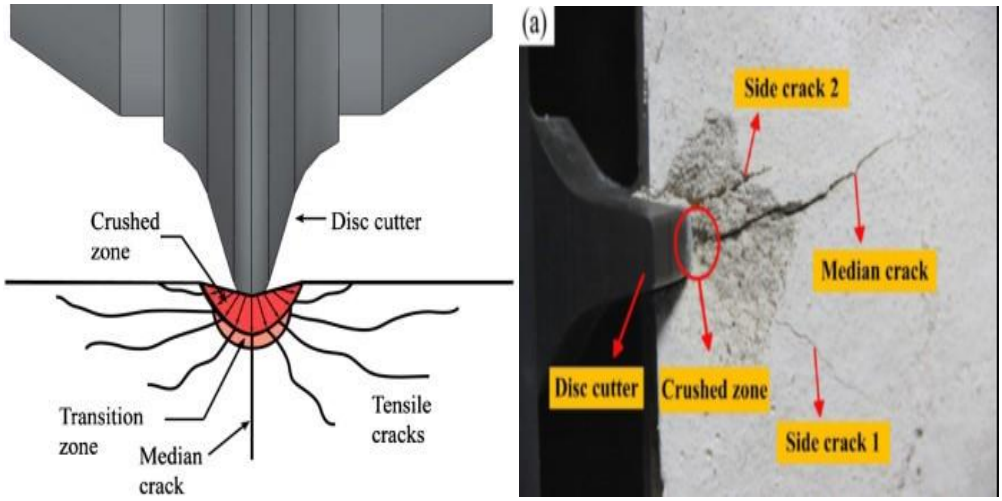

3

Figure 7. *On the left: Scheme of the crushed zone and the propagation of cracks during the contact between the rock mass and the disk cutter (Xia. Et al., 2018). On the right: a picture of the crack propagation mode and its pattern on a laboratory specimen (Lin. Et al., 2018).*

The spacing between the tools, the penetration and the properties of the rock to be excavated have a great influence on the cutting process.

In case the spacing between cutter tools is too small over crushing occurs: this effect can increase the specific energy and it's not considered economical. On the other hand, when spacing is too large, chips cannot be generated because the tools fail to efficiently penetrate the rock mass. Therefore, an appropriate choice of the cutter spacing is considered to be very significant for this process; the optimum spacing which refers to a chip detached that correspond to the best/appropriate spacing 's' between the tools. The optimum spacing is important in order to get an efficient cutting process for achieving a good overall performance of this process.

A parameter is used to define the optimal cutting geometry at a critical value of 's' the spacing of the tools and 'p' the depth of the groove, which is the ratio s/p, this effect is shown in figure 8.

According to Ozdemir et al. (1992), the optimal s/p ranges between 10 and 20, thus the optimum specific energy SE of the machine is obtained at the optimum spacing‘s’; this range can change depending on the type of rock encounter during the excavation process.

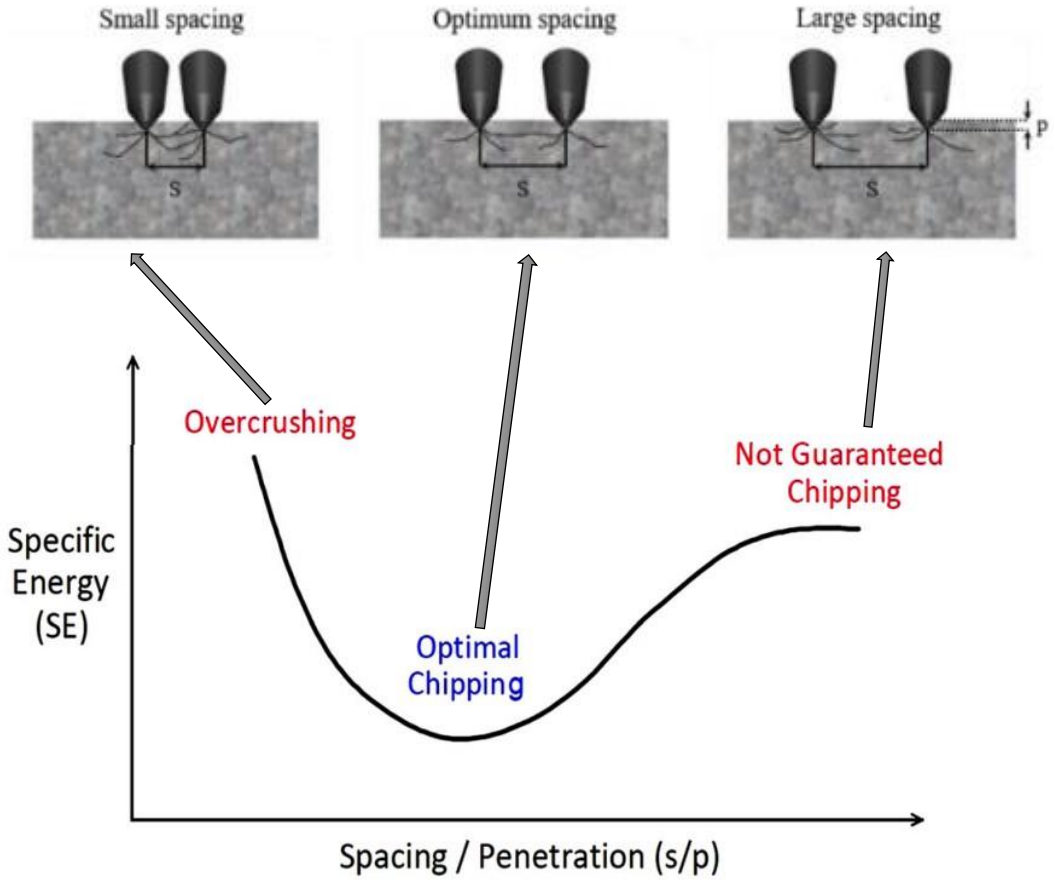

Figure 8. *Relationship between spacing/penetration ratio and specific energy consumption by means of disc cutters for the evaluation of the cutting efficiency during the excavation process (Tuncdemir et al., 2008).*

1.3 Performance of the TBM

The process for determining the most appropriate TBM has to be also justified by the performance of the machine and the cutter life assessment before its application in any tunnel construction; this evaluation depends on various parameters linked to the geological and geo-mechanical properties of the rock mass to be excavated, and also on the operational parameters of the machine. The performance of the TBM can also give us an understanding about the physical characterizations of the materials to be expected from the excavation process depending on properties of the rock mass and the parameters that were assigned to the machine.

The evaluation of the performance of the TBM can be defined by the following indices:

- **Rate of penetration [m/h]**: is defined as the boring length in a continuous phase during the effective boring time, without taking into consideration of the time required in any other operations or service during the boring process.

- **Advance rate: unit [m/h**]: is defined as the ratio of the boring length to the time required to complete all the operations and services (segment lining installation, maintenance works) required in addition to the boring time.

- **Coefficient of utilization [%]:** is defined as the ratio between the penetration rate and the advance rate.

- **Field penetration index [kN/cutter/mm/rev]:** is defined as the ratio between the total force acting on the cutterhead and the penetration rate per revolution. The penetration rate per revolution is defined as the effective boring length referring to each completed revolutions of the cutterhead.

1.3.1 Factors affecting the TBM performance

According to Bilgin et al. (2014) the factors that are affecting the TBM performance can be divided into 3 groups as follows:

- **Mechanical factors**; they refer to the machine itself and these factors can't be modified during the advancement of the machine; these factors consist of the characterisation of the TBM, such as the type of the TBM, the cutterhead and the cutter tools. The type of the machine has to be selected carefully depending on the geological and structural assessment of the rockmass and also on the economic factor of the project; a failure to do so may have a significant impact on the overall performance of the machine. The open TBM is usually preferable in small cross section TBM as it provides a good rotation speed of the cutterhead and less maintenance, compared to the shield TBM, e.g. double shield, which is, anyhow, considered to be the most sophisticated TBM type in hard rock, as its boring process is continuous and it also can be equipped with advanced mechanism for motoring and investigation of the rock mass properties ahead of the TBM's face. However, its maintenance can be time consuming compared to the gripper TBM used in smaller cross section tunnel.

  The cutterhead size is selected depending on the diameter of the cross section of the tunnel to be excavated and it has to be slightly smaller than the tunnel cross section, especially in fractured rock formation to avoid any entrapment due to an unexpected ground response or movement during the advancement of the machine. The cutterhead provides a certain thrust and rotational speed, which will define its performance; the cutterhead design is based on the specific energy required for the rock fragmentation process.

  The tools are selected based on some properties of the rock mass e.g. the abrasivity, and rock strength. The diameter, spacing and type of tools have to be selected adequately as they can also have an influence on the performance if they don't perform the cutting process efficiently. In some cases, the cutter tools can be replaced after having significantly been consumed by the wear: such delays can also affect the overall performance or the time required to complete the excavation

process. The cutter tools have to be monitored constantly during the excavation process because when a cutter tool or a group of them is damaged, the cutters might fail to exert efficiently their function; this scenario can somehow affect other tools along the same axis; as stated previously, the breaking mechanism occurs due to the collaboration among cutter tools along their axis. This effect could lead to an increase in the force required to perform the cut and also a higher consumption of the energy in the tools involved. This phenomenon can have a considerably reduction of the performance; as known, the advancement rate is a function of the cutting rate and utilization factor.

- **Geological and geotechnical factors** can considerably change during the excavation process, they refer to the properties of the medium or rockmass to be excavated such as; intact rock properties (toughness, hardness, brittlenesss, strength, mineralogy, texture, abrasivity) and the rock mass properties (discontinuities in the rock mass, squeezing and swelling, etc.).
  These parameters have a very significant influence on the performance of the machine due also to the fact that they can continuously change while the machine is excavating, especially in long tunnel, i.e. the presence of fractures in the rock can easy the cutting process and also it can induce stability problem or reduction in safety of operations/services. However, the primarily evaluations of these factors have to be as close as possible to those encounter during the excavation process and also, the machine has to be prepared to face any scenario that it was intended to or close to what it was intended to encounter during the excavation process. Furthermore, some of these factors can't be controlled, once the excavation path and the machine has already been defined, because it's almost impossible to change the geological and geotechnical properties of the rock mass.

- **Operational factors** can also considerably change: these parameters refer to the installation of supports, workers experience, and ground response during the excavation process and some onsite operations. Some of these factors don't change, such as the cross section of tunnel or its shape, and the other factors can change depending on the rock mass properties that the machine crosses during the

excavation process. Some secondary operations such as installation of primary supports or the haulage can also affect the performance if they aren't carried out adequately.

1.3.2 Prediction of TBM performance

Well-founded performance predictions and evaluations are a key issue for a successful planning and control of any risk or delays that might be encountered during the tunnel excavation process. TBM performance can be predicted by three general group of models, as follows:

- **Empirical and theoretical models** are based on some laboratory testing evaluation like the cutting force, penetration rate, rockmass properties and some in situ observations of the performance of the TBMs (Ozdemir et al., 1977). A set of parameters and tests are required to develop these models. These parameters and tests have been studied or modified by many others throughout the past years.

- **Statistical models** are based on mathematical principles and rules, they require many linear and nonlinear regression equations for the prediction of the performance. However, many authors mentioned that such models can't provide good accuracy in cases of outlier data samples in the database.

- **Computational models** are based on machine learning and also artificial intelligence. Generally, they provide a very good accuracy and low level of system error can be obtained using these models.

The most common used semi-analytical and empirical models for prediction of the cutter tools performance (penetration evaluation) and their consumption, are those developed by the Colorado School of Mines (CSM, Rostami 1997) and the Norwegian University of Science and Technology (NTNU, Bruland 1998). The NTNU empirical model is mainly based on historical data &TBMs field performance of the machine in a certain type of rockmass and the properties of that intact rock; various correlations, graph charts and equations from regression technique have been developed from the rock mass properties, ground conditions and TBM parameters to evaluate the performance. The CSM is based on laboratory tests and cutting force.

A set of laboratory testing, i.e. Cerchar Abrasivity Index (CAI), NTNU Abrasion Test (AV/AVS) for the assessment of the abrasivity of rock and cutter life of tools can be performed in request to obtain the indicators for the prediction models of the cutter tools.

The CSM have a limited set of information about the geotechnical characterization of the rockmass, this model doesn't take into consideration the influence of the joint properties of the rockmass. The joints properties correlations developed by the NTU can be used in some cases for a comparative result. The NTNU model has a better set of properties of joints obtained from similar types of rockmass but they are evaluated and measured in form of indices. This model is common used and preferred in many prediction cases, and also it provides a reliable set of data and it has been constantly updated throughout the years. However, both models provide a prediction close to each other and they both show a strong relationship with same ground characterization and TBM parameters.

Table 1 shows the input parameters of the NTNU and CSM prediction models for the evaluation of the Penetration Rate & advance rate and Utilization Advance Rate Cutter Life.

Table 1 .Shows the rockmass and TBM parameters required in the CSM and the NTNU models

Properties	CSM model	NTNU model
Rockmass properties	Uniaxial Compressive strength (UCS)	Drilling Rate Index (DRI) – fracturing , Cutter life index (CLI)
	Brazilian tensile strength (BTS)	Porosity
	Abrasiveness of the rock	Brittleness and Abrasiveness of the rock
TBM parameters	Max. thrust per cutter	Max. thrust per cutter
	Diameter of cutters	Diameter of cutters
	Number of cutters	Number of cutters
	width and spacing of cutters	width and spacing of cutters
	cutterhead diameter	cutterhead diameter
	RPM	RPM
	Cutter Radius, Spacing Penetration.	
	Torque and power	Cutters load

Moreover, In the CSM semi analytical model, the evaluation of the penetration is achieved by assigning a cutting load on linear rock-cutting machine, as shown in figure 9. The prediction of the cutter life assessment and penetration rate are based on the properties of the rock mass sample. A given force, spacing and penetration depth are

assigned on the rock sample. The CSM prediction model is performed based on following steps:

- Penetration assumptions
- Evaluation of the contact pressure
- Calculating Thrust applied to the disk cutter
- Calculation of the total torque and power

The linear rock-cutting machine (LRCM) is considered as a reliable technique for evaluating the cutting efficiency. The results of the laboratory testing using this machine can be compared with the TBM field data. Moreover, the intermediate linear cutting machine (ILCM) can also be used for assessing the penetration. As described by Cardu et al. (2021), the ILCM has several advantages for the evaluation of the penetration, e.g. reduction of the scale to facilitate the supply and transportation of the sample; this machine can also work on an intermediate scale between the full- and the small-scale.

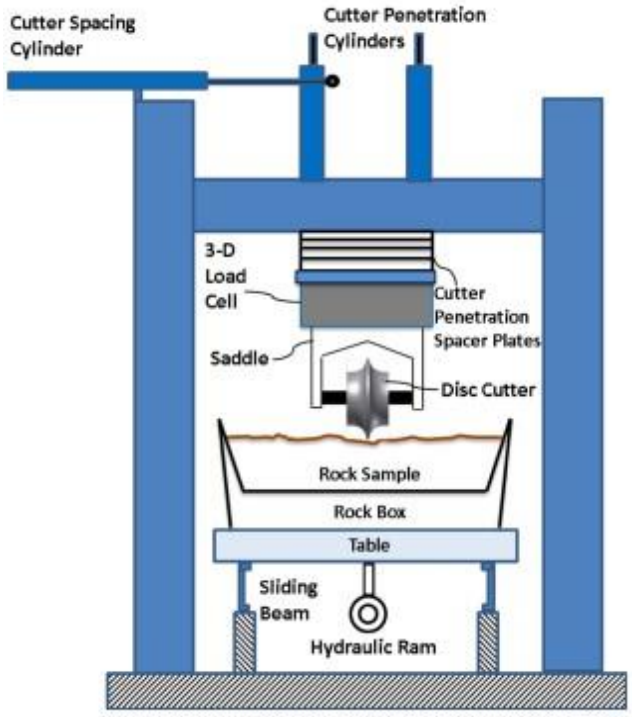

Figure 9. A scheme of the linear rock-cutting machine (LRCM) at Missouri S&T (Abu-Bakar et al., 2012)

2. Investigations to characterize the TBM muck from the Maddalena pilot tunnel

2.1. Geological overview

The muck tested in this thesis is coming from an exploratory tunnel “the Maddalena”, which is one of the parts related to the Mont Cenis Base Tunnel excavation. This tunnel is located in Northern Italy, in the Piedmont Region, precisely in the Susa valley.

The excavation of the Maddalena Tunnel was mainly released from the collection and studies of structural, hydrogeological, geotechnical data; based on the geological studies and literature review carried out, the rock mass was found to be a metamorphic massive rock of good quality.

Figure 10. Geographical position of the Maddalena tunnel in Chiomonte, Italy (Google Maps)

The tunnel crosses two main lithological formations, the first being composed of gneiss belonging to the Ambin complex, from a Pk.0 +198 m to 0+967, 0 m; as for the second one, it is composed of micascshist belonging to the Clarea complex, from Pk.1+360.0m. There's also a transition zone between Pk.0 +967.0 m and 1+360.m and it's mainly composed of gneiss and micaschists. The gneiss can somehow have better mechanical properties in comparison to the micaschist.

The Maddalena tunnel has a length of around 7.3 km. The Ambin formation (AMC) covers a length of around 1 km; the Clarea formation (CLR) covers a length of almost 6 km and a transition zone (AMD) has a smaller length, of around 200 m. ''The schistosity is on average oriented towards North and East-South east with an inclination from 10 to 50 degrees and a steeper inclination in schistosity is present within the Clarea complex" (Rispoli, 2017).

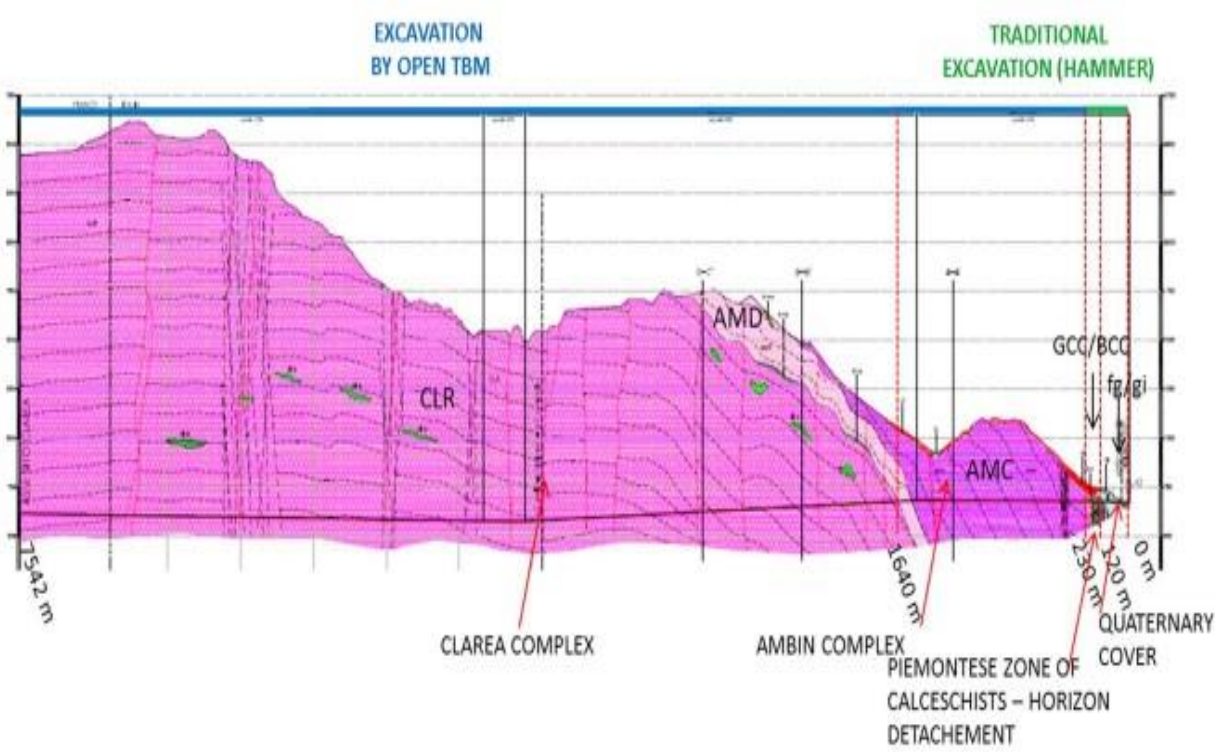

Figure 11 Geologic of the Maddalena exploratory tunnel (Parisi et al. 2015)

2.2 Mineralogical and petrographic characterization

2.2.1 Preliminary petrographic description

The petrographic analysis for the detection of the mineral composition and rock type can be performed using the macroscope or microscope depending on the level precision required for the petrographic analysis; the level of precision and choice of equipment required also depend on the data, i.e. geological information about the rock samples already available.

As a first approach, in order to determine the constituent rock or mineral types, the rock sample can be first subjected to a visual examination and also with the help of geological data. The rock sample can be inspected using a stereoscopic microscope and other appropriate means or equipment. The minerals can be detected based on the morphology (color, cleavage and twinning, etc.) and the optical characteristics of the crystal. Its description of the rock sample thanks to the petrographic classification can be done by its mineralogical composition and the rock type is named depending on the dominating minerals and texture present.

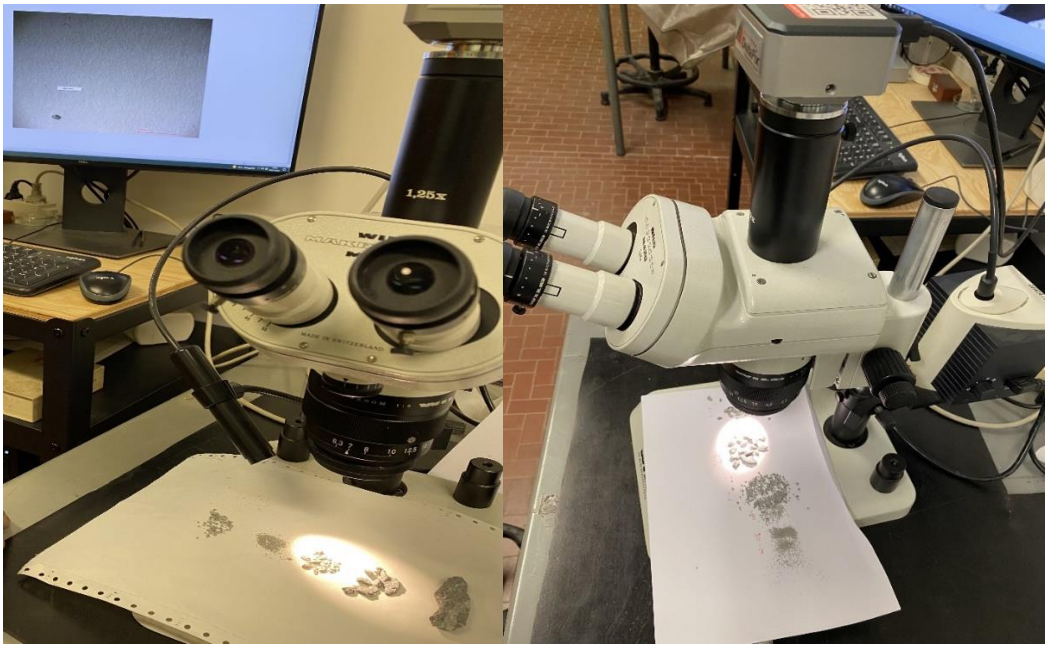

Figure 12. Macroscope used for the preliminary petrographic description

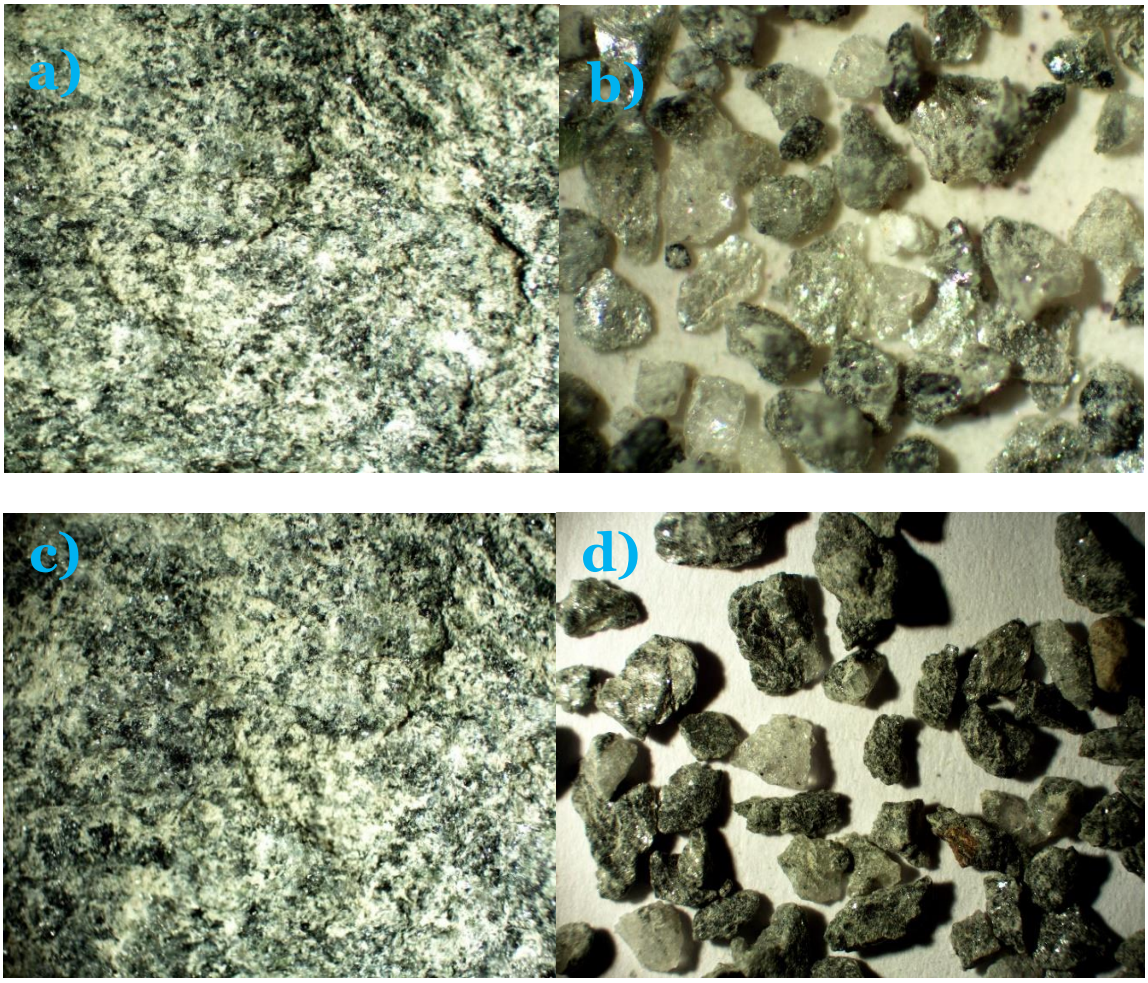

Figure 13.Macroscopic views: a) grain particle size of 12 mm; b) grain particle size of 8 mm; c) grain particle size of 1 mm and; d) grain particle size of 0.5 mm.

The rock type is found based on several observations through the macroscope, focusing on the color, texture, cleavage etc. in order to detect several minerals present in the sample. However, depending on the dominating minerals that were present, the rock type was found to be a micaschist having quartz, muscovite and chloride as dominating minerals. This investigation is important to confirm the petrographic data. Before performing the XDR analysis, the preliminary petrographic information and geological data of the rock are significantly important in order to have an efficient evaluation of the mineralogical assessment.

2.2.2 XRD Analysis for Quantitative mineralogical assessment

2.2.2.1 Overview

The qualitative assessment of the minerals present in the muck is very significant for the purpose of an efficient reuse of the muck itself. A high quantity of certain minerals in the muck can affect the durability of concrete when the muck is used as aggregates for concrete. By example for the reuse of muck in the concrete as aggregates, the muck shouldn't have a higher amount of minerals such as clay, gypsum, garnet and talc and also fibrous minerals like graphite and micas; such minerals can also create reactions that will compromise the strength of structural concrete.

The geological data and petrographic description about the sample provide a primarily characterisation of the mineralogical composition of the muck; however, based on the previous evaluations conducted on the material, the rock was identified as a mica schist.

The quantitative analysis was performed using the X-ray diffractometer with advanced detector from Rigaku SmartLab SE, which is a multipurpose powder diffraction analytical machine that can determine the crystalline phase identification (phase ID) and quantification, crystallinity percent (%), crystallite size and strain, lattice parameter refinement, Rietveld refinement, and molecular structure. This method is widely used for a phase analysis of poly-crystalline materials in order to obtain a qualitative and quantitative evaluation of materials.

Figure 14. XDR Rigaku Smart Lab SE, from DIATI (Politecnico di Torino) used to carry out the tests

The samples used for this test are those obtained from the sieving method. The fraction of the samples retained on the sieve of 125 -250 microns, 125-63 microns and min. 63 microns were selected.

The samples were further crushed to a finer powder in order to make them suitable for the test, then they were poured and uniformly pressed in a slide holder plate.

2.2.2.2 Methodology

An X-ray diffraction pattern is based on core elastic scattering to plot the intensity of X-rays scattered at different angles to produce from each phase a unique diffraction pattern. The detector in the machine moves in a circle around the sample and its position is recorded as the angle 2theta (2θ) and the number of x-rays observed are also records at each angle 2θ. The sample or the tube will also rotate in order to keep the X-ray beam properly focused. The 2θ incidence angles with a span of 4°as start angle to 80° as stop angle, with a speed of 10 s, step of 0.100, and incident slot 2/3 are considered for this experiment. The runtime for the analysis was about 15 min for each sample.

The reference patterns are compared to the XRD data, which contain all major peaks to determine the different phases that are present in this experiment. Each phase produces a different combination of peaks which are properly calibrated in order to obtain the amount present in each phase of the sample and the x-ray diffraction pattern is the sum of the diffraction patterns produced in each phase.

The qualitative analysis is done by calculating the unit cell dimensions at the diffraction peak positions using the Bragg's Law for the conversion of the observed peak positions and to determine the Miller indices (hkl) of the diffraction peaks from the reference pattern obtained:

$d_{hkl} = \lambda / 2\sin\theta$

where:

λ is the characteristic wavelength of the X-rays impinging on the crystallized sample;

d is the interplanar spacing between the rows of atoms;

θ is the angle of the X-ray beam with respect to the planes.

The weight fraction of each phase is calculated when the calibration constant is known. The calibration constant is determined from empirical measurements, reference intensity ratio (RIR) or by calculating them with Rietveld refinement.

2.2.2.3 Results

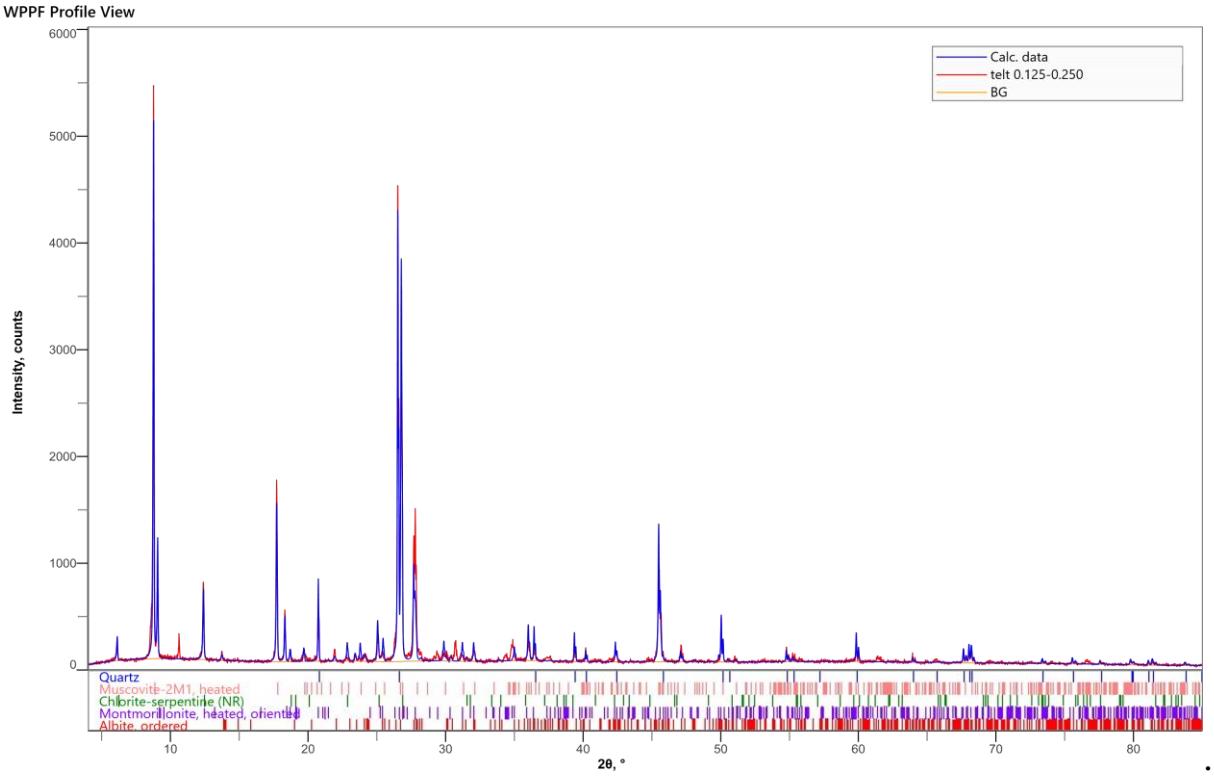

*Figure 15.*Sample 1: test spectral results.

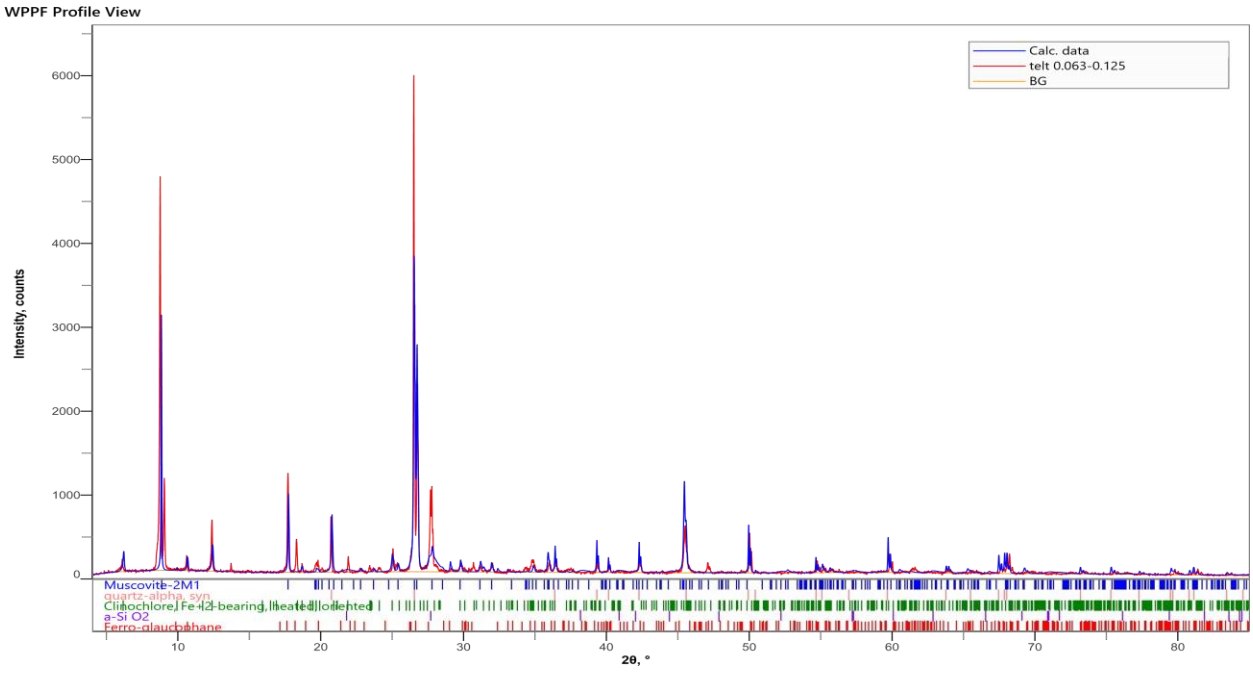

Figure 16.Sample 2: test spectral results

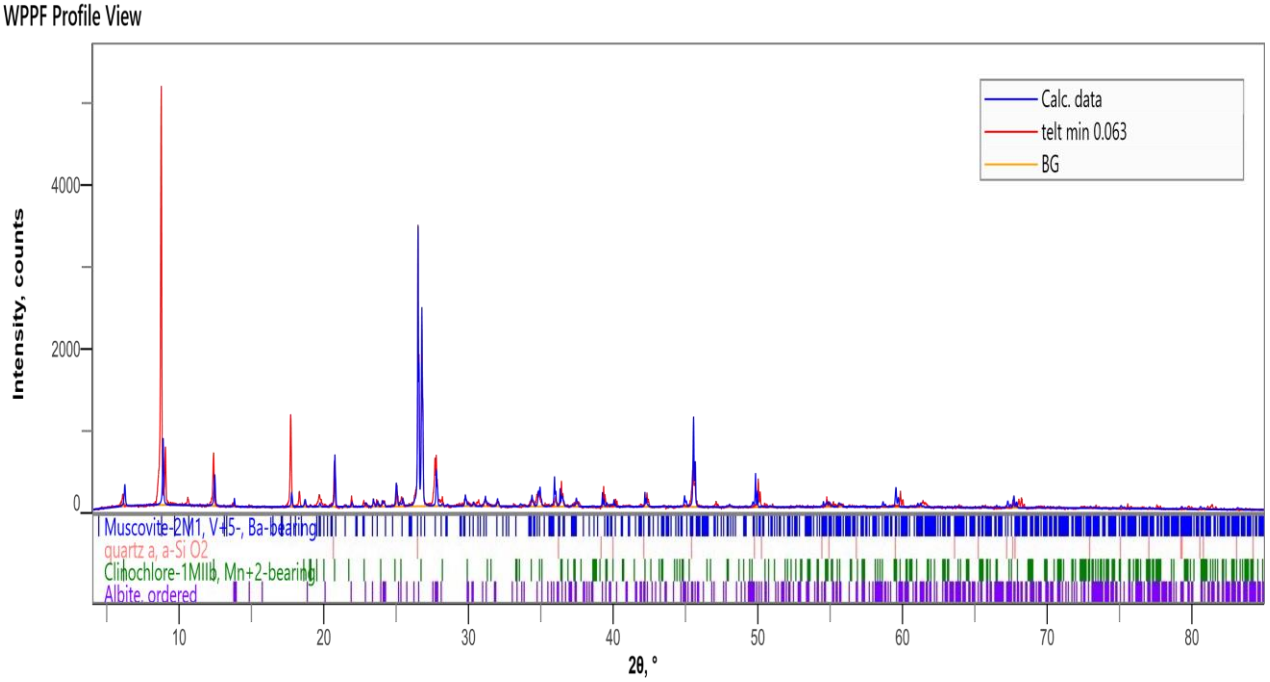

Figure 17. Sample 3: test spectral results.

The mineralogical composition detected in all of the three samples examined are mainly composed of silicate minerals (quartz, muscovite, chloride) and some other minerals. The quartz and muscovite represent at least 75 % in all of the three tests performed. The results obtained about the rock type from the XDR analysis match with the preliminary petrographic evaluation. The sample was identified to be a mica schist, and the mineral proportions of each sample are shown in Figures 18-20.

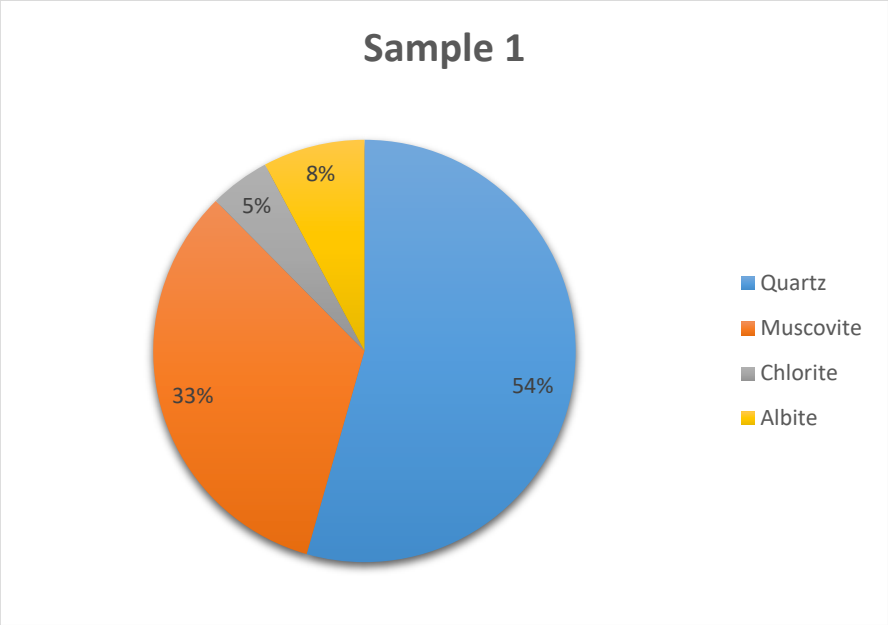

Figure 18. Graph for mineral composition in percentage for sample 1.

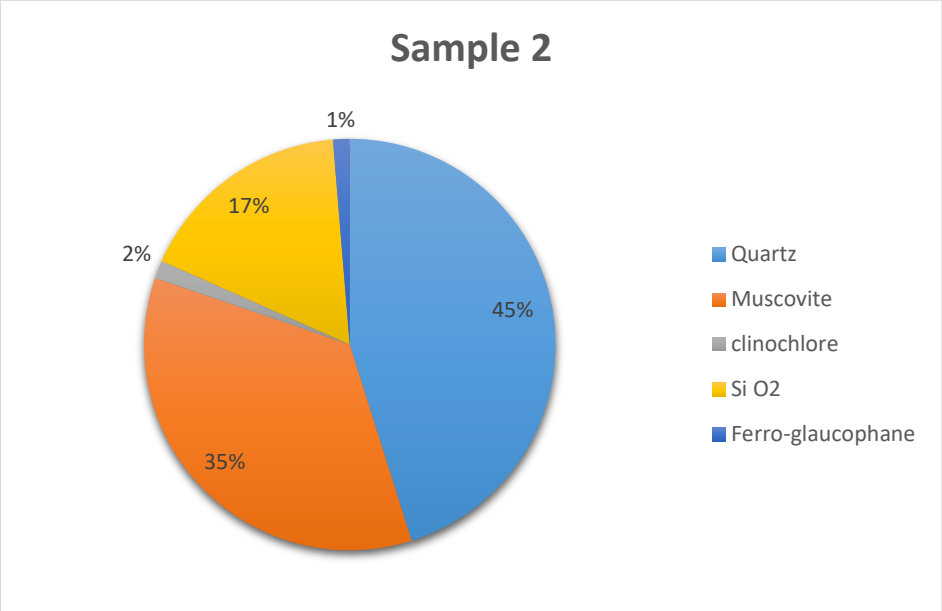

Figure 19. Graph for mineral composition in percentage for sample 2.

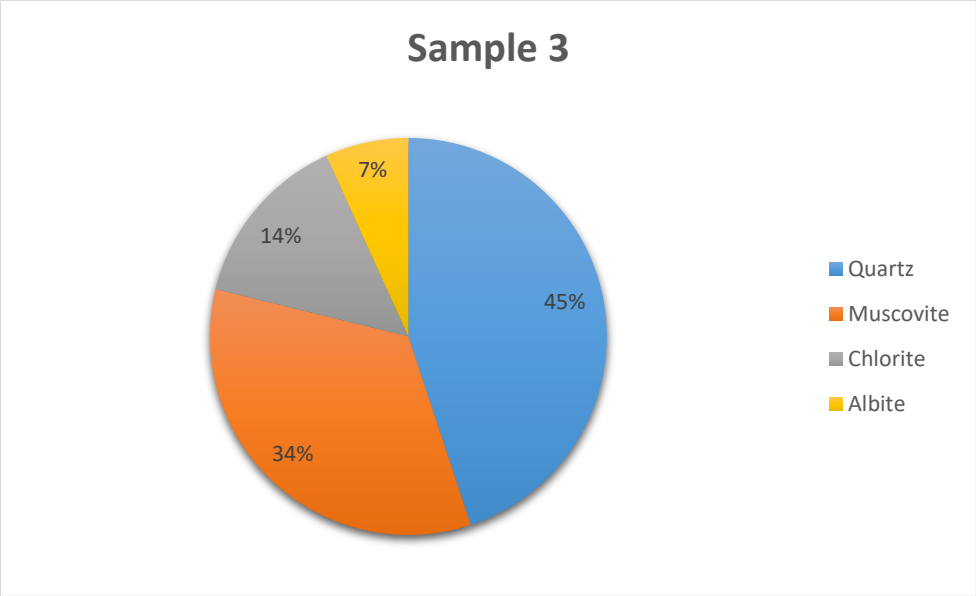

*Figure 20.*Graph for mineral composition in percentage for sample 3.

2.3 Laboratory tests for identifying the geometrical properties of the muck

2.3.1 Overview

The laboratory tests were performed in order to characterize the muck on the geometrical point of view. These tests involved verifications on the size, angularity and shape (content of elongated and flat particles).

These properties play an important role for the performance and requirements of the reuse of aggregates as a construction material; they generally provide a primarily evaluation on the quality of the muck. These tests could also give an idea about the technique to be implemented in order to improve the quality of the muck if required, depending on the targeted reuse, e.g. in the concrete mix design the flaky and elongated particles could lower the workability of concrete mixing due to high surfaces area/volume ratio.
The laboratory tests and standards for investigating the geometrical properties of aggregates are specified in table 2.

Table 2. Tests for geometrical properties of the muck in accordance with the standards

Laboratory test	Standard
Preparation of the laboratory sample	EN 932-2 Standard
Determination of the particle size distribution	UNI EN 933-1:2012 Part 1
Determination of particle shape: Flakiness index	UNI EN 933-3:2012 Part 3
Determination of particle shape: shape index	*UNI EN 933-4:2008 Part 4*

2.3.2 Determination of particle size distribution of the muck-sieving method

2.3.2.1 Methodology

The determination of the particle size distribution was performed according to **UNI EN 933-1:2012 Standard Part 1** and each test sample should be prepared in accordance with the **EN 932-2 Standard,** therefore the samples used for this test were dried for few hours in the oven and the boulder/cobbles particles were brushed in order to make the sample fit for the test. This test is used to grade the muck, the particle size distribution is considered as one of the primary criteria used to verify whether if the muck can be suitable for any reuse. The test consists of separating the dry muck into several particle size classes in a decreasing order by means of a set of sieves; the selected sieves opening and the number of sieves have been selected based on the nature and intended reuse of the muck.

Figure 21. Sieve shaker used to perform the tests.

For the particles size with a D≤ 31, 5 mm, the sieving was performed mechanically through a sieve shaker. On the other hand, for the particles size D ≥ 31, 5 mm the sieving was done manually with a scale. The test was performed on 3 samples of about 50 kg each, taken from different big bags of materials collected during the tunnel excavation process.

The sieves were arranged depending on their opening, larger to smaller sieve (D/d) and the column of sieves was placed on the sieve shaker and a portion of sample was pour on; the sieving process was performed through the sieve shaker for more of less 15 min for each portion of the sample.
This test was performed for three samples and the weight of the sample fraction retained on each sieves was expressed as cumulative percentage and retained percentage.

Moreover, the characterization of the grain size particle can also be represented by the coefficient uniformity and curvature. The coefficient of curvature refers to the ratio of the sieve size through which 60% by weight of the grain particles pass to the sieve through which 10% by weight of the grain particles pass. A value of CU greater than 6 refers to densely graded aggregates, whereas a value of CU less than 4 refers to open graded aggregates, the CU can be calculated with the following formula:

$C_U = D_{60} / D_{10}$

and the coefficient of curvature CC is calculated with the following formula:

$$C_C = \frac{{D_{30}}^2}{D_{60} \times D_{10}}$$

where:

D60 is the dimension corresponding to 60% of passing aggregate in the particle-size distribution curve.

D30 is the dimension corresponding to 30% of passing aggregate in the particle-size distribution curve.

D10 is the dimension corresponding to 10% of passing aggregate in the particle-size distribution curve.

Figure 22. Example of the sieved boulder/ *cobbles particles with D ≥ 31, 5 mm that were performed manually*.

2.3.3 Determination of particle shape: Flakiness index

2.3.3.1 Methodology

The flakiness index was performed according to **UNI EN 933-3:2012 Standard Part 3**; the samples used for this test are the samples obtained from the sieving test. The classes used for this test correspond to some of the sieves classes from the sieving test with square openings that were previously used to determine the grain particle distribution, as indicated in the standard.

A set of sieves bar sieves with parallel slots are used to sieve each particles size fractions in order to determination the particle shape: flakiness index.

Moreover, all the apparatus is conformed to the general requirements of **EN 932-5 standard** and the test portions were prepared according to the standard **EN 932-2.**

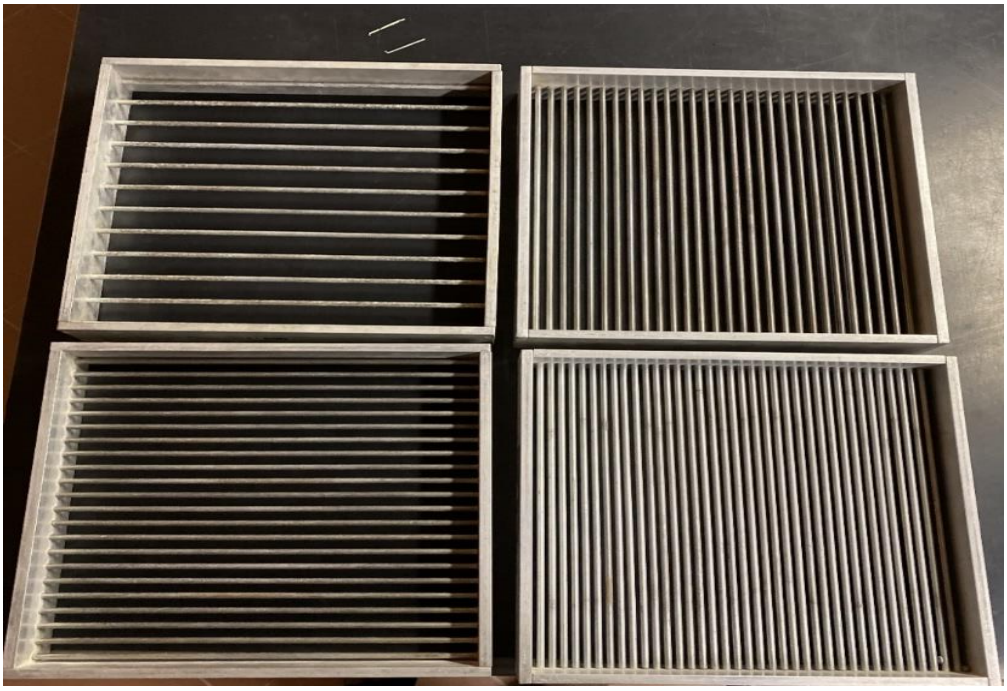

Figure 23. Bar sieves with parallel slots used for the determination of the flakiness index.

The flakiness index of each particle size fraction di/DI can be calculated as the mass of particles passing the corresponding bar sieves, which is expressed as a percentage by mass of that particle size fraction.

The overall flakiness of the sample can be calculated as the total mass of particles passing through the bar sieves, which is expressed in percentage with respect to the total mass of that sample.
The overall flakiness index Fi can be calculated from the following equation:

Fi= (M2/M1) *100

where:

M1 is the sum of the masses of the particles in each of the particles size fraction di/Di, [g];

M2 is the sum of the masses of the particles in each particle size fraction passing the corresponding bar sieve of slot width Di/2 [g].

The overall flakiness Fi has to be recorded to the nearest whole number.

The flakiness index for each size fraction Fi can be calculated, with the following equation:

Fi= (mi/Ri) *100

where:

Ri is the mass of each particle size fraction di/Di[g];

Mi is the mass of the material in each particle size fraction di/Di which passes through the corresponding bar sieve of slot width Di/2 [g].

The results of these tests are shown in in the table 3, 4 and 5 and the overall flakiness index is represented in figure 17.

2.3.4 Determination of particle shape: shape index

2.3.4.1 Methodology

The shape index test was performed according to the **UNI EN 933-4:2008 Standard Part 4;** this test consists of classifying a portion of each sieve sample fraction in accordance with the standard and the nature of the materials. The classification is based on the ratio of the length L to the thickness E of particles using a particle slide gauge.
The shape index for each sample is calculated as the mass of the particles with a ratio of dimensions L/E more than 3 expressed in percentage with respect to the total mass of particles.

The designation of aggregate in terms of lower (d) and upper (D) sieve sizes, expressed as d/D and fraction of an aggregate passing the larger (Di) of two sieves and retained on the smaller (di).
The test was carried on each particle size fraction di/Di, where Di ≤ 2di.
Test portions from samples for which D≥ 2d shall be separated into particle size fractions d1/Di where Di ≤2di during the subsequent test procedure.

Moreover, all the apparatus is conformed to the general requirements of **EN 932-5** standard and the test portions were prepared according to the standard **EN 932-2.** The separation to obtain the particle size fraction required to perform the test was done through the Jonson separator in accordance with the standard **EN 933-1.**

The shape index is performed using a double caliber and it can be calculated using the following formula:

$$SI = (M2/M1) * 100$$

where:
M1 is the total mass of the tested particles [g];
M2 is the mass of the non-cubic particles[g].
The shape index has to be recorded as the nearest whole number.

Figure 24. The *Jonson separator used to obtain the particle size fraction.*

Figure 25. The particle double caliper used to perform the shape index

2.3.4 Test Results

The results given in table 3 can be used to produce the grain size distribution curves for the cumulative passing percentage.

Table 3.Sieving results for determining the passing percentage of particle size.

	SAMPLE 1			SAMPLE 2			SAMPLE 3		
D [mm]	**Weight [g]**	**Fraction %**	**Cum. Passing %**	**Weight [g]**	**Fraction %**	**Cum. Passing %**	**Weight [g]**	**Fraction %**	**Cum. Passing %**
> 200	3640	7.22	100.00	10690	23.15	100.00	12800	28.59	100.00
150	3290	6.53	92.77	1530	3.31	76.85	3200	7.15	71.40
100	6160	12.22	86.25	3860	8.36	73.53	4950	11.06	64.26
31.5	8535	16.93	74.03	4900	10.61	65.17	3650	8.15	53.20
14	8755	17.37	57.09	7180	15.55	54.56	5800	12.96	45.04
8	4155	8.24	39.73	4020	8.71	39.01	2620	5.85	32.09
4	3325	6.60	31.48	3600	7.80	30.30	2470	5.52	26.23
2	1745	3.46	24.89	1960	4.25	22.50	1455	3.25	20.72
1	2018	4.00	21.42	1620	3.51	18.26	1330	2.97	17.47
0.5	3109	6.17	17.42	1200	2.60	14.75	1085	2.42	14.50
0.25	1017	2.02	11.25	1030	2.23	12.15	990	2.21	12.07
0.125	795	1.58	9.23	1290	2.79	9.92	1335	2.98	9.86
0.063	1264	2.51	7.66	2150	4.66	7.13	2045	4.57	6.88
< 0.063	2598	5.15	5.15	1140	2.47	2.47	1035	2.31	2.31
	∑W= 50406	∑%= 100.00		∑W= 46170	∑%= 100.00		∑W= 44765	∑%= 100.00	

The cumulative retained percentage is shown in figure 26; this information about the size of the particle grains can be used as a primarily classification or characterization of the geometrical properties of the aggregates.

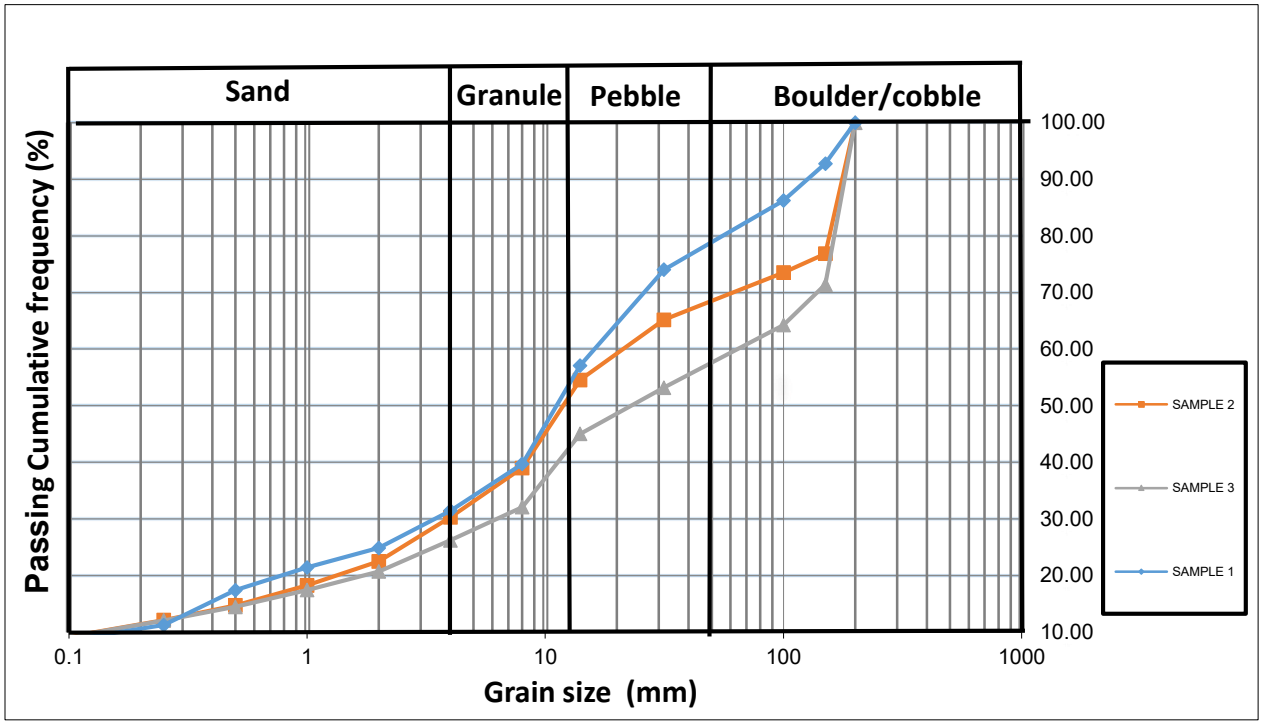

*Figure 26.*Grain size distribution curves obtained from the tests

On the basis of the ISO 14688-:2002 classification, the grain size distribution curves represented in figure 26 shows that the larger amount of particle grains are categorized as gravel (4-64 mm): they represent at least 45% of the total weight in all the three sample tested. The sand class represents more or less 25% of the total weight in each sample. As for the boulder/cobble particles, they represent at least 20 % of the total weight in each tested sample. The cumulative passing percentages for the sand and gravel classes in the tested samples are relatively close to each other in comparison with the boulder/cobble classes.

Table 4.Sieving results for determining the cumulative retained percentage of particle size to evaluate the crossness index

	Sample 1			Sample 2			Sample 3		
D (mm)	**Weight [g]**	**%**	**Cum. retained %**	**Weight [g]**	**%**	**Cum. retained %**	**Weight [g]**	**%**	**Cum. retained %**
+ 100	13090	25.97	25.97	16080	34.83	34.83	20950	46.80	46.80
-100+31.5	8535	16.93	42.90	4900	10.61	45.44	3650	8.15	54.95
-31+14	8755	17.37	60.27	7180	15.55	60.99	5800	12.96	67.91
-14+8	4155	8.24	68.51	4020	8.71	69.70	2620	5.85	73.76
-8. +4	3325	6.60	75.11	3600	7.80	77.50	2470	5.52	79.28
-4+2	1745	3.46	78.57	1960	4.25	81.74	1455	3.25	82.53
-2+1	2018	4.00	82.58	1620	3.51	85.25	1330	2.97	85.50
-1	8783	17.42	100.00	6810	14.75	100.00	6490	14.50	100.00

The cumulative retained percentages obtained in table 4 are used to calculate the coarseness index and the absolute grain size in the next chapter for a comparison between the muck size and the TBM parameters.

The results given in tables 5-7 show the flakiness index for each particle size, as well as the total flakiness index obtained for each sample.

Table 5. Results for the flakiness index of each particle size fraction and overall flakiness for sample 1.

Sample 1				
Particle size class [mm]	Flakiness sieve [mm]	Ri: mass of each size fraction [g]	Mi: mass passing through the sieve[g]	Fi=mi/Ri*100
>200	100	3640	0	0%
200-150	75	3290	1290	38%
150-100	60	6160	2549	41%
100-31.5	20	8535	2240	26%
31.5-14	8	8755	1500	17%
14-8	5	4155	1070	26%
8-4	2.5	3325	1075	32%
		M1:total mass class in g	M2: mass passing to sieve in g	Fi=m2/m1*100
		37860	9724	26%

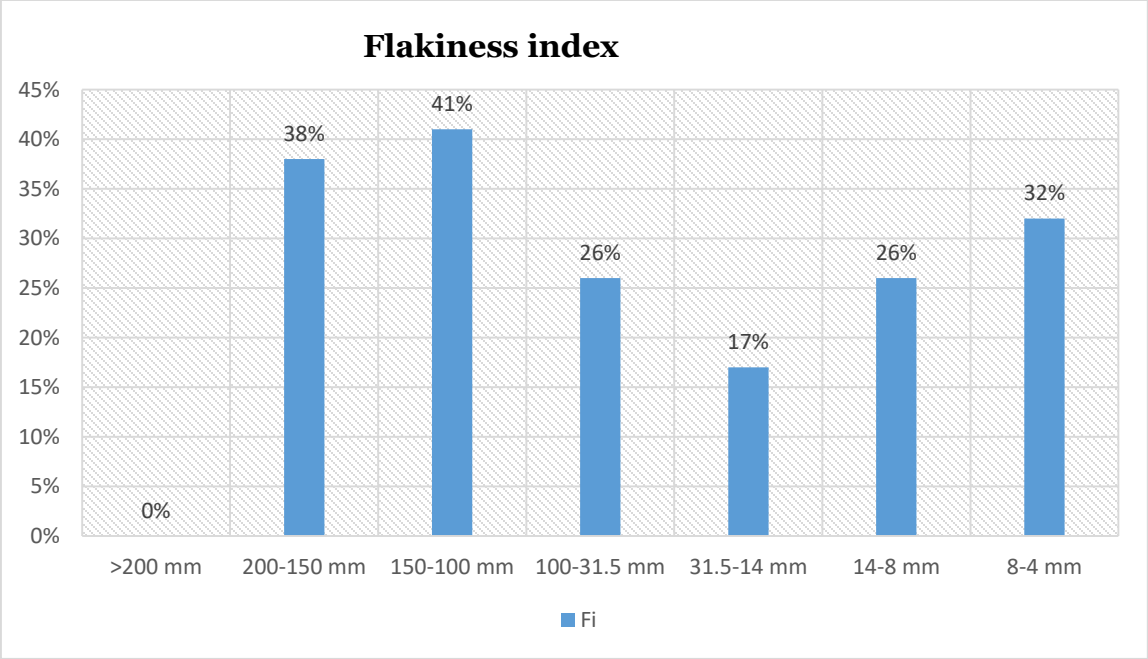

Figure 27 .Graphical representation of the flakiness index for sample 1

*Table 6.*Results for the flakiness index of each particle size fraction and overall flakiness for sample 2.

Sample 2				
Particle size class [mm]	Flakiness sieve [mm]	Ri: mass of each size fraction [g]	Mi: mass passing through the sieve[g]	Fi=mi/Ri*100
>200	100	1069	0	0%
200-150	75	1530	465	30%
150-100	60	3860	3100	80%
100-31.5	20	4900	1640	33%
31.5-14	8	7180	1130	16%
14-8	5	4020	1100	27%
8-4	2.5	3600	1170	32%

	M1:total mass class in g	M2: mass passing to sieve in g	Fi=m2/m1*100
	26159	8605	33%

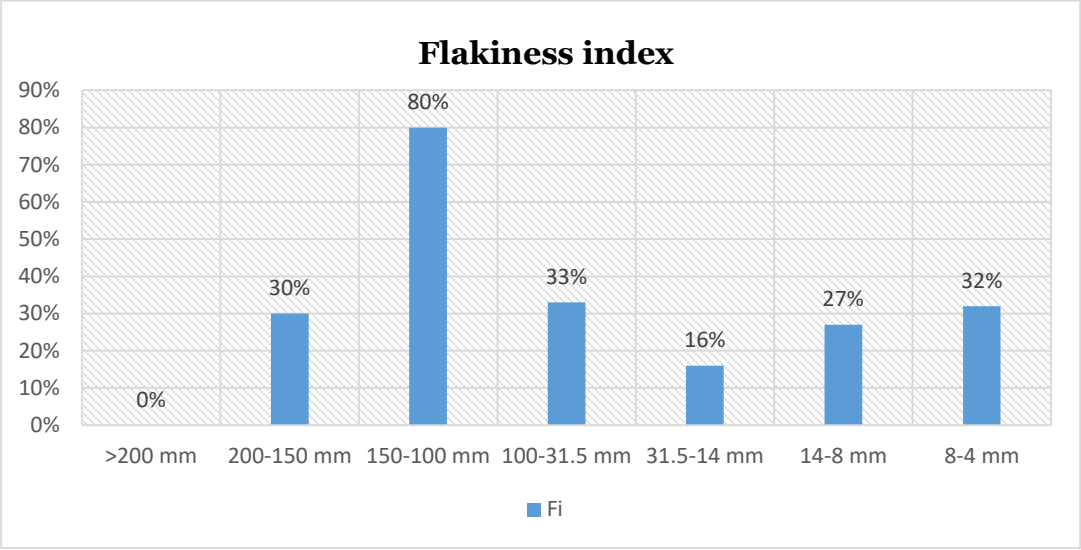

Figure 28.Graphical representation of the flakiness index for sample 1

*Table 7.*Results for the flakiness index of each particle size fraction and overall flakiness for sample 3.

Sample 3				
Particle size class [mm]	Flakiness sieve [mm]	Ri: mass of each size fraction [g]	Mi: mass passing through the sieve[g]	Fi=mi/Ri*100
>200	100	12800	1370	11%
200-150	75	3200	2180	68%
150-100	60	4950	3280	66%
100-31.5	20	3650	940	26%
31.5-14	8	5800	865	15%
14-8	5	2620	590	23%
8-4	2.5	2470	705	29%
		M1:total mass class in g	M2: mass passing to sieve in g	Fi=m2/m1*100
		35490	9930	28%

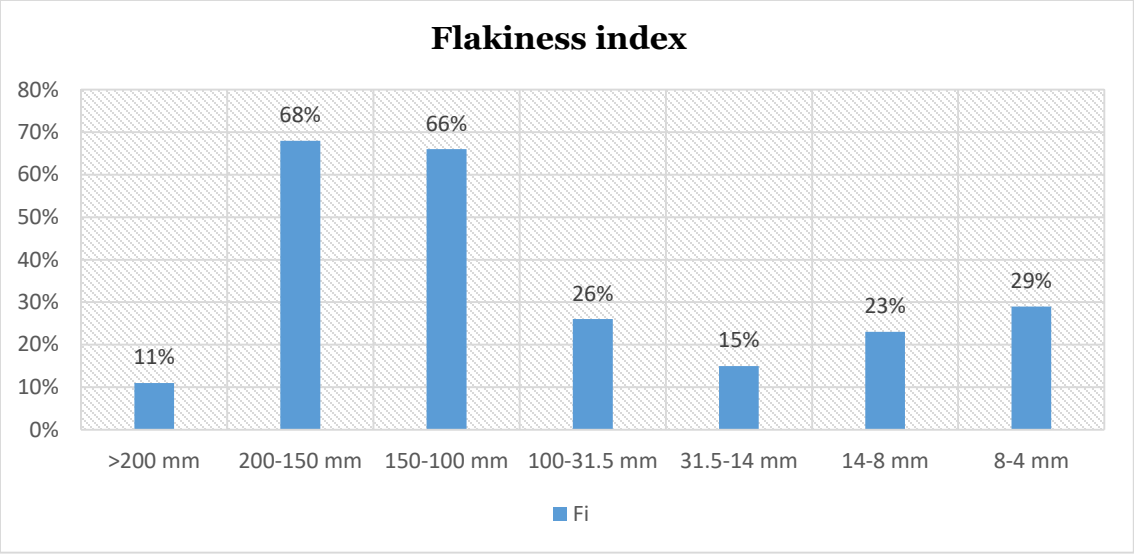

Figure 29 graphical representation of the flakiness index for sample 1

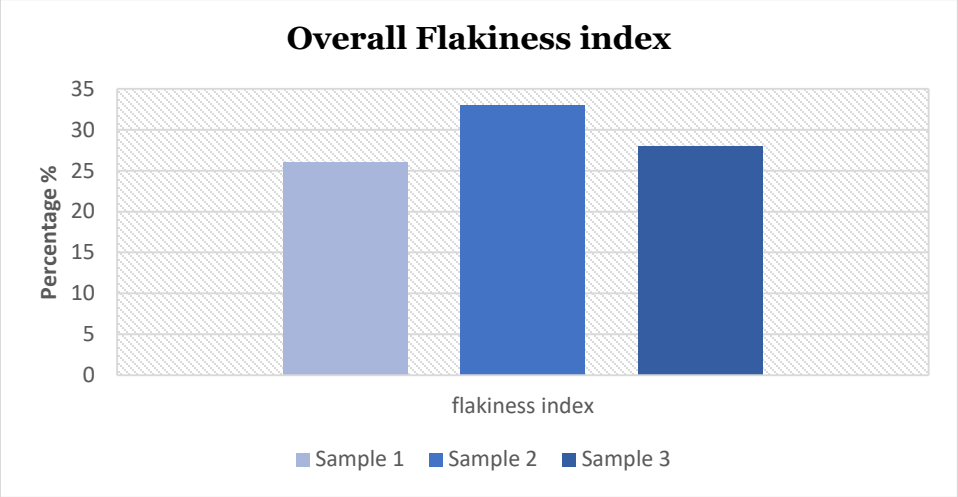

Figure 30. Graphical representation of the overall flakiness index

The results of the flakiness index obtained in tables 5-7 show that there's a significant amount of flaky and elongated particle grains; the flakiness index in the gravel classes are relatively smaller in comparison with the boulder and cobble classes. A similar observation was also made by other authors, e.g. D'Aloia et al. (2019). Somehow, this noticeable large amount of such particle grains shape is also related to the excavation technique adopted, e.g rock TBM excavation .

The results given in tables 8 -10 show the shape index for each particle size class.

Table 8. Results for the shape index of each particle size fraction for sample 1.

Sample 1			
Particle size fraction class /di/Di Where Di ≤ 2di	Mass M1 [g]	Mass M2 [g]	Shape index SI % = (M2/M1) *100
100-31.5 mm	4350	1776	41%
31.5-14 mm	2170	1010	47%
14-8 mm	470	230	49%

Table 9. Results for the shape index of each particle size fraction for sample 2

Sample 2			
Particle size fraction class /di/Di Where Di ≤ 2di	Mass M1 [g]	Mass M2 [g]	Shape index SI % = (M2/M1) *100
100-31.5 mm	2399	763	32%
31.5-14 mm	1445	803	56%
14-8 mm	251	140	56%

Table 10. Results for the shape index of each particle size fraction for sample 3

Sample 3			
Particle size fraction class /di/Di Where Di ≤ 2di	Mass M1 [g]	Mass M2 [g]	Shape index SI % = (M2/M1) *100
100-31.5 mm	1990	850	43%
31.5-14 mm	1170	575	49%
14-8 mm	370	190	51%

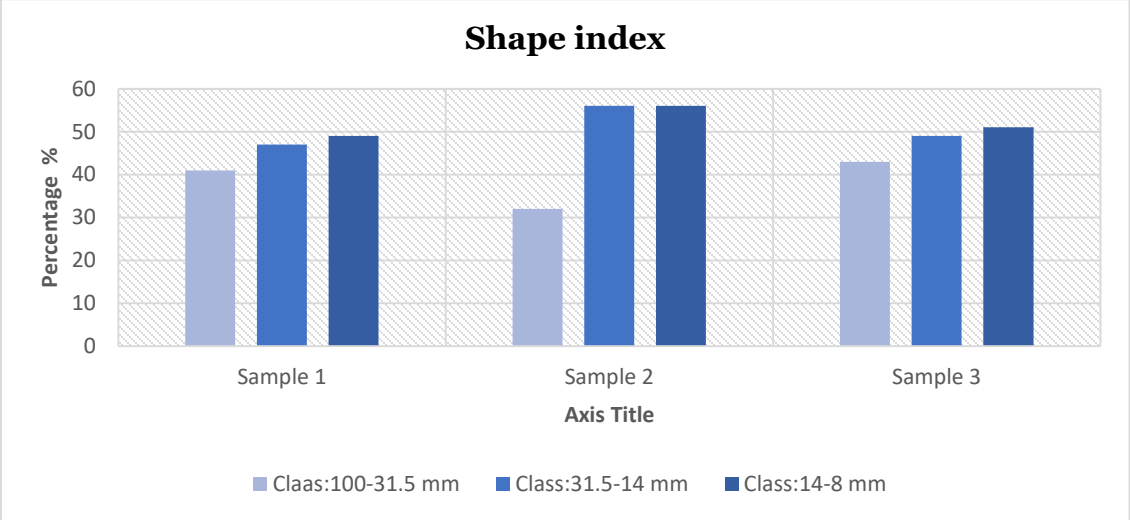

*Figure 31.G*raphical representation of the shape index

The results of the shape indexes obtained for each sample in table 8- 10 show that in the gravel classes they are relatively small in comparison with the boulder and cobble classes. These higher values are also related to the presence of a large amount of flat and elongated particle grains in the tested samples; this observation on the particle grains shape is also related to the excavation technique adopted, e.g rock TBM excavation.

2.4. 2D geometrical analysis of the TBM muck by means of sensors and cameras

2.4.1 Background review and methodology

The 2d photogrammetry techniques are considered to be more suitable for evaluating the grain size distribution of a lager quality of muck. The need to implement a photographic technique for assessing a larger quality of muck is often a must in larger underground infrastructures project. The traditional method can be very time consuming when a larger quality of the muck has to be investigated for the grain size distribution properties.

Different photographic methods for assessing the grain size distribution of a larger quality of muck (3 m^3 or more) have been studied and applied by many authors throughout these past years (Alecci, 2018; Rispoli et al., 2017; Detert & Weitbrecht, 2012 and 2014).

The method developed by Alecci (2018) involved an evaluation of a larger quality of muck by means of Image processing using MATLAB and digital photogrammetry. These techniques can be considered as time and cost saving for the evaluation of grain size distribution curve of a very larger quality of muck. In this method, the Image processing involves the application of algorithms and mathematical morphology operators using MATLAB for the evaluation of the geometrical properties of particles for assessing the granulometric distribution of the grain particles. The digital photogrammetry is mainly based on the 3d reconstruction of the sample using watershed algorithms for the classification of the grains; however, the imaging processing is considered to be more reliable for produce the grain size distribution assessment because this process encounters lesser overestimation and underestimation of the fines and coarse grains. The 3d reconstruction provided in this approach can also be used to further determine others geometrical properties of the grains (by example, shape of the particle grains).

Rispoli et al. (2017) methodology involves onsite assessment of the particle size distribution without any inference with the excavation process using photographic imaging thanks to the split desktop software. A larger quantity of muck (about 3 m^3) was investigated on a daily basis using this method; this evaluation was performed at a lesser time and lower cost.

The MATLAB based technique for an automated assessment and evaluation of the grain size distribution using top-view photograph, presented by Detert & Weitbrecht (2012, , is about an object detection and an automatic separation of the grains; this method also allows the use of a graphical interface for detection and correction of the data collected during the pre and post processing steps .Moreover, this method also provides additional parameters (the ratio of the minor axis and the major axis, the area of the grains, perimeter of the grains, the center of coordinates, and the orientation of each grain in the horizontal plane) to further characterize the materials tested .This method can give outstanding and robust results for coarse grains ; the evaluation of finer grains using this techniques is very limited. The following steps are required for the determination of the grain size distribution and properties:

- Detection of interstices using a double grayscale threshold approach, this step involves a transformation and conversion of the top view photograph in grayscale image.
- Detection of interstice using a morphological bottom-hat transformation on the grayscale image for a deeper evaluation and a further determination of the interstices.
- Determination of interstices by edge detection techniques using two gradient filtering method.
- A separation using a watershed transform, this step refers to the separation of each grain areas.
- The final step, involves the determination of the properties of each grains and other additional parameters.

Furthermore, a more sophisticated approach based also on MATLAB automatic detection by means of the BASEGRAIN software for the analysis of the grain size using top view photographs and line sampling of the materials; it was developed by the same authors (Detert & Weitbrecht, 2013). In this approach the grain size analysis is carried out following five important steps. This software provides a more efficient way to avoid over-segmentation using watershed algorithms. These techniques and methods were studied and implemented for the evaluation of the granulometric of the gravel on a river bed.

The MATLAB methodology approach using BASEGRAIN software is adopted for the processing of the data collected during this experiment.

2.4.2 Data collection

A larger amount of muck was taken, including also the 3 muck samples that were used to perform the traditional grain size distribution, flakiness index and shape index for the 2D analysis of the grain size distribution. The muck was put on the floor for this 2D experiment, as shown on the left of figure 32.

Figure 32 .The cameras, sensors and other equipment mounted on a rolling device around the muck column for the collection of the data.

Two sensors and cameras were mounted on the top of the rolling device for the collection of data.

The first sensor, SPECIM FX 17, is a hyperspectral imaging sensor with high sensitivity and detection accuracy for recording the line imaging and calibration of the colors for the identification of the materials. The sensor was connected to the software to save the data for each line recorded for every advancement. For a better accuracy in the processing; the advancement for each line imaging was about 5 mm.

The second sensor and 3 cameras were connected to the RIKOLA ltd. software for acquiring and capture of the imaging at the beginning and the end of each advancement. The second sensors was also needed for acquiring the calibrate hypercube and save the hyperbolic curved generated for each petrographic advancement step. A calibration was also done at the beginning in order to identify and correct the dark colors before the collection of the data.

Furthermore, a total station was used to track the location of the material and record the positioning and coordinates during each advancement step. Then, the prism on the top of advancement device were used to maintain the location while the advancement of each step occurred.

Figure 33.On left: the total station used for the positioning & tracking; right: the frame positions for geo-referencing (in square white paper) to be recorded by the total station for the advancement step.

2.4.3 Data Processing

The software BASEGRAIN, developed by Detert and Weibrecht (2012) and PebbleCounts algorithm, developed by Purinton and Bookhagen (2019) are used for processing the data during this experiment.

The BASEGRAIN software provides an automated evaluation of the imaging by measuring and identifying the grain geometrical properties in each photographic image of the sample. The BASEGRAIN software is based on MATLAB automatic detection; it involves a comparison of each grain to a corresponding ellipse. The necessary geometrical parameters required for the comparison are already implanted in this software.

This software can estimate the granulometric distribution of a larger sample faster than the traditional sieving method.

The Pebble Counts Auto is composed of an open-source algorithm developed in Python: the technique consists of identifying the grains through k-means algorithms where the separation of each grain particle and the geometrical parameters for the selected grains will be provided in order to assess the grain distribution of the sample. During this evaluation, a problem of over segmentation is present due to the proportion of the fines gain particles in the muck and, for these reasons, the BASEGRAIN evaluation was more appropriate for the elaboration of the grain size particle diagram.

In the BASEGRAIN, the image processing of the samples is done according to the following steps:

- Importation and geo-referencing of the data that were collected, as described previously.
- Pre-processing of the imaging, which involves some modifications like scaling/ image cropping, whenever required.
- Processing of the images for the recognition of the grains properties, then the separation of different grains is obtained by means of watershed algorithms.
- Post processing: in this stage, manually corrections can be performed whenever there's a presence of excessive segmentation from the watershed algorithms.
- Assessment of the grain size distribution, thanks to the Fehr line-sampling method.

The granulometric curves obtained using these techniques can also be compared with the grain size distributions obtained from the traditional sieving method.

Note: The three samples used in the traditional sieving method were again used in this test, in order to provide a comparison between the results obtained by both methods .This experiment shows only the granulometric results from those 3 samples.

Figure 34. Sample 1: 2D photographic image after pre-processing

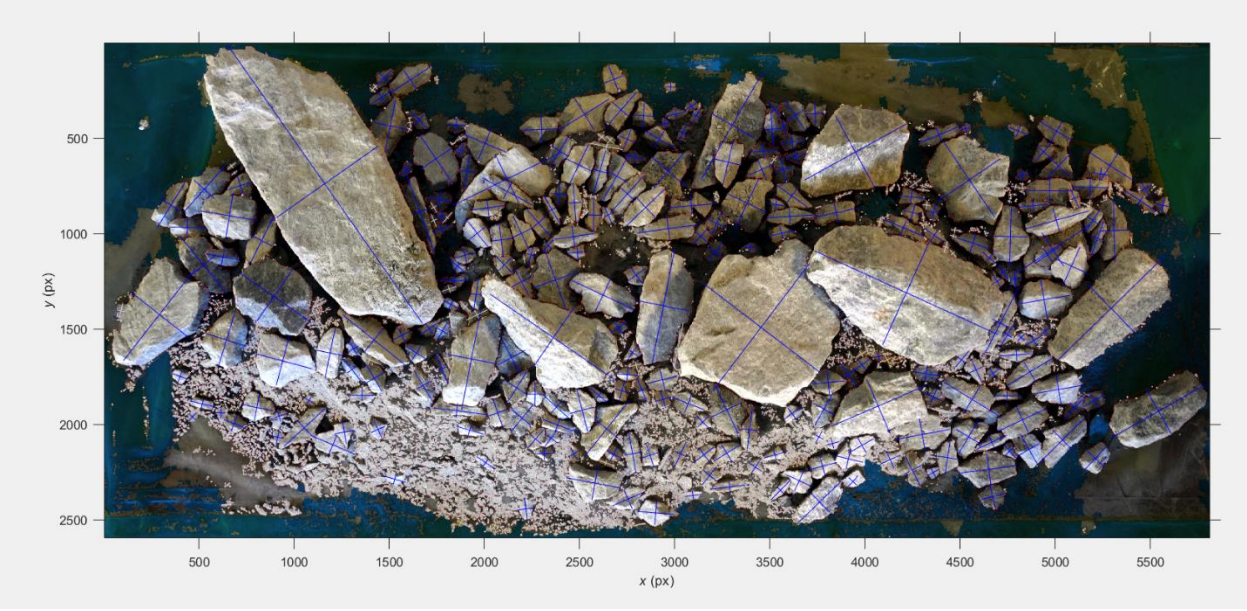

Figure 35. Sample 1: 2D processing photographic image after post-processing for the final detection of the grain size and other geometrical parameters

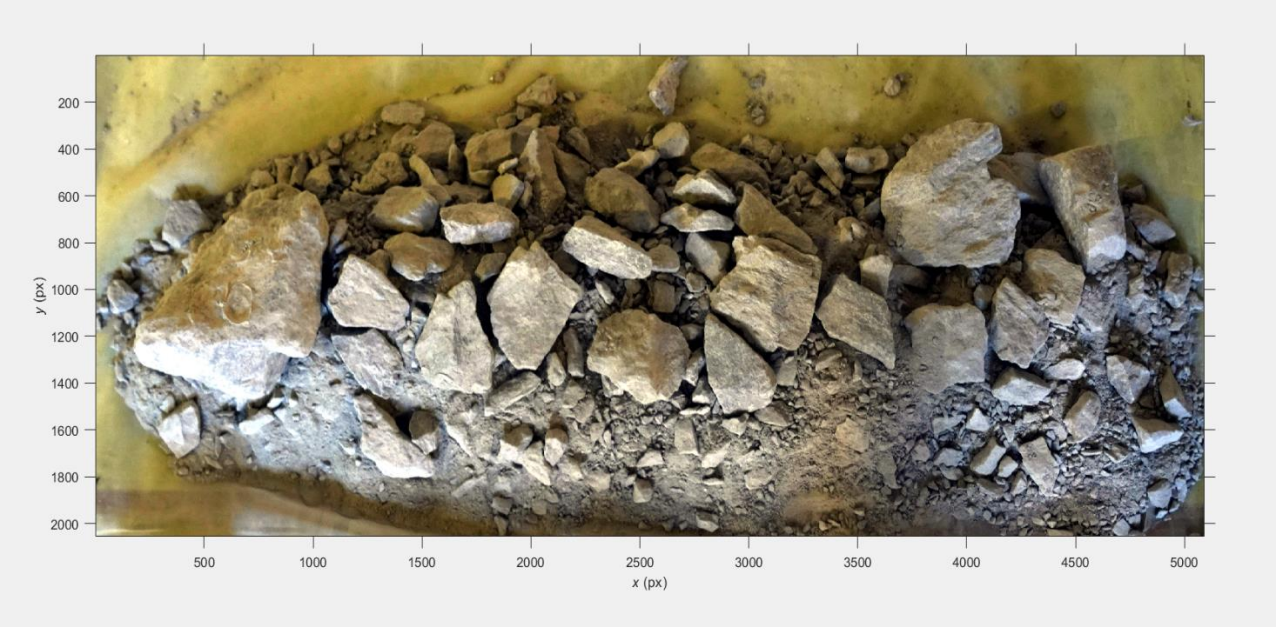

Figure 36.Sample 2: 2D photographic image after pre-processing

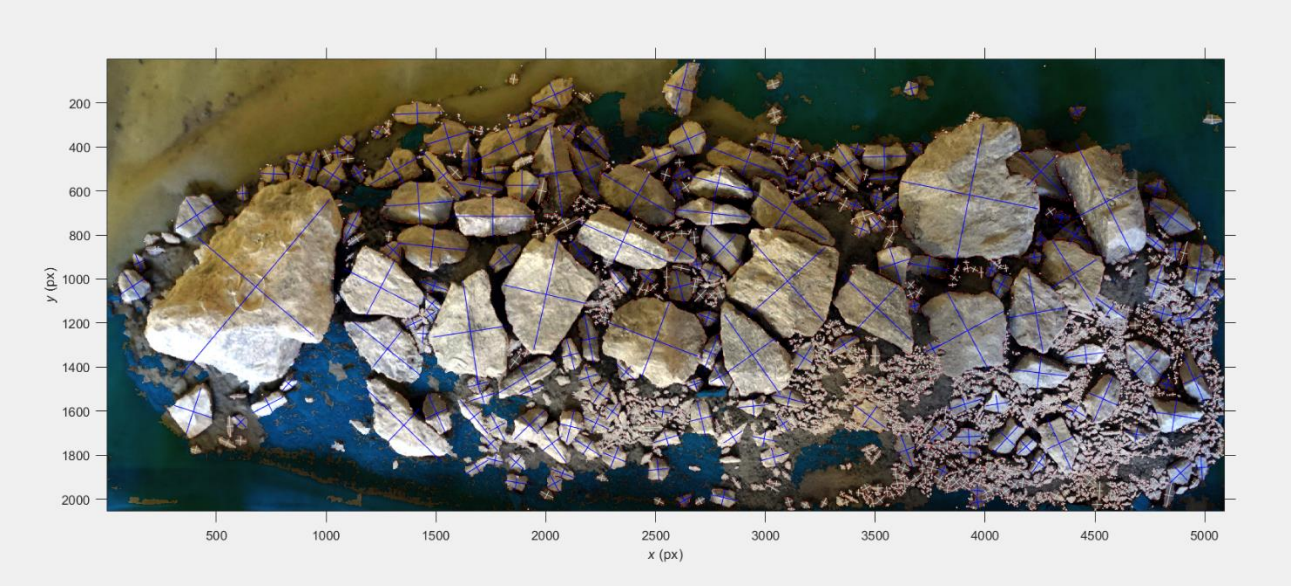

Figure 37.Sample 2: 2D processing photographic image after post-processing for the final detection of the grain size and other geometrical parameters

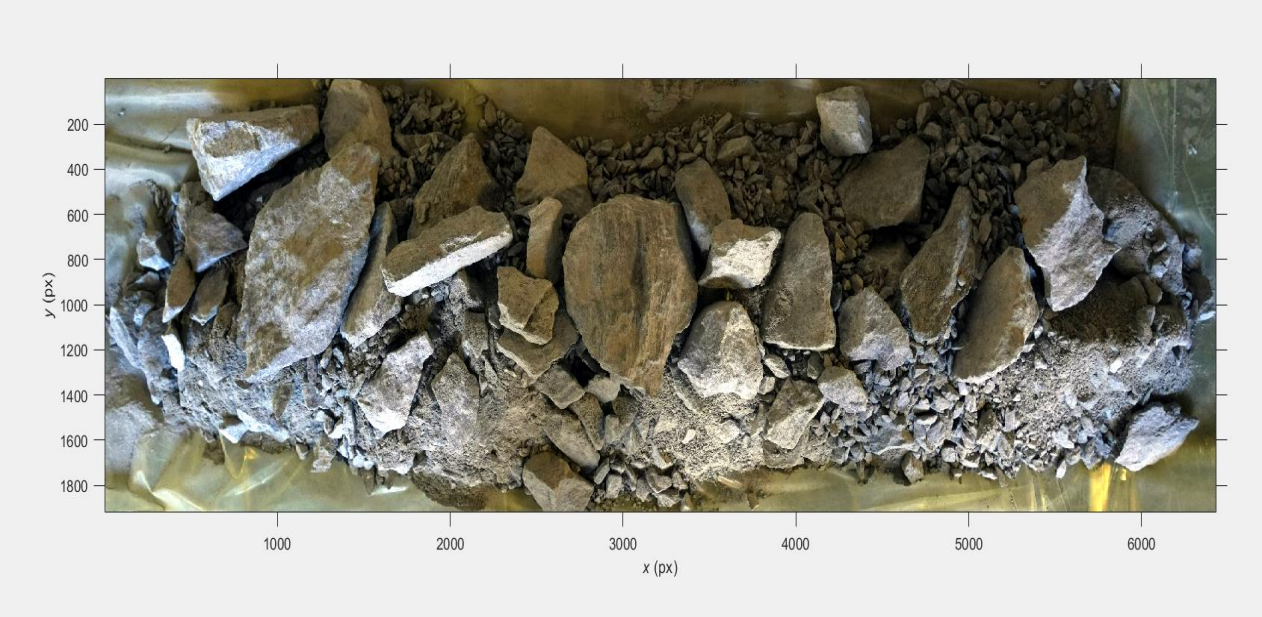

Figure 38.Sample 3: 2D photographic image after pre-processing.

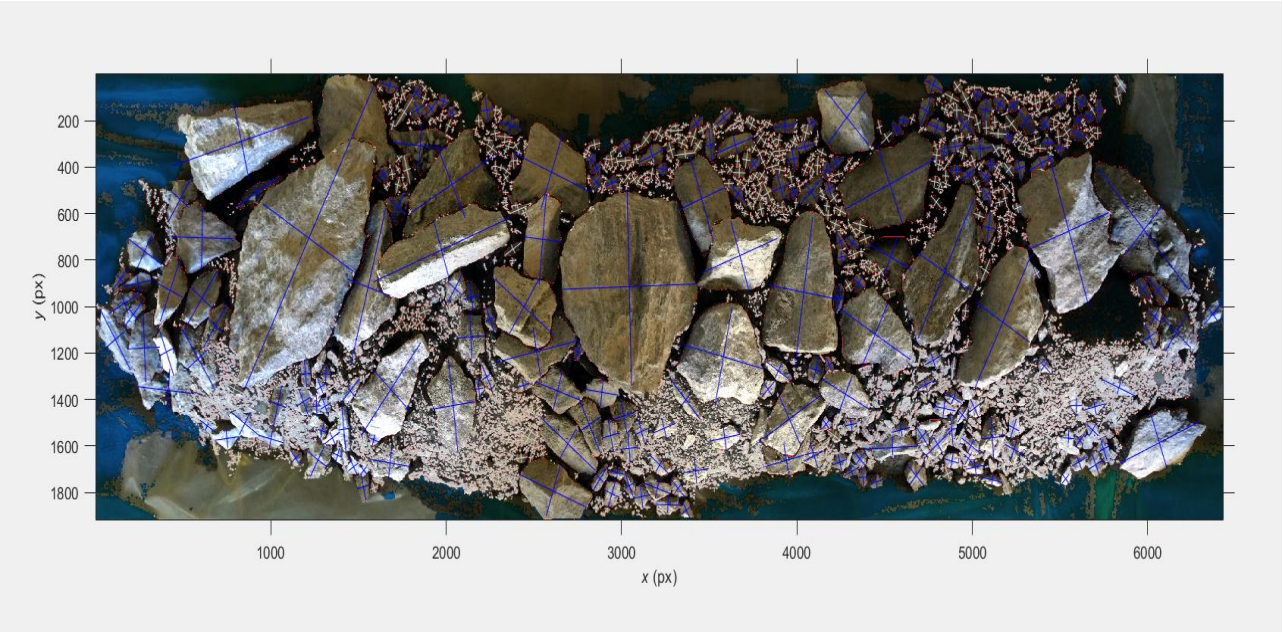

Figure 39.Sample 3: 2D processing photographic image after post-processing for the final detection of the grain size and other geometrical parameters

The straight lines (in blue color) represent the axis of ellipses for the fitting of each object using normalized second central moments of the object areas processed

2.4.4 Test results

2.4.4.1 Grain size distribution results and discussion

The results obtained in terms of grain size distribution are shown in figures 40-43. The estimation of fines and the pre-estimation of the percentage of non-detected fines from over segmentation are respectively evaluated, then represented on the grading curves. The reference data from in-situ line sampling are combined with the automated photo analysis for producing the final photo analysis and grading curves. Moreover, some others parameters (d_{30}, d_m, d_{90} and p_i) are represented to further characterize the materials. The BASEGRAIN software couldn't give a proper representation of the finer particle grains due to a problem of overestimation; further improvements were performed in order to have an adequate representation of the finer particles. This software is more efficient for the evaluation of the coarse grain size particles.

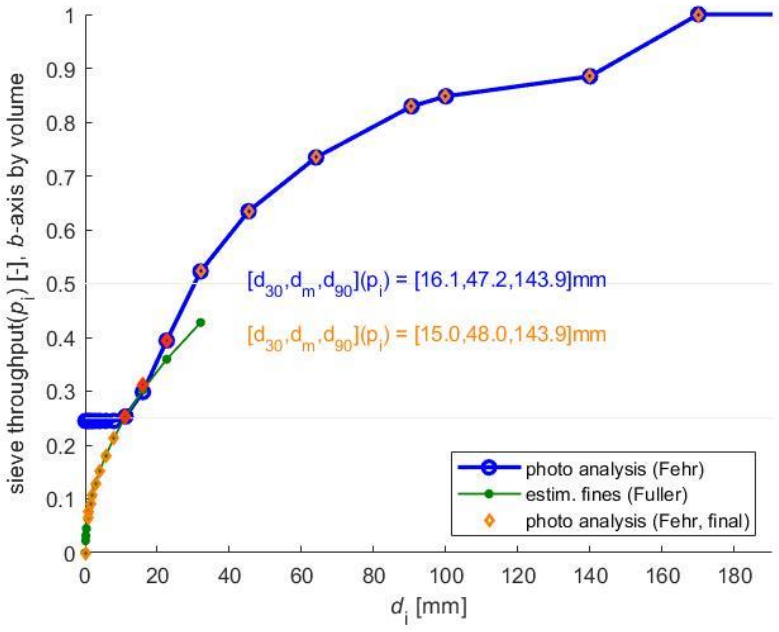

Figure 40.Sample 1: BASEGRAIN software grading curve of the tested material resulting from automatic photo analysis of image using Fehr's parameters.

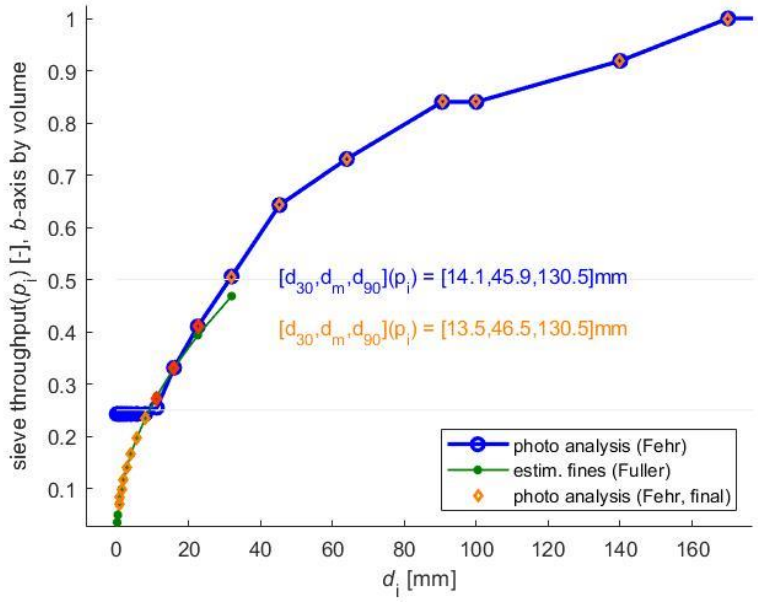

Figure 41.Sample 2: BASEGRAIN software grading curve of the tested material resulting from automatic photo analysis of image using Fehr's parameters.

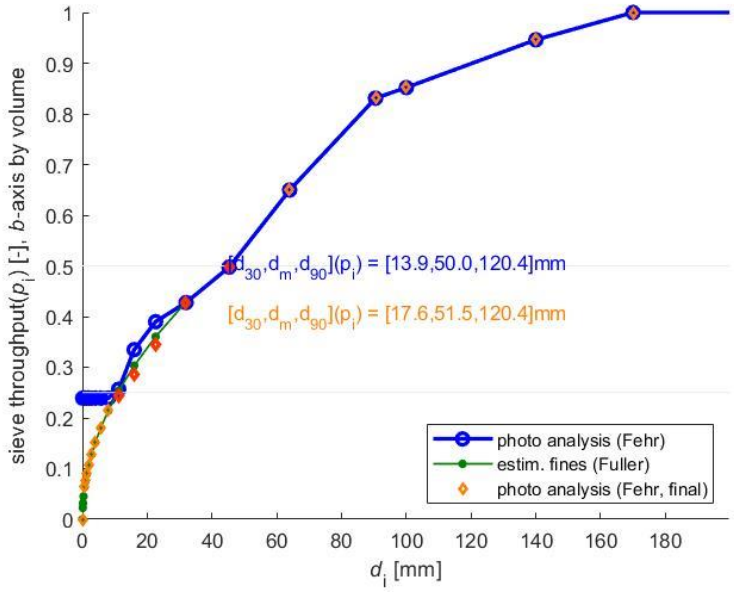

Figure 42.Sample 3: BASEGRAIN software grading curve of the tested material resulting from automatic photo analysis of image using Fehr's parameters.

Table 11.BASEGRAIN software Data used to produce the grain size distribution curves

di: size in mm	Sample 1			Sample 2			Sample 3		
	Photo analysis data	*Data for estimation of the fines*	*Photo analysis & fines estim. Cum %*	*Photo analysis data*	*Data for estimation of the fines*	*Photo analysis & fines estim. Cum %*	*Photo analysis data*	*Data for estimation of the fines*	*Photo analysis & fines estim. Cum %*
0.088	0.245	0.022	2.2	0.242	0.025	2.46	0.239	0.022	2.25
0.177	0.245	0.032	3.2	0.242	0.035	3.48	0.239	0.032	3.19
0.354	0.245	0.045	4.5	0.242	0.049	4.92	0.239	0.045	4.51
0.707	0.245	0.064	6.4	0.242	0.070	6.96	0.239	0.064	6.37
1.000	0.245	0.076	7.6	0.242	0.083	8.28	0.239	0.076	7.58
1.410	0.245	0.090	9.0	0.242	0.098	9.83	0.239	0.090	9.00
2.000	0.245	0.107	10.7	0.242	0.117	11.70	0.239	0.107	10.72
2.830	0.245	0.127	12.7	0.242	0.139	13.92	0.239	0.128	12.75
4.000	0.245	0.151	15.1	0.242	0.166	16.55	0.239	0.152	15.16
5.660	0.245	0.180	18.0	0.242	0.197	19.69	0.239	0.180	18.04
8.000	0.245	0.214	21.4	0.242	0.234	23.41	0.239	0.214	21.44
11.200	0.253	0.253	25.3	0.255	0.277	27.27	0.257	0.254	24.29
16.000	0.299	0.302	31.3	0.331	0.331	33.06	0.335	0.303	28.55
22.600	0.394	0.359	39.4	0.410	0.393	41.02	0.390	0.360	34.41
32.000	0.523	0.428	52.3	0.506	0.468	50.58	0.428	0.429	42.77
45.300	0.634	0.509	63.4	0.643	0.557	64.25	0.497	0.510	49.74
64.000	0.734	0.605	73.4	0.731	0.662	73.09	0.650	0.606	64.97
90.500	0.829	0.719	82.9	0.840	0.787	84.01	0.831	0.721	83.09
100.00	0.848	0.756	84.8	0.840	0.828	84.01	0.852	0.758	85.19
140.00	0.885	0.894	88.5	0.919	0.979	91.86	0.946	0.897	94.62
170.00	1.000	0.986	100.0	1.000	1.079	100.00	1.000	0.988	100.00

The results given in table 11 can be used to produce the grain size distribution curves for the cumulative passing percentage. Additionally, figures 43- 46 provide comparisons among the grain size distribution curves obtained using both methods (2 D photographic and traditional sieving method).

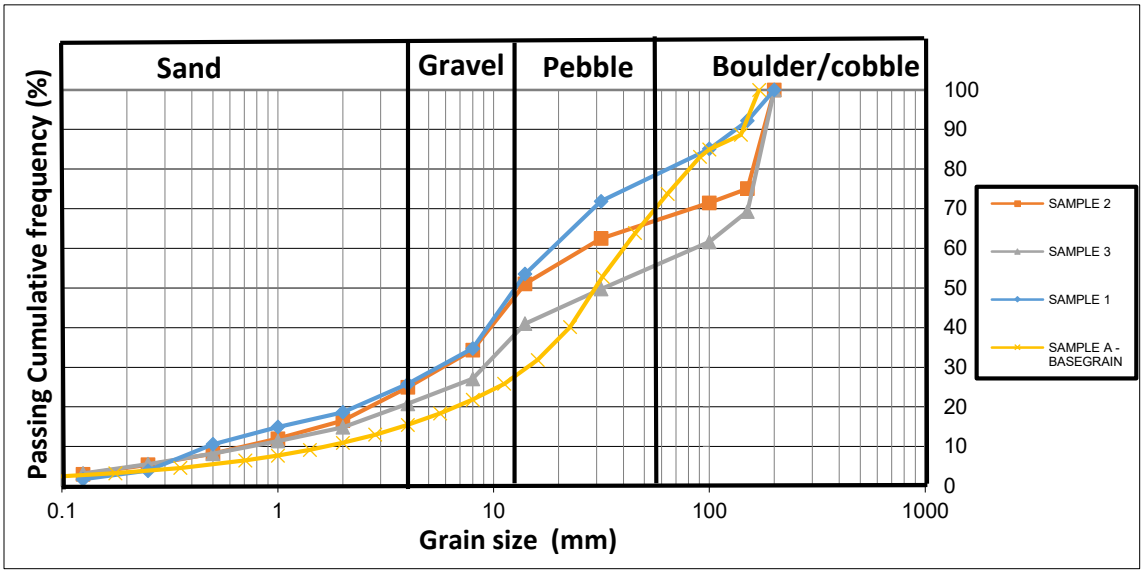

Figure 43.Comparison between the grain size distribution curves obtained with the traditional sieving method and the BASEGRAIN grain size distribution curve for sample 1

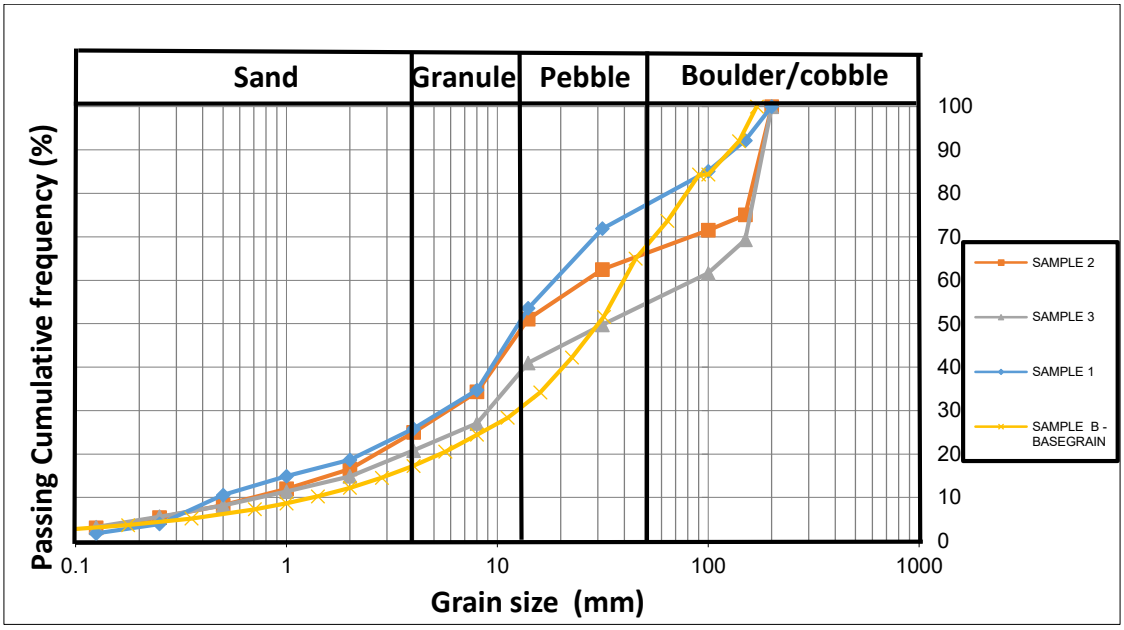

Figure 44.Comparison between the grain size distribution curves obtained with the traditional sieving method and the BASEGRAIN grain size distribution curve for sample 2

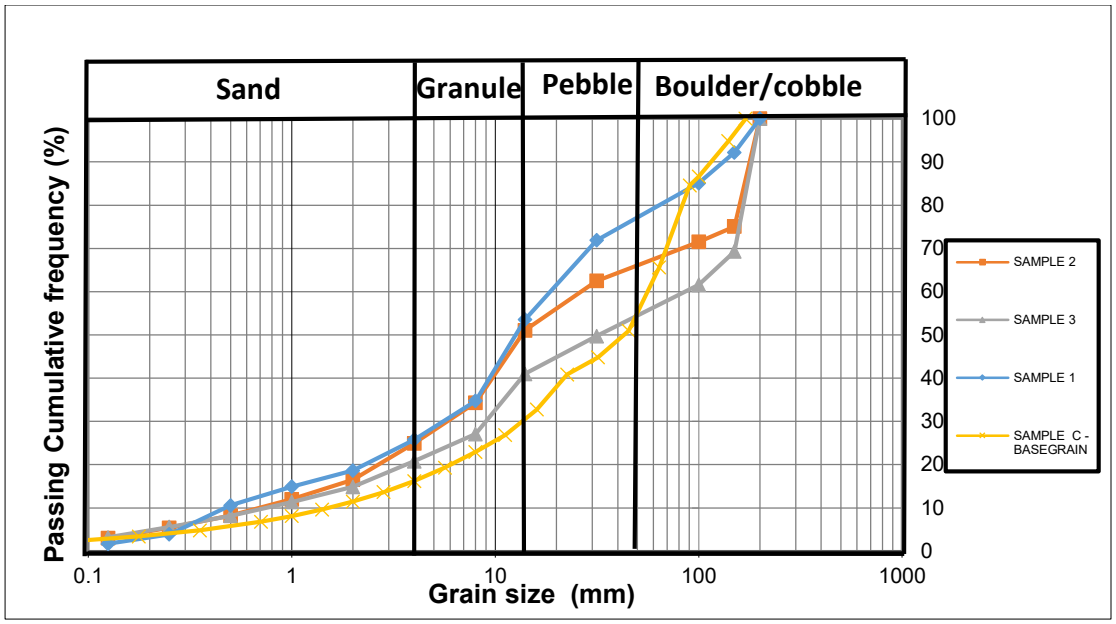

Figure 45.Comparison between the grain size distribution curves obtained with the traditional sieving method and the BASEGRAIN grain size distribution curve for sample 3

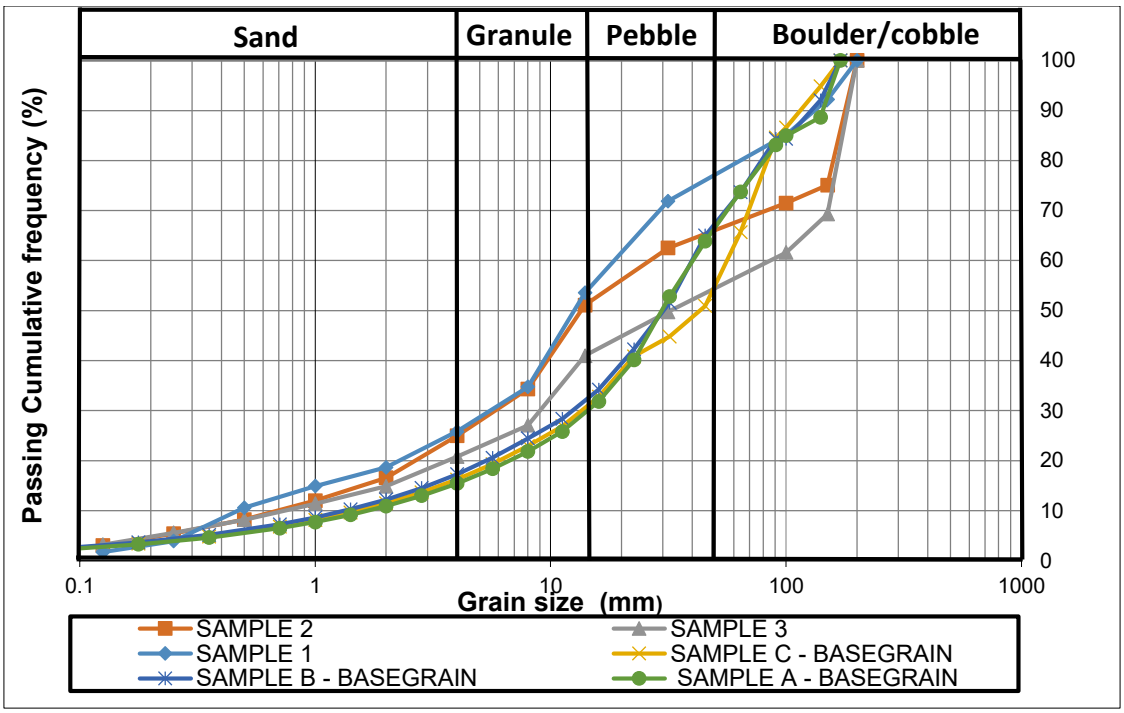

Figure 46.Comparison between the grain size distribution curves obtained with the traditional sieving method and the BASEGRAIN grain size distribution curves

The grain size distribution curves given in figure 46 and obtained using both methods are relatively alike. The grain size results obtained using the 2D photographic methodology show that the larger amount of particle grains size are also categorized as gravel (granule and pebble). Both methods (2D photographic methodology and conventional sieving method) used to evaluate the grain size have approximately produced comparable results.

2.4.4.2 Particle shape: elongation index results and discussion

In accordance with the **BS 812-105.2: 1990** (Methods for the determination of the particle shape — Section 105.2 referring to the Elongation index of coarse aggregate), the elongation index is the length of particle grains more than **1.8 times** of their mean sieve size; this index is expressed in percentage i.e. a particle grain is characterized as ''elongated'' when its length **L** is more than **1.8 times** the middle size **B**. Using the software output data for each particle grain detected during the photographic image processing; the **l/b** ratio of grains is calculated on an average basis for each particle sieve classes. The results of the average elongation ratio for each class is shown in table 12.

Table 12. Elongation values for coarse aggregates

Granulometric class	Average elongation ratio		
	SAMPLE 1	SAMPLE 2	SAMPLE 3
>200 mm	2.2	1.5	2.5
200-150 mm	1.8	-	-
150-100 mm	1.9	1.6	2.0
100-31.5 mm	2.0	1.9	1.9
31.5-14 mm	1.5	1.6	1.5
14-8 mm	1.2	1.2	1.1

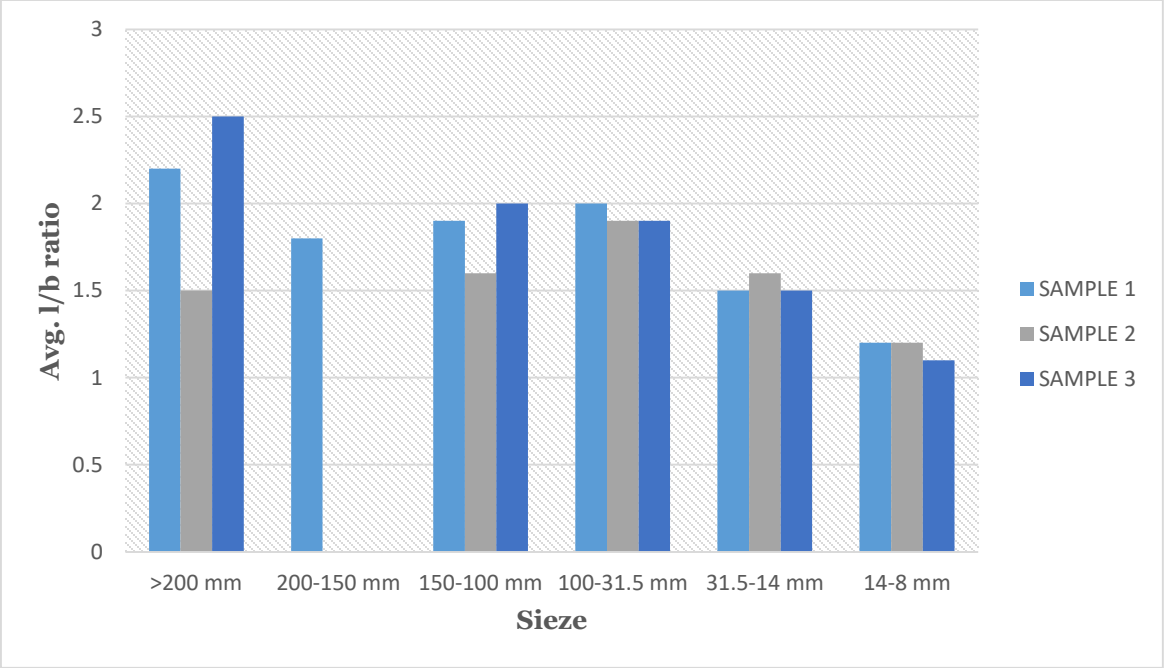

Figure 47.Graphical representation of the elongation results

The results obtained for the shape particle show that the flakiness and shape index were higher for the boulder/cobble particles in comparison to the gravel particles. The same observation is also present for the elongation ratio; the elongation ratios are higher for the boulder particles in comparison to the gravel particles. Somehow, these comparisons show that the muck index are related to each other for the purpose of characterizing and describing the particle shape.

3. Correlations among TBM parameters, rock mass properties and size of the chips tested.

3.1. Background review and discussion

Recently many authors have studied and found that there are significant relationships between the TBM parameters and size of the muck depending on the rockmass properties (Cardu et al., 2021; Heydari et al. ,2019; Rispoli et al., 2017; Xia et al., 2017; Abu Bakar et al., 2014; etc.). These relationships are not only important for making the assessment or for predicting the TBM performance, but also to have an understanding of the size and shape of muck produced during the excavation process; in order to establish such correlations, a set of data about the properties of the rock mass i.e. RMR, GSI, strength and joints properties encounter for each boring cycle or a certain advancement length, the muck parameters and the TBM parameters & characteristics that were used during the excavation of the muck tested are required. Furthermore, they can also be compared or evaluated in laboratory using linear rock-cutting machine (LCM) or the intermediate linear cutting machine (ILCM).

The quality of the muck produced can be another indicator for estimating or regulating the TBM operational parameters, while the machine is excavating; when observing the muck passing through the conveyor belt of the machine, we can somehow judge by the quality of the muck produced if the operations are well fitted for the ongoing excavation process. The properties of the rock can't be changed but the parameters of the machine are controllable. The lasted model of hard rock TBM, i.e. double shield, as previously mentioned, can also be equipped with advanced technology to study the properties of the rock ahead of the face of the tunnel; the chips size and shape produced can also be a good indicator of the rockmass properties.

Moreover, according Yin et al. 2014, the onsite stress on the tunnel face can also have an impact on rock mass boreability and chipping efficiency. This effect can easy the failure of the rock, it occurs when the stress on the face are high enough; thus the rock boreability index can considerably decrease. Villeneuve et al. (2017) also stated that the strength of the rockmass can be a good parameter for evaluating and controlling the thrust force

required by the disk cutters for the chipping and the penetration; the net thrust force applied can also be consider as a good indicator for chipping mechanism efficiency and the performance of the TBM during the excavation process.

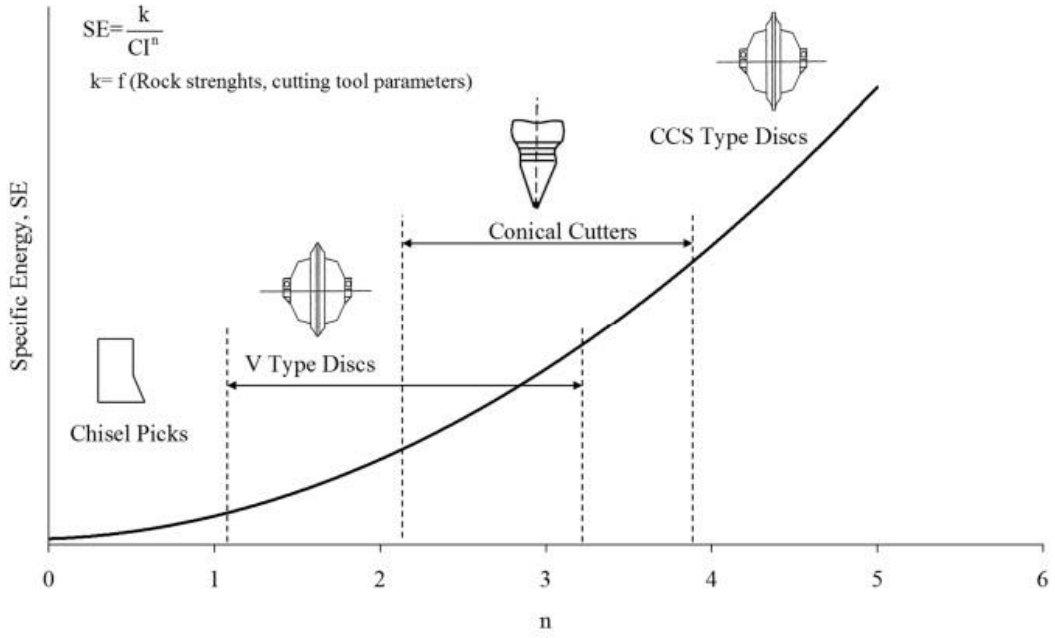

Figure 48. The efficiency of the boring process based on the fragment size and also a correlation among SE, CI and type of tools (Bond and Rittinger law)

The muck can be characterized by some parameters, like the coarseness index, the absolute grain size from the Rosin-Rammler Diagram, or also by the coefficient of curvature and uniformity for its evaluation and comparison with TBM parameters and rockmass properties.

Many past investigations and studies have shown that the coarseness index CI can be a good indicator of the cutting efficiency; an increase in cutting spacing or penetration can produce large and finer particle size depending on specific energy SE and rockmass properties i.e. the present of fractures in the rockmass can considerably affect the chips size. The specific energy SE decreases with increasing of the coarseness index CI (Tuncdemir et al., 2008) and CI follows an inverse trend with respect to SE; thus the

muck size and shape are good indicators for the efficiency of the rock chipping process on the tunnel face (Heydari et al., 2018).

The rock cutting efficiency correlation with the muck parameters (i.e. the absolute grain size and the coarseness index) shows that there's a strong relationship among the specific energy, the absolute grain size and the coarseness index CI; thus these muck parameters increase when the specific energy decreases (Abu Bakar et al. 2012).

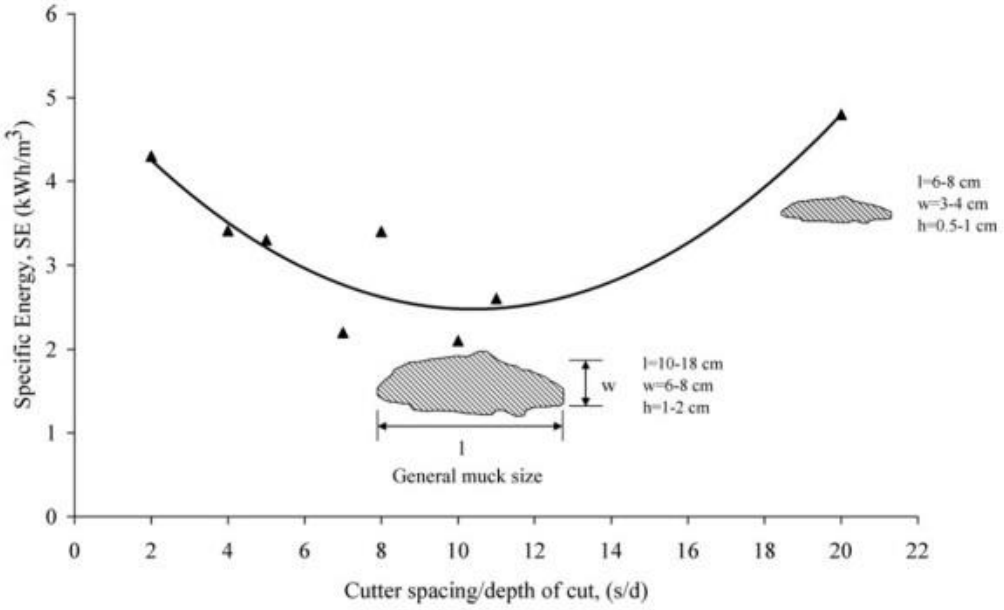

Figure 49.Shows the influence of spacing and penetration depth (s/d) ratio on the specific energy SE (Tuncdemir et al., 2008)

Biichi et al., 1994 found that the chip thickness increases by 60% when the cutter spacing between tools is increased by about 50%.

Rispoli et al., 2017 provide an investigation based on a petrographic analysis for analyzing the muck size distribution, and the relationships among the onsite machine parameters collected during the excavation process (e.g. FN, RPM, ROP, FPI, Torque SE), the rockmass properties (discontinuities and joints in the rockmass, strength) and muck parameters (coarseness CI) for its characterization. The results show a significant

relationship between the FPI and SE with respect to the coarseness CI, but no strong relationship between the ROP and CI was found; this can be also due to the presence of discontinuities i.e. fractures in the rockmass; and also the same occurs with the rockmass properties: no strong relationships were found between the CI and the rockmass properties.

To conclude, based on the past studies and literatures, the muck size and shape are clearly related to the efficiency of the cutting process and to the onsite properties of the rockmass encountered during the excavation (fractures in the rock mass, joint spacing, etc.); the efficiency of the cutting process also depends on the TBM operational parameters applied, based on the rockmass properties.

3.2 Evaluation of the parameters

3.2.1. Muck parameters

In accordance with the investigation carried out previously, the muck can be represented by some parameters in order to further characterize them and evaluate their comparisons.

The absolute grain size (d, d') from Rosin-Rammler equation is a specific parameter for the grain sizing at which about 36.8 % weight of material is retained. This parameter can also be used to verify whether the material tested is fine or coarse. The Rosin – Rammler equation $R\ (d)$ is a well-known distribution in mining and cement industry.

$$\boldsymbol{R\ (d) = 100\ \exp((-\frac{d}{d'}))^{n}}$$

where:

R (d) is the cumulative percentage of material retained on the sieve;

n is the uniformity index

The Rosin Rammler diagram, as shown in figure 28, is obtained from MATLAB using the same data (sieves size and retained percentage of materials) from the traditional sieving method.

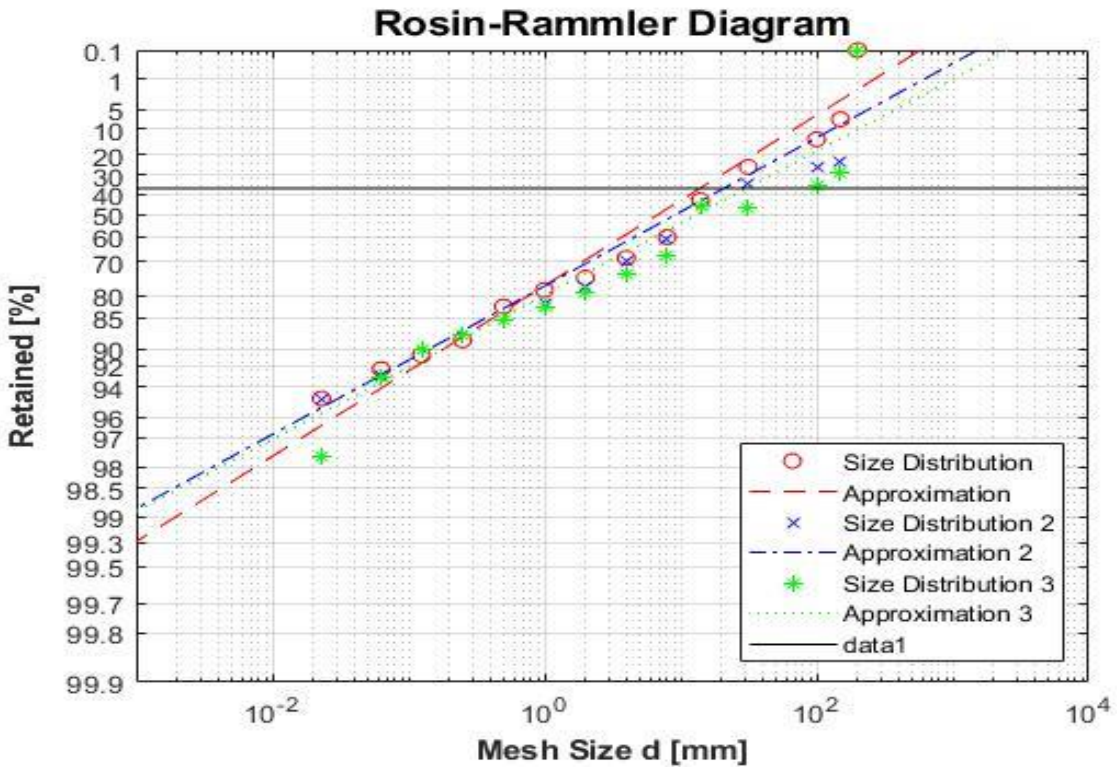

Figure 50.The Rosin-Rammler diagram: the grain size distribution and approximation of the 3 samples for the evaluation of the absolute grain size

The muck grain size distribution can also be represented by a non-dimensional number called **'coarseness index' CI**, which is defined as the sum of the cumulative mass (%) of the muck retained on every particle size sieve.

The Coarseness index (CI) and the absolute grain size are somehow related to the specific energy required for the cut and, therefore, the production rate and instantaneous cutting rate (ICR) can also be used as indicators for the evaluation of the TBM performance (Abu Bakar et al., 2014).

Table 13. The coarseness index and the absolute grain size values

Muck parameters	Sample 1	Sample 2	Sample 3
Coarseness index (CI)	404.77	414.19	421.08
Absolute grain size	17.1 mm	26.5 mm	34.57 mm

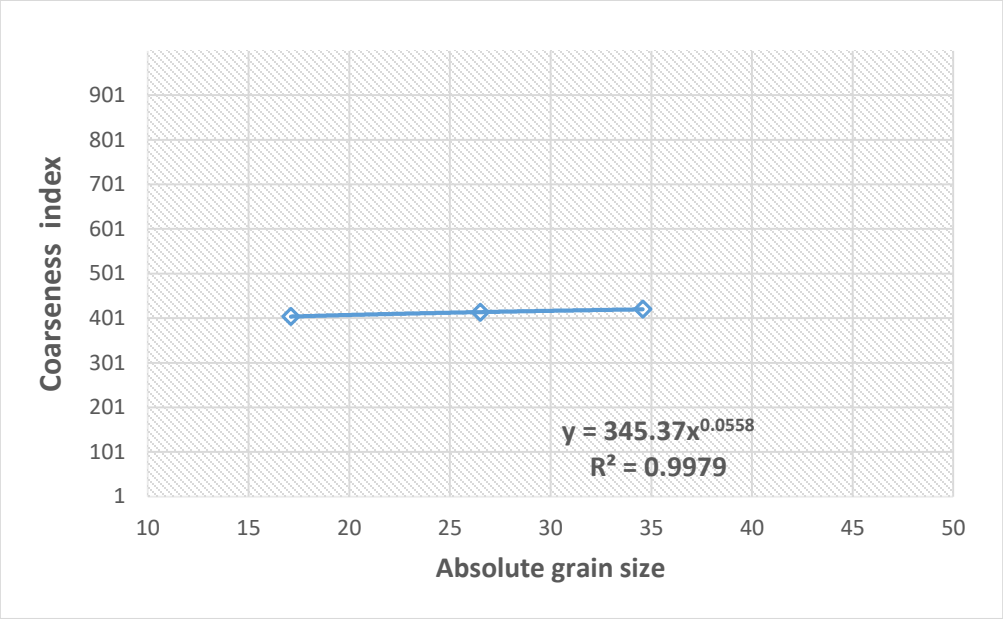

Figure 51. Relationship between the coarseness index and the absolute grain size

Figure 51 shows that there is a linear relationship between the coarseness index and the absolute grain size, with a correlation coefficient R^2=0.99.

3.2.2. Rock parameters

The discontinuities, the rockmass quality and the rockmass strength can be investigated using geotechnical classification systems, i.e. rock mass rating (RMR) by Bieniawski (1973) or geological strength index (GSI) by Hoek (1994). Generally, the GSI is estimated by means of charts provided by Hoek and field observations/tests of the rock mass conditions, e.g. fractures and/or discontinuities in the rockmass. The RMR is the most used classification in rock engineering and tunneling; its modification RMR89 is usually preferable. The RMR/ RMR89 can be evaluated using the following parameters:

- A: strength of the intact Rock: Uniaxial compressive strength (UCS)/the Brazilian tensile strength (BTS) and point load test can also be performed.
- B: Rock quality designation, RQD
- C: Average joint spacing
- D: Joint wall conditions (J_c)
- E: Ground water condition (dry and wet).

As suggested by many authors (Somodi et al., 2021; Hoek et al., 2013; Vasarhelyi et al, 2016) the relationship between these classification systems (Rock Mass Rating/RMR89 and the GSI) can be obtained using the following formula:

- $GSI = RMR89 - 5 \text{ for } RMR89 > 23$

RMR89 is calculated through the following formula:

$$RMR89 = A1 + B2 + C3 + D4 + E5$$

- $GSI = 0.5\,RQD + 1.5\,J_c$

Table 14.Rock mass rating by Bieniawski (1973).

Value	Rock quality
RMR:81-100	Very good
RMR:61-80	Good
RMR:41-60	Fair
RMR:21-40	Poor
RMR<21	Very poor

Referring to the past studies and data (Rispoli et al., 2020), the rock formation under exam was characterized as a massive rock, with RMR and GSI average values over 70 in the AMC complex and lesser than 60 in the CLR. The general average of RMR was between 80 and 40.

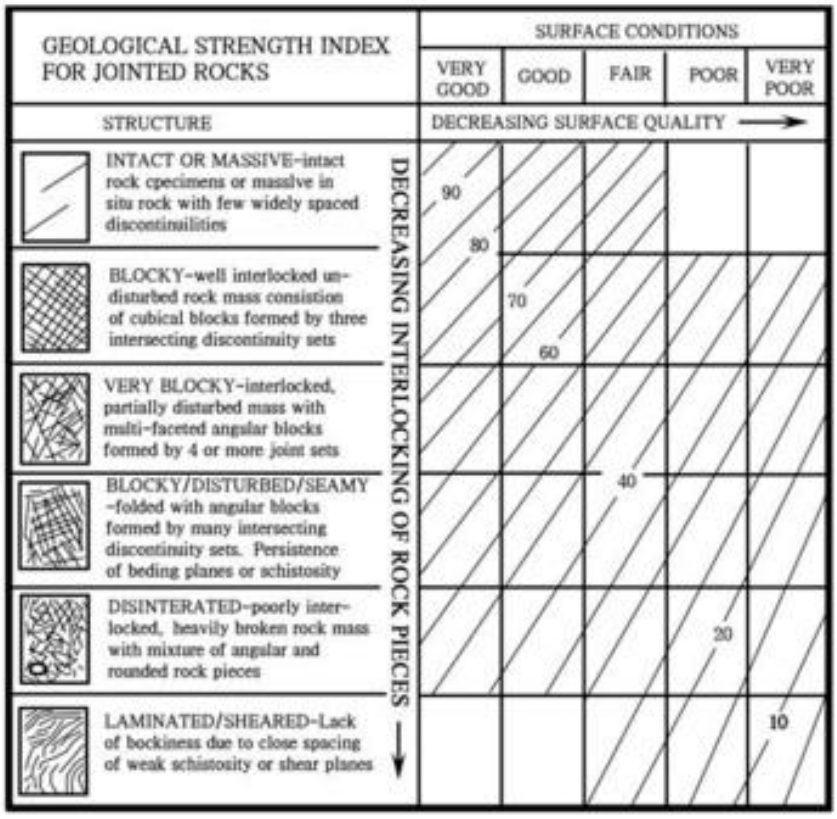

Figure 52.Chart for determining the geological strength index (GSI) value of a jointed rock mass (Hoek, 1994)

3.2.3. TBM parameters

The main TBM parameters can be provided by the manufacturing company as shown in table 10, and the main TBM data (penetration rate, cutter head rotational speed, torque, normal force) related to its performance during the excavation process or advancement has to be recorded for each boring cycle. They can also be estimated by predictive models for the evaluation of the penetration, when all data required about the machine and rockmass properties are available.

Table 15. Some of the most important parameters required for the correlation among the TBM parameters, muck and rockmass properties.

Rock mass properties	Unit	Muck parameters	Unit	TBM parameters	Unit
Geological Strength index (GSI)	-	Absolute grain size	-	Normal force (FN)	kN
Rock Mass Rating (RMR)	-	Coefficient f curvature (CC)	-	Cutterhead rotational speed (RPM)	rev/min
Joint spacing (js)	mm	Coefficient of uniformity(Cu)	-	Rate of penetration (ROP)	mm/rev
Uniaxial compressive strength (UCS)	MPa	Coarseness index (CI)	-	Field penetration index (FPI)	kN/min
Brazilian tensile strength (BTS)	Mpa	Mean grain size	mm	Torque	kN-m
Rock quality designation				Specific energy (SE)	MJ/m^3

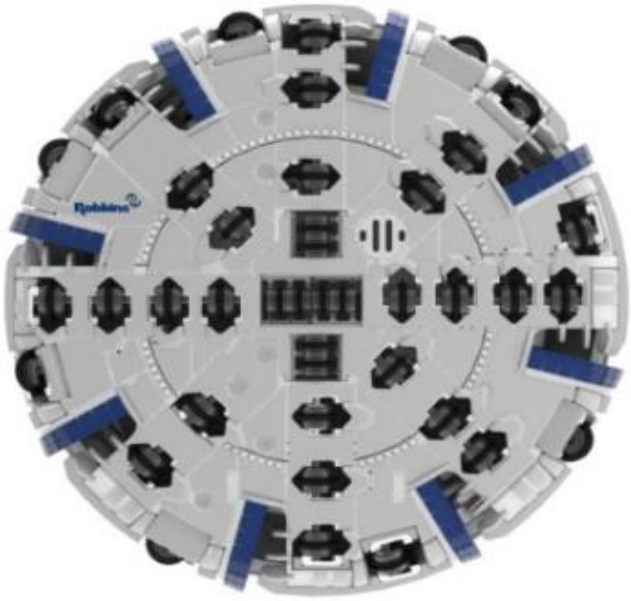

Figure 53. Hard rock TBM disk cutters mounted on the cutterhead (Robbins Company)

Table 16. Main characteristics of the Robbins TBM (''Main Beam'' Gripper TBM) used for perform the excavation at the Maddalena exploratory tunnel (Rispoli et al., 2017)

TBM diameter	6.3 m
Cutterhead Thrust	12800 kN
Machine thrust	13700 kN
Cutterhead power	2203 kW
Cutterhead torque	2083 kN-M
Cutterhead speed	0-11 rpm
Thrust cylinder stroke	1830 mm
Number of main thrust cylinders	4
Gripper total force	36400 kN
Numbers off disk cutters	43 (2 for overcutting)
Disk cutters size	432 mm
Average cutter spacing	77 mm

Furthermore, a preliminary evaluation of the penetration rate can be done following the NTNU approach on the basis of the previous studies and excavation performed in the same type of rock formations with similar TBM characteristics. According to Cardu et al. and Rispoli et al. (2020), based on Theoretical and Experimental Laboratory Tests with the intermediate linear cutting machine (ILCM) and also the hard TBM performance prediction investigations carried out the Maddalena pilot tunnel and the Mont Cenis Base Tunnel, the rock mass rating RMR was estimated to be on average between **40 and 80**; the joint spacing was ranging from **0.5 to 1.2 m**. and for the uniaxial compressive strength was on average **85 MPa**, with a minimum value of **48 Mpa** and max. value of **125 MPa**. The schistosity was on average oriented towards North and East-South East with an inclination from **10 to 50** degrees. Schistosity refers to the mode of foliation that can occur particularly in a metamorphic rock. It has been estimated to be between a range of **5 to 10 cm**.

3.3. NTNU penetration rate and net advancement evaluation

The prediction of the penetration rate and net advancement can be evaluated on the basis of TBM characteristics provided and the rock mass properties estimated, following the steps below:

- **Determination of the fracture class**

It's an evaluation based on the max. spacing between the weak planes with the estimated schistosity value; the corresponding fracture Class can be obtained from table 14.

Table 17.Fractures class (Bruland, 1998)

Fracture class (Joints:Sp/fissures:St)	Distance between Planes of weakness
0	-
0-I	160
I-	80
I	40
II	20
III	10
IV	5

- **Calculation of the angle between the discontinuities and the tunnel axis**

It can be calculated from the equation: $\propto = \boldsymbol{arc}\ \mathbf{sin}(\mathbf{sin}\ \boldsymbol{\alpha_f}\ .\mathbf{sin}(\boldsymbol{\alpha_t} - \boldsymbol{\alpha_s})$

where:

$\propto$: The smallest angle between discontinuities and tunnel

α_f : The dip

α_t : The tunnel axis

α_s : The strike

- **The Fracturing Factor, Ks**

It can be obtained graphically, by plotting the $\propto$ angle obtained with respect to the fracture class.

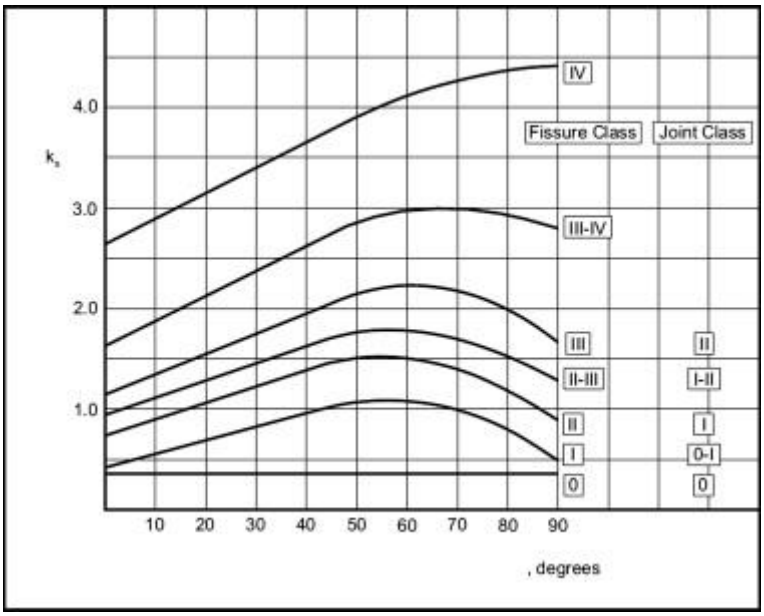

Figure 54.Graph for the determination of the fracturing factor (Bruland, 1998)

- **The determination of the Drilling Rate Index, DRI, and the correction factor, K_{DRI}**

It can be obtained from the geotechnical and geo-mechanical tests carried out, the survey data can be used in this evaluation. These values, as well as DRI, can be read graphically and then plotted on the graph in order to obtain K_{DRI}.

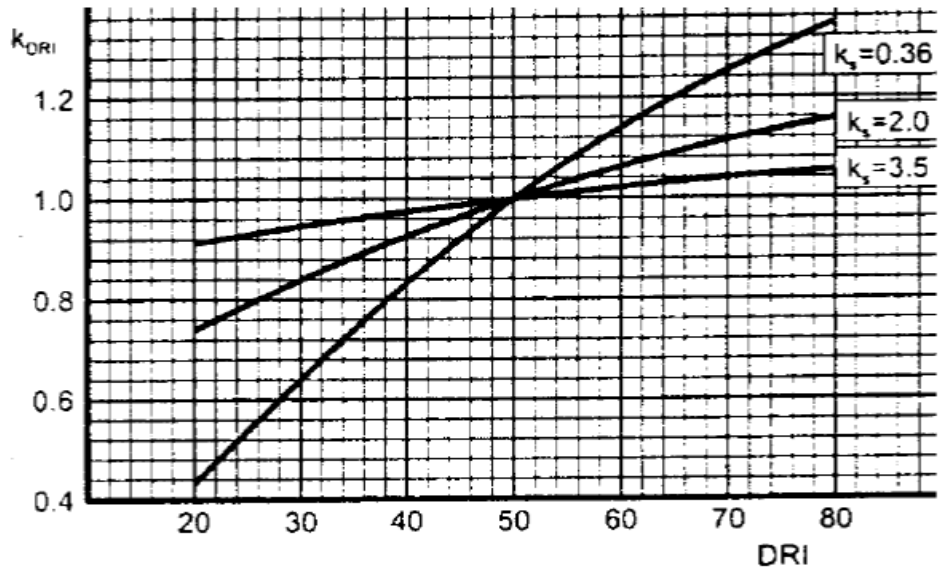

*Figure 55.*Graph for the determination of the correction factor *(Bruland, 1998)*

- **Correction factor for cutting diameter Kd**

For the Kd value, the diameter of the disk cutters are required. By plotting this value on the given graph, the Kd value can be obtained.

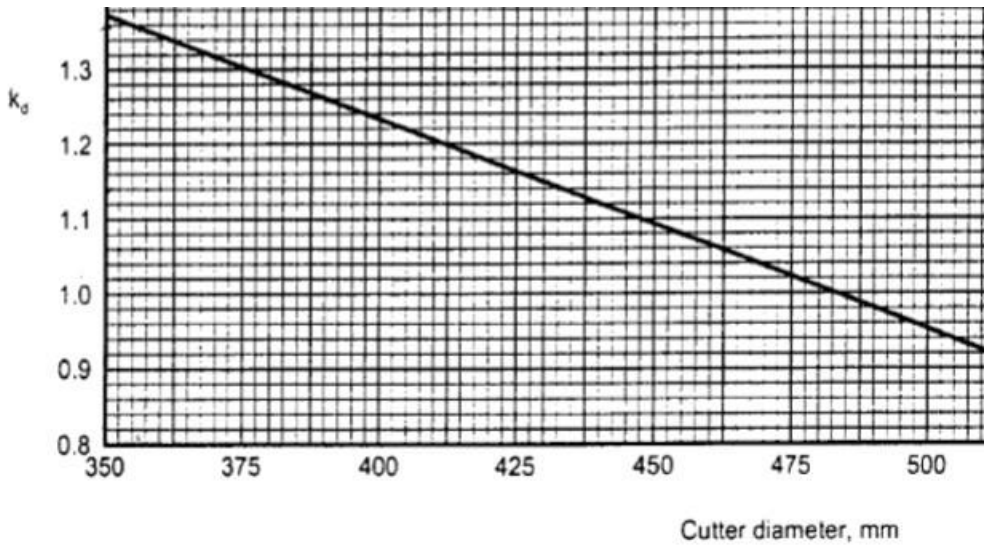

*Figure 56.*Graph for the determination of *the correction factor for cutting diameter (Bruland, 1998)*

- **Correction factor for average cutting spacing K_a**

The average cutter spacing is a function of the cutter-head diameter and the number of disk cutters. Based on the diameter and number of the tools, the spacing can be calculated by the following formula: $\boldsymbol{S = \frac{Dtbm}{2*Ntools} * 1000}$

By substitution; once the spacing is known, the factor K_a can be obtained graphically.

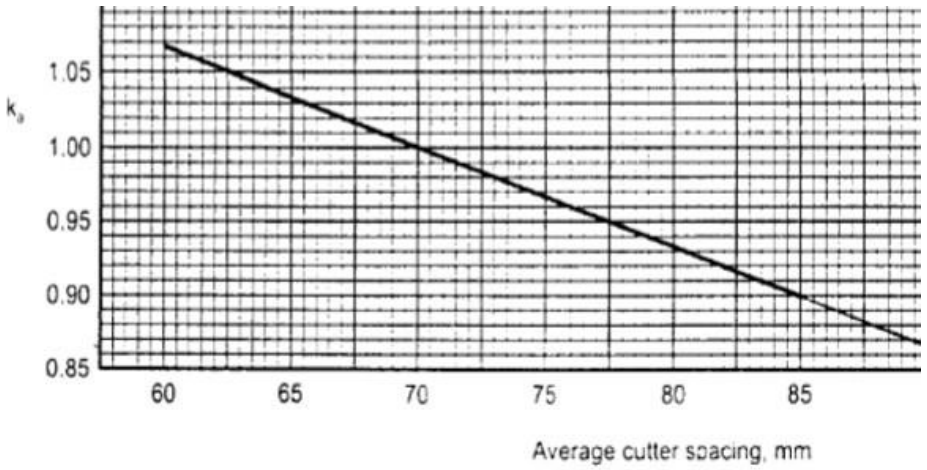

*Figure 57.*Graph for the determination of *the correction factor for average cutting spacing K_a (Bruland, 1998)*

- **Correction factor for porosity K_{por}**

It can be obtained graphically as well, the porosity value depends on the type of rock.

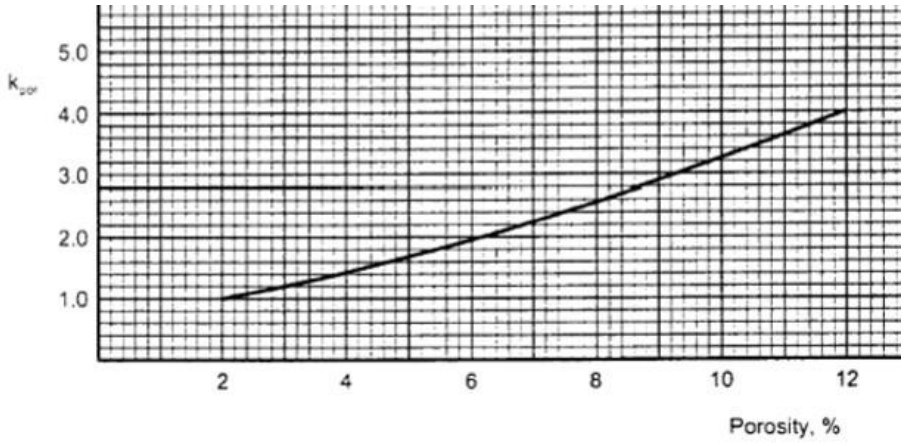

*Figure 58.*Graph for the determination of *the correction factor for porosity (Bruland, 1998)*

- **The equivalent fracturing factor, KeKv**

It can be calculated by the following formula: $KeKv=Ks.Kdr.Kpor$

- **The equivalent thrust per cutter, M_{ekv}**

It can be defined as the product of the max. Thrust per cutter, the correction factor and the cutter diameter. It's calculated by the following formula: $M_{EKV}= M_B.K_d.K_a$

- **The critical thrust (M1) and the penetration coefficient (b)**

They are a function of the KeKv and they can be obtained graphically.

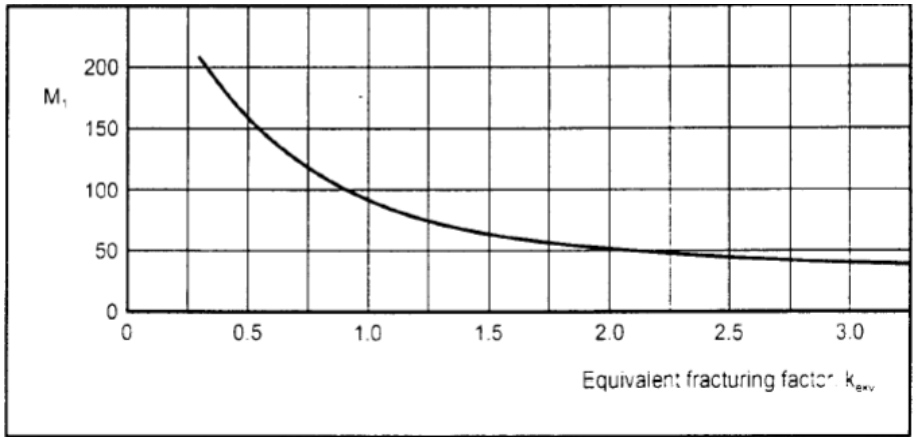

Figure 59.Graph for the determination of *the critical thrust (Bruland, 1998)*

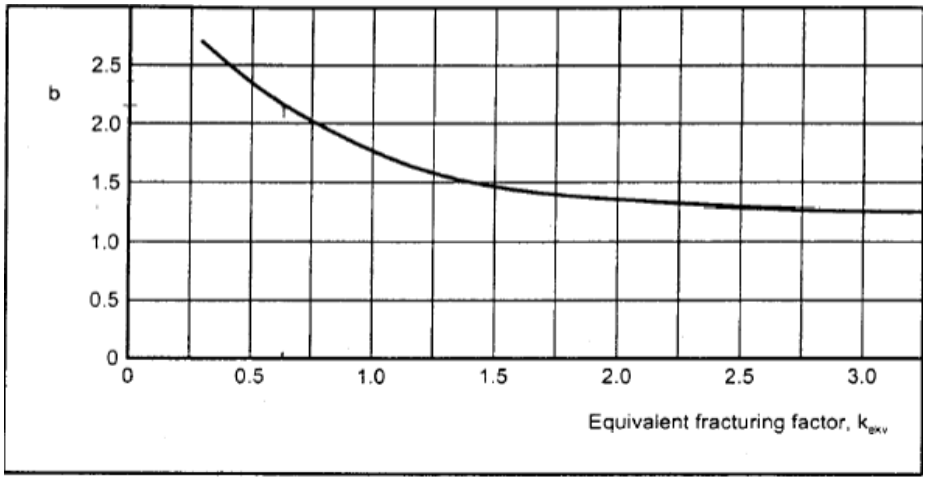

Figure 60.Graph for the determination of *the penetration coefficient (Bruland, 1998)*

- The penetration rate and net advancement

After the M_{ekv} value is obtained, the penetration rate (i_o) and the net advancement can be calculated by the following formula:

$$i_0 = \left(\frac{M_{ekv}}{M_1}\right)^B \text{ in [mm/rev]}$$

$$I\left[\frac{m}{h}\right] = io * RPM * \frac{60}{1000}$$

where

RPM, is the cutterhead rotational speed.

Finally, the NTU estimation can also be verified by means of the graph in figure 61.

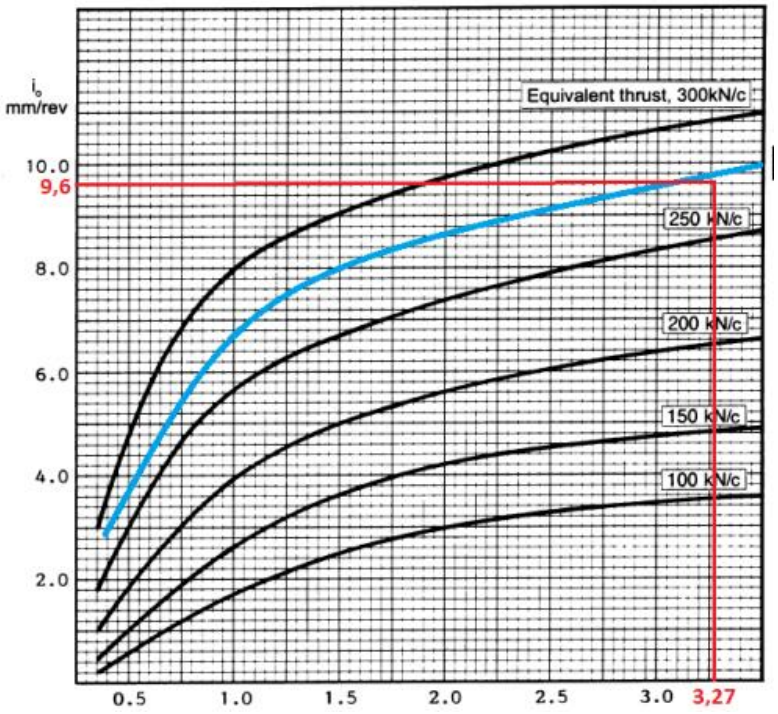

*Figure 61.*Graph for the verification of the penetration rate and net advancement values *(Bruland, 1998)*

3.3.1. Penetration rate and net advancement results

The penetration rate and the net advancement results is obtained in the following:

- Consider a schistosity value of **10 mm** that corresponds to a fracture of class III from the table 14 provided.
- The angle between discontinuities and the tunnel axis ($\propto$) considering a dip angle of 50 °is equal to **4 °**
- The Fracturing Factor, Ks with an angle of 4 ° for fracture class III is **1.2**, this value is obtained graphical.
- For a rock mass with an UCS between 50-125 Mpa the brittleness value **S20** is assumed to be **45%** and **SJ as 15 mm**. The determination of the Drilling Rate Index, DRI, and the correction factor, K_{DRI} are obtain graphical. The DRI value is **50** and the K_{DRI} is **0.95.**
- For a diameter of 432 mm, the Correction factor for cutting diameter Kd is equal to **1.1**1.
- For a cutterhead of diameter 6.3 m with 42 disk tools, spacing between tools is **75 mm**, thus the correction of the average cutting spacing Ka value is equal to **0.98**.
- Since the rock type was found be to metamorphic, therefore the porosity can be considered as **2**, the Correction factor for porosity K_{por} is equal to **1.**
- The equivalent fracturing factor, KeKv is equal to **1.14**.
- Considering the max. thrust force provided by the TBM manufacturing company and also the max. allowable range of thrust forces in hard rock excavation respectively, thrust forces of **200kN, 240 kN and 290 kN** are considered for the evaluation of the equivalent thrust per cutter. The equivalent thrusts per cutter, Mekv are equal to **217.6 kN, 261.1 kN, 315 kN,** with estimated these thrust forces for each disk cutter.
- The critical thrust and penetration coefficient M1 and b is respectively equal to **85 kN** and **1.6.**

- Finally, the penetration rates (i_o) are: **4.5 mm/rev, 6 mm/rev and 8.2 mm/rev** and the net advancement (I) are: **1.6 m/h, 2.2 m/h and 2.9 m/h** net with an average cutterhead rotational speed (RPM) of **6 rpm**.

Table 18 Summary of the NTNU penetration rate and net advancement results

Parameters	Value
Fracture class	Class 3
Angle between discontinuities and the tunnel axis ($\propto$)	4 °
Fracturing Factor	1.2
Drilling Rate Index(DRI)	50
Correction factor (K_{DRI})	0.95
Correction factor for cutting diameter (Kd)	1.11
correction of the average cutting spacing (Ka)	0.98
Correction factor for porosity K_{por}	1
Equivalent fracturing factor, KeKv	1.14
Max.thrust per cut (M_b) [kN]	200
	240
	290
Equivalent thrust per cutter (M_{ekv}) [kN]	217.6
	261.1
	315
The critical thrust (M1)	85
Penetration coefficient(b)	1.6
Penetration rate (i_o) [mm/rev]	4.5
	6
	8.2
cutterhead rotational speed (RPM)	6 rpm
Net advancement(I) [m/h]	1.6
	2.2
	2.9

Moreover, from the TBM characteristics provided by the manufacturing company and the penetration rate evaluated or recorded for each unique excavation advancement step, other TBM parameters (Normal force FN, specific energy SE, etc.) can be calculated using the following formula:

$$F_N = \frac{FT}{N_{cutter}}$$

$$FPI = \frac{F_N}{ROP}$$

$$SE = \frac{2.\pi.RPM.T}{PR} \quad \text{Or} \quad SE = \frac{4*1000*P_0}{PRev*RPM*60*\pi*d_{TBM}^2} \quad \text{(Bilgin et al., 2014)}$$

$$BI = \frac{F_N}{PRev}$$

$$CC = \frac{F_r}{F_N}$$

where:

F_N : Normal force (kN/cutter) ;FT: Total cutterhead thrust (kN);N_{cutter}: Number of disk cutters;FPI: Field penetration index (kN/cutter/ mm/rev);ROP: Rate of penetration (mm/rev);SE: Field specific energy (MJ/m3);RPM: Rotational speed (rev/min);T: cutter Head torque (MN-m);PR: Penetration rate (m3 /min);$PRev$: Penetration per cutterhead revolution (mm/rev);BI: Boreability index (kN/cutter/mm/rev)CC: Field cutting coefficient,F_r: Cutter rolling force P_0: Cutterhead power (kW);d_{TBM}: Diameter of TBM (m).

The TBM parameters values mentioned above are important for a precise evaluation in real time during the excavation process in order to efficiently connect the muck parameters to the TBM parameters and also to the rockmass properties.

Table 19.Rock mass parameters Rispoli et al. (2017)

VALUE	UCS	RMR	JOINT SPACING
Min. value	48 MPa	40	0.5
Avg. value	85 MPa	60	0.85
Max. value	125 MPa	80	1.2

Although, the UCS and RMR can impact the excavation process; however, no strong relationships were found among the RMR, UCS and the coarseness index.

To further understand the concepts discussed previously in this chapter, the following relationships were found and arranged on the basis of the literature review, and also on the basis of the preliminary data evaluated in table 13 and 18.

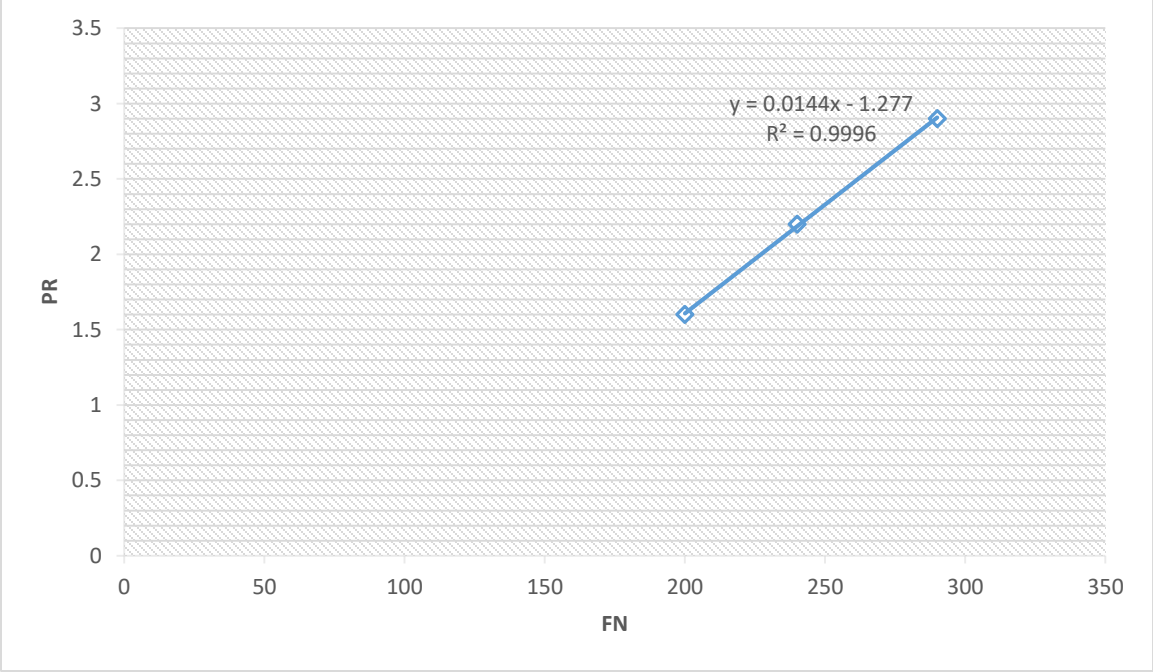

Figure 62. Relationship between the cutter head force FN and the Penetration rate PR

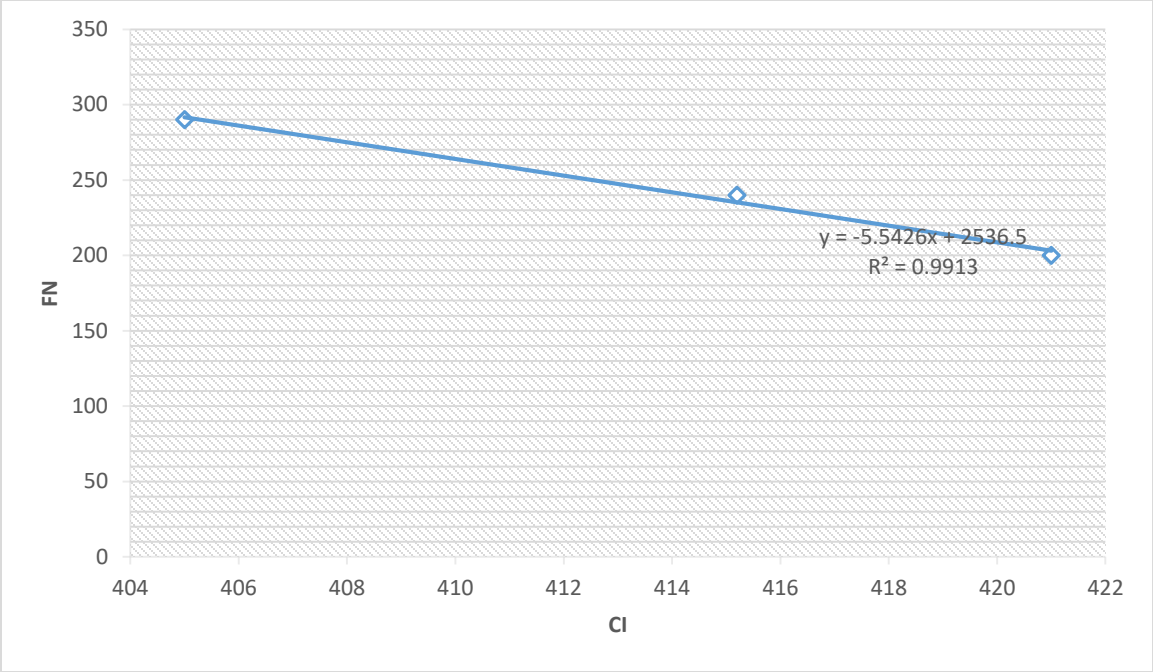

Figure 63.Relationship between CI and FN

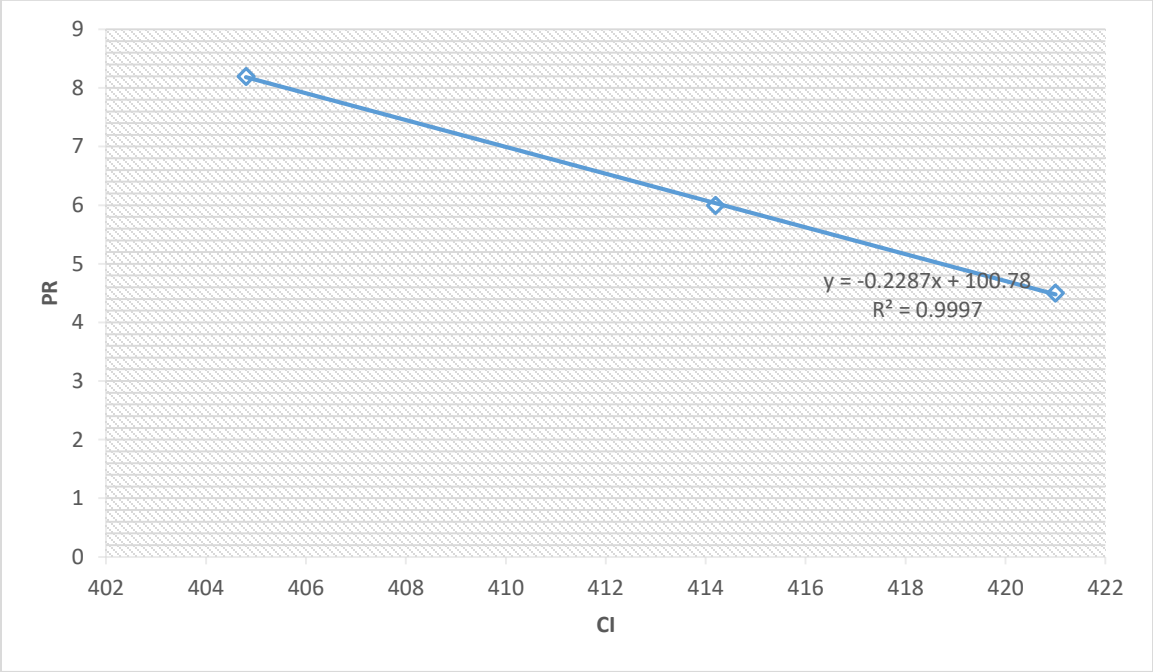

Figure 64. Figure 65.Relationship between CI and the NTNU penetration rate values.

The results in terms of mineralogy and petrographic analysis show that the rock tested is a micaschist belonging to the Clarea Complex (CLR) and also to a transition zone (AMD). As shown in table 20, the study carried out by Rispoli et al. (2018) at the Maddelena tunnel provided the parameters recorded during the excavation of the tunnel on an average basis from the Clarea Complex (CLR) and the transition zone (AMD). These parameters refer to: FN, normal cutter force; T, torque; RPM, rotational cutterhead speed; PR, penetration rate; ROP, rate of penetration; FPI, field penetration index; SE ,Field Specific Energy; spacing/penetration, S/P .

Table 20.The Maddalena tunnel TBM excavation parameters (Rispoli et al. ,2018)

Lithology formation	Parameter	F_N (kN)	T (kNm)	RPM (rev/ min)	P (kW)	PR (m/ h)	ROP (mm/ rev)	FPI (kN/cutter/ mm/rev)	SE (MJ/ m^3)	s/p (–)
AMD	Average	234.3	659.4	8.6	590.9	1.5	2.8	93.2	50.1	29.6
	St. dev	48.3	136.6	0.6	143.4	0.4	0.8	41.5	14.4	8.9
CLR	Average	178.5	572.7	7.2	446.3	1.5	3.5	57.7	34.5	24.1
	St. dev	46.6	207.4	1.4	205.8	0.4	1.1	28.2	12.6	7.9

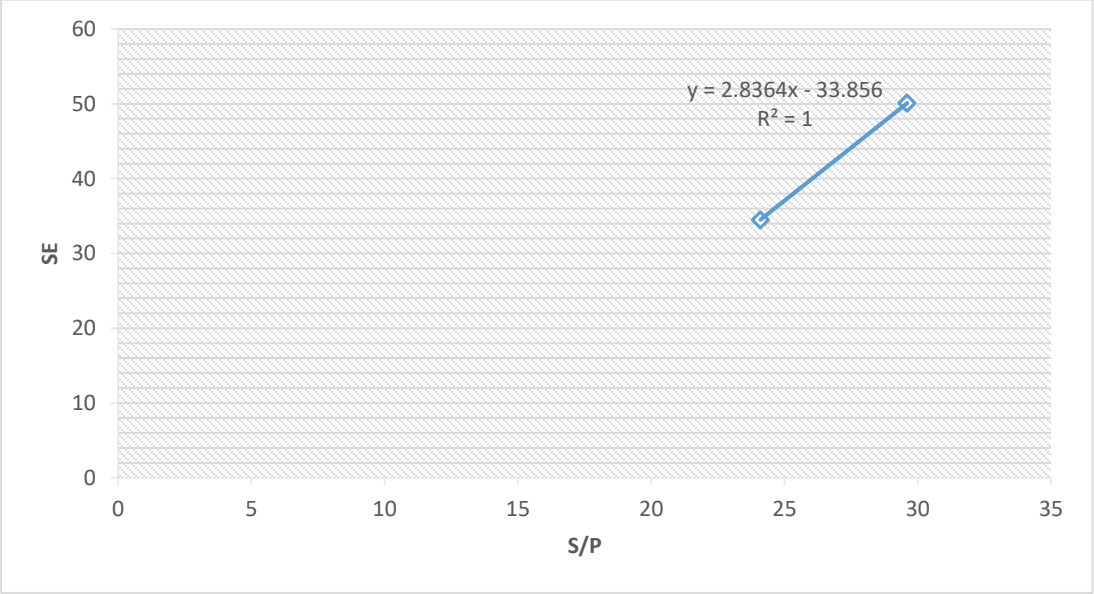

Figure 66.Relationship between specific energy SE and spacing / penetration ratio (s/p) from the Maddalena tunnel data.

As it can be seen in figure 68, the results of the tests performed on the same type of rock with similar characterizations show that there's a strong relationship between the CI and TBM parameters. In addition, the s/p values in table 20 and the CI values obtained in table 13 are very alike to the tread characteristic in figure 68.

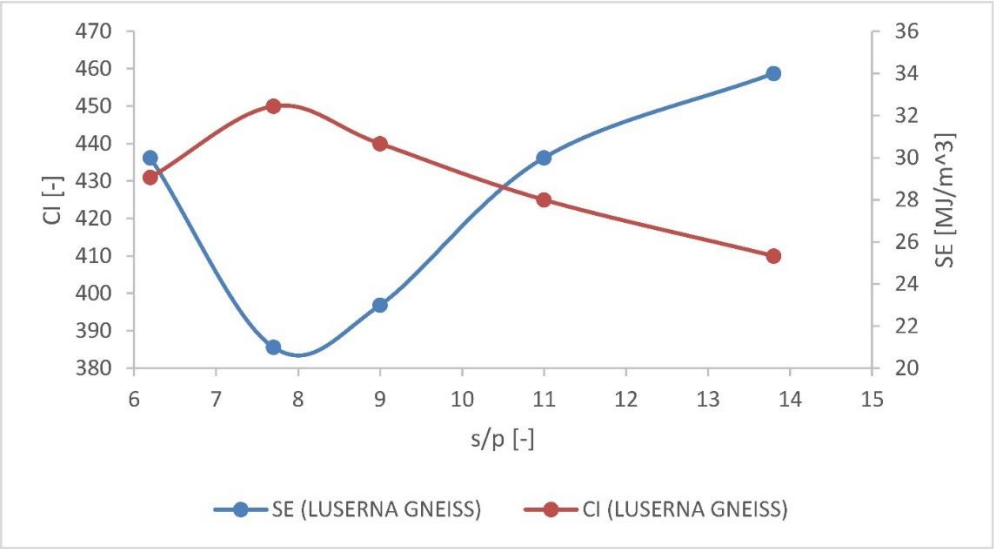

Figure 67. Relationship between specific energy SE, coarseness index CI and s/p ratio obtained from experimental tests with the ILCM on a gneiss (Cardu et al., 2021).

4. Sustainable reuse of TBM muck for construction application

4.1 Tunnel re-mucking background review

The need of remucking is becoming very important since the end of the 20th century, especially in the northern regions of Italy and the all alpine regions due to the large number of ongoing infrastructure projects ,and also due to those projects within their planning stages referring to the alp-transit for further route extension in order to establish a better and an efficient road or railways connection within the European Union; the large amount of muck generated during the excavation of such large infrastructures can also efficiently contribute to the raw materials demand (aggregates) during the construction of these infrastructures.

Re-mucking has been implemented in many various tunnel infrastructure projects throughout the past years. The muck from tunnel excavation can be reused in various construction applications, such as refilling material, railway ballast road construction, structural concrete mixing or asphalt mixing, and also as a source for raw material for industrial purpose.

By example, the reuse of tunnel muck was successful implemented for an onsite production of construction aggregates and other applications in the Swiss base tunnels of Lötschberg and Gotthard; the tunnels are of length 34.6 km and 57 km respectively. They are part of the alp transit project. The excavation process of the Gotthard base tunnel generated a total of 24 Mt of muck. The reuse/recycling goal for the onsite production of the aggregates follows an approach to minimize the environmental impact and obtain the optimum reuse of the tunnel debris. The muck of good quality was used as aggregates for structural concrete, whereas the muck of lower quality (which couldn't be used as aggregates for concrete on site) was reused as filling materials for environmental restoration and railway embankments. About 46 % of the muck recycled in this tunnel was reused as aggregates for concrete and embankments and the remaining 54 % was

used as materials for various environmental restoration and landfills (Bellopede et al., 2011).

The case study of the Gotthard base tunnel highlighted also the need for a successful reuse the muck for various applications by implementing efficient treatment plants and a good management technique to reach an optimum reuse or the end use targeted depending on the qualities of the muck generated from the excavation process.

As an initial step, the rock characterization has to be investigated and understood, then the implementation of an efficient processing facility for a successful and optimal recycling has to be done. For a sustainable re-utilization of tunneling muck, further processing can be required for enhancing this goal in various construction applications.

In every tunneling project, the final target for the reuse of muck depends on various factors (geological, ecological, environmental, economic and so on). These factors refer to the quality of the rock, installation of facilities for processing the muck around or near the construction site, free spaces around the construction site for storage (Bellopede et al., 2011). The recycling is also implemented according to guidelines and requirements specified in the waste framework directive e.g. 2008/98/EC for spoil management; by establishing a comparison between the muck characterizations and the waste recycle requirements.

The muck from hard rock TBM excavation generally shows a good quality in strength; however, the muck can be primarily targeted for a suitable application as aggregate in concrete and also road pavements construction. As highlighted by Voit et al. (2015), several past re-mucking tunnel projects and studies have shown that initially a lower portion of TBM muck with respect to the total volume of muck produced in large tunnel infrastructures is found to be suitable for a direct reuse as aggregates in structural construction in comparison with other construction applications or waste.

Another example, based on the primarily evaluation that was done for Brenner base tunnel for the recycling and sustainable reuse of muck as aggregates for concrete, based on the total of 43 m tons of muck generated from that tunnel, a prediction was made with respect to all the factors (environmental, economic, etc.) that were involved in this project and it was found that only about 6 % of the muck was suitable for reuse as aggregates in

concrete and about 15% was suitable as land filling material. The remaining volume of muck was primarily evaluated as waste for disposal, more importantly this evaluation shows also the need to further improve the recycling process for an optimum reuse of TBM debris.

This is also due to the fact that the debris from TBM excavation are generally of lamellar shape; as mentioned earlier, the excavation process affects the shape and size of the muck, therefore a larger quantity of lamellar grains in the mix will decrease the workability of the concrete, as they might allow some water to be trapped in and also they tend to form horizontal planes in the concrete mixing phase.

However, with further improvement and treatment of the muck, an optimum reuse or an enhancement can be obtained also for several other construction applications depending on its characterization. The environment goal in large tunnel infrastructures is to reach the maximum possible muck recycling.

Riviera et al. (2013) also investigated the tunnel muck for a possible reuse as aggregates in road construction, by evaluating the muck excavated using different excavation methods, and coming from different sites for a potential reuse of the muck in road construction. This study also highlighted the goal of maximizing the muck recycling for its reuse in several applications.

Generally, the muck from a good hard-rock quality requires minimal treatments (e.g. washing, drying) before its reuse as aggregates in road pavements construction or structural concrete. Hard rock of good quality is usually considered as a good source for production of construction aggregates, however an important key issue about the size and shape has to be considered for the muck from TBM, (typically flat and elongated shape). The size and shape can reduce its suitability for its application as aggregates in concrete. Moreover, all the requirements not only related to physical properties, but also to chemical and mechanical behavior have to be satisfied.

Modifications can be also implemented if required for improving the muck grain size in order to meet the requirements for its reuse; usually these modifications refer to a physical improvement. Regardless the intended reuse of the muck, the physical properties of the aggregates generally refer to their grain size, shape, mineralogy type and also to the

bulk density of the materials, whereas the mechanical properties mainly refer to the ability of the material to withstand any degradation that can compromise its strength; and as for the chemical properties of the material, they refer to reactive minerals, and are significantly important especially when the materials is mixed with blinders like in concrete or asphalt mixing i.e. sulfate compounds or alkalis-silica reaction (Gertsch et al .,2000).

For example, based on the experiments carried by Olbrecht and Studer (1998) on different type of muck from TBM excavation, the concrete mix generated from these muck samples had a high shrinkage and a low modulus of elasticity in comparison to the conventional concrete; furthermore in fiber concrete with further improvements and a proper amount of fiber steel, the muck from TBM excavation can fit well as aggregates and shows good mechanical properties and an increase in the compressive strength (Voit et.al, 2015).

The study carried out by Oggeri et al. (2015) on the TBM muck recycling highlighted the need for classifying the muck on the basis of various parameters for finding out all the possible reuse applications and, also, the study proposes a methodology during the processing of the muck on the basis of scenarios that may occur during the planning of a tunnel.

For all possible reuse applications of tunnels debris, the evaluation can be carried out according to the European standards available for each application. The following European standards are the most commonly required for the classification and investigations of aggregates for construction applications:

- UNI EN 12620: Aggregates for concrete.
- EN 13043: Aggregates for bituminous mixtures and surface dressings for roads and other trafficked areas.
- EN 13139: Aggregates for mortar
- PrEN 13055: Lightweight aggregate mortar, grout, bituminous mixtures, surface treatments and for unbound and bound applications
- EN 13242: Aggregates for unbound and hydraulic bound materials for use in civil engineering work and road construction.
- EN 13285: Unbound mixtures - Specifications.

- PrEN 13450: Aggregates for railway ballast.

These standards established all the properties and requirements to be met for a sustainable reuse of the TBM muck as construction aggregates. A set of investigations and laboratory tests have to be performed for each particular application. Those requirements and properties generally refer to the grading, shape, quality resistance to fragmentation, resistance to water, water absorption, petrographic description, chemical reaction, resistance to freezing and so on.

4.2 Aggregates requirements for concrete

4.2.1 Geometrical requirements

The geometrical requirements mainly refer to some of the investigations (grain size, grading, flakiness index, shape index) carried out in the second chapter. The geometrical requirements should be evaluated in accordance to clause 4 (UNI EN 12620 standard).

The size and grading have to be categorized; the fines and coarse aggregates have to be selected based on the requirements and specifications provided in Table 2 (UNI EN 12620); and also to limits specified in table 3 (UNI EN 12620). The size of the grains is expressed as d and D respectively, d refers to the lower size and D to the upper size. The D/d ratio for the coarse grain shouldn't be lesser than 1.4 and the finer grains are selected in accordance to the requirements provided in table 4 (UNI EN 12620). Generally, in construction the common size of coarse aggregate is 20 mm for concrete. Aggregates between 4.75 mm to 40 mm can be considered as coarse aggregate and those lesser than 4.75 mm as fines aggregates. The size and range also depend on the strength requirements to be achieved.

The flakiness and shape index refers to the shape/geometry of the grains, the flakiness and shape index have already been determined in the first chapter in accordance to the UNI EN 933-3. The shape plays an important role in the concrete mix, as known the flaky and elongated particles can have a lower compatibility and higher breakage and the shape of aggregates can affect the workability of the concrete. An index value ranging from 15 % to 25 % can be considered as a good value for aggregates in the concrete mixing design.

Moreover, the maximum values of the shape index can be categorized as specified in table 8 and 9 (UNI EN 12620).

Furthermore, for the requirements referring to the fines quality, fines content, and shell content of coarse and all-in aggregates; they should be as specified in the causes 4.5 to 4.7 (UNI EN 12620). All the coarse aggregates refer to a mixture of coarse and fines aggregates and they shall comply to the general grading requirements as given in the table 2. The fines content can be determined in accordance with UNI EN 933-1 standard. As known, a high content of fines can compromise the water requirements and workability in the concrete mix design as well.

4.2.1 Mechanical requirements

The mechanical requirements for aggregates depend on the end use targeted. The evaluation of the toughness and strength of aggregates are not very significant in concrete design mix due to the fact that the cement matrix will provide most of the strength and stability required, the primary concerns are on the shape, size, petrographic and chemical composition (Gertsch et al., 2000).

The mechanical properties of the muck should be investigated as specified in clause 5 (UNI EN 12620). For the evaluation of the mechanical properties of aggr*e*gates; if required the following tests have to be performed:

- **Resistance to fragmentation**: is determined using the Los Angeles testing method, and the test results are represented in terms of Los Angeles coefficient, thi coefficient can be expressed as specified in table 12 and 13 (UNI EN 12620) for Categorizing the maximum values of Los Angeles coefficient
- **Resistance to wear**: Micro-Deval (MD) test is the most common test used for evaluating the resistance to wear of aggregates. Micro-Deval coefficient – *M*DE should be expressed as stated in table 14 (UNI EN 12620)
- **Particle density**; can be determined in accordance with the clause of EN 1097-6
- **water absorption**; can be determined in accordance with the clause of EN 1097-6
- **Bulk density**; can be determined in accordance with EN 1097-3 standard

- **Resistance to polishing** for application in surface courses; can be determined in accordance with EN 1097-6 standard
- **Resistance to surface abrasion**: can be determined in accordance with EN 1097-8 standard
- **Resistance to abrasion from studded types for application in surface courses**; can be determined in accordance with EN 1097-8 standard

4.2.1.1 Durability

It's very critical to make a good assessment of the properties of the aggregates since some destructive reactions may occur during the life time of the concrete. And such reactions may lead to deterioration of the concrete. The durability of concrete is assessed based on Freeze-thaw resistance of coarse aggregates, Magnesium sulfate soundness of coarse aggregates, volume drying stability-shrinkage, and alkali -silica reactivity.

Freeze-thaw resistance: the investigation to frost resistance of aggregates in a freezing and thawing environment is evaluated with reference to the EN 1367-1 or EN 1367-2 standards. The results should be represented and conformed as stated in table 18 and 19 (UNI EN 12620). The water absorption evaluation can be used as a screening test for this requirement. The water absorption is determined in accordance with the EN 1097-6, the results obtained should be conformed, as stated in table 28 (EN 1097- 6 water absorption at 24 h), which provides maximum categories for values of water absorption.

Magnesium sulfate soundness of coarse aggregates: when required it can be determined in accordance with the magnesium sulfate soundness test in EN 1367-2.
This evaluation refers to resistance of courses aggregates to weathering with reference to the categories as specified in the standard.

Volume drying stability-shrinkage: It can be evaluated using EN 1367-4 standard and the value shouldn't exceed 0,075 %. As known, the drying shrinkage in the aggregates for concrete use can contributed to disruptive shrinkage cracking of the structural concrete.

Alkali -silica reactivity: also refers as "concrete cancer "this phenomenon happens when certain types of aggregates can react with alkaline hydroxides in the pore solution of concrete, this leads to a formation of deleterious swelling reaction that will damage the concrete. For natural aggregates, as stated in Annex c (BS EN 12620), the most common form of reaction that can occur in the concrete is the alkalis-silica reaction. Another form, which is less common form of reaction refers to the alkali-carbonate reaction. It's necessary to evaluate the mineralogy and reactivity of the recycled concrete aggregates and make sure that their end use in the structural concrete doesn't contain any reactive that will damage the concrete. Reactive minerals generally contain fined grained/ deformed silicate minerals (quartz, feldspar, mica) in metamorphic (schist, gneiss). Also precautions can be taken in the binder composition to minimize the total alkali-content in the concrete mx. Some important precaution can be taken, especially when lacking the long term disruptive reactivity of the materials, the following precautions can be considered: The alkali content (lithium, sodium, potassium, rubidium and cesium) in the concrete mixing has to be limited, the use of cement with a lower alkali content, the use of non-reactive aggregates, and also the degree of saturation between the concrete and water can be limited.

4.2.1 Chemical requirements

The chemical requirements shall be determined in accordance to the clause 6 (UNI EN 12620 standard); and they mainly refer to the Chlorides, Sulfur containing compounds, Constituents affecting the setting and hardening of concrete, and also others requirements such as: the Free mica and Carbonate content for concrete pavement surface courses of fine and all-in aggregates. The petrographic analysis is considered as a first step for this investigation, the mineralogical data are required for the evaluation of the chemical requirements.

4.2.1.1 Chlorides

The chlorides amount in aggregates is very important, especially in reinforced concrete. The chlorides present in the aggregates muck won't directly damage the concrete, but

contribute to the corrosion of the steel reinforcement. The chlorides can be present in form of sodium and potassium salts; such salts impact also to the alkali reaction in the concrete. Moreover, for recycled aggregates, the chlorides may also be combined in the form of calcium aluminate. Generally, for recycled aggregates, the chlorides content is likely to be low, it can be determined with reference to the EN 1744-5 and EN 1744-1:2009. As stated in the standard annex F (UNI EN 12620), the chlorides content shouldn't be greater than 0.01% for concrete aggregates.

4.2.1.2 Sulfur containing compounds

The sulfates in aggregates can bring up a significant disruptive effect, which could lead to a damage in concrete. The sulfur compounds shall be investigated following the approach in the clause 6 (EN 12620 standard). For recycled aggregates, the water –soluble sulfates are determined in accordance with en. 1744-1. the results should be categorized as specified in table 21 (UNI EN 12620 standard) for the maximum value of acid and sulfate soluble content reactive sulfates such as gypsum plaster in aggregates can lead also to expansive disruption of the concrete.

The total sulfur content of aggregates can be determined in accordance with EN 1744-, the results should be categorized as specified in table 24 (BS EN 12620 standard) for the maximum values of total sulfur content. Furthermore, in case of unstable minerals in of form iron sulfide, like pyrrhotite, the permissible total content of sulfur is 0.1% as s. the total content in accordance to the clause 11 (BS EN 12620 standard) shall not exceed – 2% s by mass for air-cooled blast furnace slag; and - 1% s by mass for aggregates other than air-cooled blast furnace slag.

4.2.1.3 Constituents affecting the setting and hardening of concrete

Organic matters affecting the setting and hardening of concrete can be determined in accordance with EN 1744-1, generally these organics matters refer to humus and sugar-type materials and also some type of clay minerals. The presence of such minerals can affect the durability of concrete and also the development of the required strength in the concrete. When required the sugar type minerals can be tested on the basis of the stiffening time and compressive strength requirements as specified EN 1744-1.

The present of these minerals types or organic amounts shouldn't:

-Increase the stiffing time of the concrete mortar by more than 120 min;

-Decrease the compressive strength of concrete by more than 20 % after 28 days of curing.

4.2.1.4 Others requirements:

Carbonate content for concrete pavement surface courses of fine, and all-in aggregates:

The carbonate content can be evaluated in accordance with EN 196-2. The test for controlling the carbonate content can be prepared as specified EN 1744-1.

Classification of the constituents of coarse recycled aggregates:

The standards EN 933-11 and EN 12620:2013 can be for the evaluation to determine the fractions of constituent materials in coarse and all-in recycled aggregates and the results should be represented as specified in table 22 (BS EN 12620 standard).

Free mica:

A significant amount of free mica can lead to an increase in the water requirement and also reduce the compressive strength in the concrete. The content of free mica is influenced by the quantity, type of gain and the grain size and it can be evaluated using the XRD analysis.

The table 15 shows the requirements and characteristics for aggregates intended for use in concrete base on the mandate given under the EU Construction Products Directive (89/106/EEC)

Table 21"Requirements for concrete aggregates for use in buildings, roads and other civil engineering Works: BS EN 12620:2013 standard"

Essential Characteristics of the aggregates for concrete	Requirements properties, clauses/standards
Particle shape, size and density	Aggregate size, Grading, Particle shape of coarse and all-in aggregate, Particle density
Cleanliness	Fines content, Fines quality, Shell content of coarse and all-in aggregate
Resistance to fragmentation	Resistance to fragmentation
Composition/content	Petrographic description, Classification of the constituents of coarse recycled aggregates, Chlorides, Acid soluble sulfates, Total sulfur, Water soluble sulfate content of recycled aggregates, Constituents which affect the rate of setting and hardening of concrete, Carbonate content of fine and all-in aggregates for concrete pavement surface courses, Influence on initial setting time of cement (recycled aggregates), Influence on initial setting time of cement (recycled aggregates)
Volume stability	Volume stability, drying shrinkage, Constituents which affect the volume stability of air-cooled blast furnace slag
Water absorption	Water absorption
Dangerous substances e.g. heavy metals, hydrocarbon, etc.	EN 16236:2013, 5.3.4 Knowledge of the raw material EN 16236:2013, 5.3.5 Management of the production
Durability -Freeze-thaw resistance	Resistance to freezing and thawing, Resistance to freezing and thawing in the presence of salt (extreme conditions)
-Durability against studded tires	Resistance to abrasion from studded tires to be used for surface course
-Durability against alkali-silica reactivity	Alkali-silica reactivity

4.3 Reuse of the muck as aggregates in structural concrete

4.3.1 Background reuse of TBM muck

An efficient washing, removal of finer particles and good storage of the aggregates can considerably reduce the negative effect of various chemical reactions that may occur in the concrete (e.g. sulphate reaction, mica); these reactions can lead to the deterioration of the concrete.

According to Hugo et al. (2019), one of the most challenging problem encountered for the optimal reuse of the muck from Villarodin-Bourget/Modane access tunnel was related to a high concentration of sulphate content in a very large portion of the muck produced in that tunnel. The materials excavated over a length of about 10 km had a significant amount of sulphate over the limitations provided in the dedicated standard. The muck from this tunnel had a sulphate content of more than 0.2 %. According to the standard, the aggregates shouldn't have a sulphate content of more than 0.2 %. The sulphate was in form of gypsum (40%) and anhydrite (60%).However, despite several other good properties of the muck from Villarodin-Bourget/Modane access tunnel; this higher sulphate content could have limited the reuse of about 1.7 million tons of muck, which represented almost 24 % of the materials that were required in the production of concrete.

For maximizing the reuse, several innovative solutions were adopted to minimize the effect of sulphate in concrete in order to obtain the required concrete strength and durability. These solutions consist of the use of special cements, additives and replacement/removal of finer particle grains. The lab experiments carried out in that study shows that the sulphate content was most accessible in grain smaller than 1 mm and for grains larger than 1 mm, the higher concentration of sulphate were found at the periphery.

Two solutions were considered for the reduction of sulphate contents in the muck:

(1) Extend the washing time of the muck using a temperature of 20°C to enable the reduction of sulphate content from 3.5 % to 2.5 %; (2) The removal of finer sand particles; this was done due to the fact that the grains of size 315 µm had a sulphate content 6 times greater than other grain size classes; thus as result, the sulphate content was lower down to 1.9 %.

To further reduce the sulphate content, an additional solution was implemented, which consists of the use of special cement (Super Sulphate Cement and Portland cement with a very low C_3A content settled for aggregates having a high sulphate content).

Finally, several concrete mix were suggested with the processed muck using special cement types, as well as additives for introducing fine air into the fresh concrete, as well as improving the consistency and setting of cement. A good strength e.g. C30/37 was developed from these mixing; the concrete produced was subjected to several experiments and investigations for the evaluation of its performance.

For 1 m3 of concrete, the mixing components were arranged as follows:" - **Cemen**t: 400 kg (reference 300kg of CEM I + 100 kg of fly ash); - **Sand** 0/4 mm: 770 kg - **Grit** 4/8 mm: 280 kg - **Gravel** 8/16 mm: 700 kg - **Crushed gypsum**: depending on the SO3 content of the aggregates" (Hugo et al. 2019)

4.3.2 Main aspects for determining the concrete composition using TBM muck and its performance

Generally, TBM muck can be considered as a good replacement of coarse aggregates in the concrete mix: commonly, coarse aggregates of size 10- 20 mm are the most required in construction. Although, there's a considerable amount of flat and elongated particles, as well as boulder particles in the sample tested; the pre-processing (i.e. washing, crushing, screening, liming) of the TBM muck coming from good competent rock is usually minimal. When the geometrical characterization are met, the muck could only require washing/cleaning for the removal of finest particles or some impurities for its

direct use as coarse aggregates in structural concrete. However, further treatments on the muck could modify the cost/benefit ratio from both an economical and environmental points of view due to the fact that a processing plant and a large amount of water may be required and also the mud generated has to be handled. This management approach has to be defined clearly from the earliest stages of the work until the end in order to put in place a successful circular economy principle.

Depending on the quality of the muck tested, several alternatives could be considered for the reuse of the muck as aggregates in the concrete mixing. As discussed previously, for obtaining a good quality of concrete using TBM muck, it is necessary to follow the requirements (physical, mechanical and chemical) defined by the conventional dedicated standards (EN 12620 standard); However, on the basis of the muck quality and the targeted concrete strength class (e.g. C20/25) to be obtained; the TBM muck can be fully or partially used in structural concrete as aggregates. The attention shouldn't only be given to the aggregates quality, but also to other components in the concrete mix, such as the type of cement, additives (e.g. fly ash), water and cement ratio (w/c); these components type and amount in the concrete mix can also be modified in request to obtain the same workability as conventional concrete, as well as the strength required at maturation (e.g. after curing 28 days) of the hardened concrete.

"The workability of concrete is the property of the mortar that determines the ease with which it can be mixed, placed, consolidated, and finished to a homogenous condition" (American concrete institute). Low workability in the mortar can lead to high porosity since the concrete with low workability can't easily fully compact; the workability of fresh concrete is commonly determined by the slump test.

It is also necessary to highlight that the TBM muck from long tunnel can be subjected to variations in quality during the tunnel excavation depending on the geological conditions. When the muck is used as aggregates for concrete, some of these variations can be very significant due to the fact that they can considerably affect the constructional performance (consistency, durability, strength, etc.) of the concrete. The main components of the structural concrete consist of water, cement, and aggregate; the muck can be used to substitute fine or coarse aggregate in the concrete mix; therefore the

mechanical and chemical properties of concrete can change. Several concrete mix can be proposed, thus in return several type of concretes with different properties can be obtained on the basis of the properties of the muck tested. The use of additives, fiber reinforcements and special cement type can also be considered for improving the quality of concrete or shortcrete.

When required, the hardened concrete can be tested in accordance with the EN-12390 Part 1-18 (Testing hardened concrete) for the evaluation of its performance. These tests refer to the determination of the following:

- Flexural strength
- Compressive strength
- Density of the hardened concrete
- The carbonation resistance
- The chloride resistance and migration
- Secant modulus of elasticity in compression
- Tensile strength
- Shrinkage, creep of concrete in compression,
- Depth of penetration of water under pressure
- Consistency of the concrete mortar
- Heat released during the concrete hardening process
- Strength assessment during curing of concrete

Additionally, the design of structural concrete can be made following the recommendations and specifications stated in following standards:

- BS 8110-1:1997 standard (Structural use of concrete — Part 1: Code of practice for design and construction),
- EN 206. 2021 *Concrete - Specification, performance, production and conformity*.
- EN 1992-1-1. 2004 *Eurocode 2: Design of concrete structures–Part 1–1: General rules and rules for*

  Buildings.

5. Conclusion and recommendations

A successful implementation of the reuse of muck requires sufficient knowledge of the characteristics of the raw muck for their targeted reuse; the implementation of an efficient processing plant also plays a key role with regard to the reusing implementation success.

On the basis of the laboratory test results obtained from the grain size and shape analysis, it was found that some of the materials tested require an improvement in shape and size in order to maximize their reuse as coarse aggregates in structural concrete. The samples had a significant portion of boulder particles with respect to their total weight. The indices (flakiness index, shape index, elongation ratio) used to characterize the shape were also higher in some classes in comparison to the permissible percentage range. These results obtained regarding the geometrical characteristics of the muck tested are compressible and much related to the excavation method adopted and also to the rock mass conditions.

The excavation technique certainly affects the size and shape of tunnel muck; it was found that, on one hand there is a strong relationship between the TBM parameters and geometrically properties of the muck, on the other hand no strong relationships were found between the muck parameters and the rock mass properties. Additionally, these results show the need to better understand and further study the choice of the excavation technique or machine type and all the aspects related to the production of the muck from TBM excavation as a first approach to minimize this effect on the size and shape (elongated and flat) of the muck. Alternatively, another approach could be to provide physical modifications on shape and size; and treatment for a reduction of the boulder particles and also of a portion of the flat and elongated particles in the samples tested.

Such physical modifications occur by breaking the targeted particle grains in such a way to obtain a proper size and shape (polyhedral) in order to reduce the overall percentage of the flat and elongated particles with respect to the total volume of the coarse muck. These modifications could lead to a more appropriate grain size distribution for the intended use of coarse aggregates. Another solution to reduce this effect includes the use of special binding agents and/or some type of additives in the concrete mixing. All the

requirements suggested above for the improvement of the materials have also to fit with the budget and the environmental requirements.

It was also found that the fine contents represent more or less 20% of the total weight of the muck tested; consequently, further investigations need to be carried out to evaluate whether or not the fine contents can be used as fine aggregates for concrete application e.g. backfilling. Nevertheless, the use of special cement type, additive could be considered for optimizing the reuse of these fine particles.

Referring to The XRD analysis performed on the muck, no sulfur compounds or sulfur bearing mineral were detected above the maximum range in all the three tested samples. The mineralogical qualitative assessment doesn't show the presence of chlorides salts in the form of potassium or sodium in all the samples. Moreover, the XDR analysis carried out for the mineralogical quantitative assessment shows that the materials tested contain a high amount of silicates minerals, mainly quartz, muscovite and others minerals. Therefore, further investigations and precautions have to be considered while preparing the concrete mix with the tested aggregates in order to minimize/control the alkali-silica reaction. Furthermore, when required, the use of special cement type and additives (fly ash) can also be suggested for reducing the reactions that may lead to the deterioration of concrete, as well as improving the quality and strength of the concrete.

Past reuse of the muck coming from the TELT section of Villarodin-Bourget/Modane access tunnel showed that the optimal reuse of the muck was initially limited because of a high concentration of sulphates in a large portion of the muck. However, several other chemical tests/investigations need to be carried out in the future on the muck examined in this work in order to have a robust characterization about chemical properties of the muck in accordance with the dedicated standards, to verify if the muck meet all the necessary requirements for a possible reuse in concrete applications.

The 2D photogrammetric methodology used for investigating the muck size and shape was efficient to some extent; the results and characteristics of the muck obtained were very alike in comparison to those obtained using the traditional/conventional methods from the standards. Since the rock mass condition and mineralogy of the muck coming from long tunnel infrastructure may continuously change; as a suggestion for further

studies and future directions on this topic in request to increase accuracy and facilitate or speed up the investigation of a large volume of muck, both a continuous geometrical and petrographic analysis can be implemented for continuously assessing the properties of the muck. Although, it may have a significant increase in the cost; it could bring up various benefits. However, with further innovation and improvement e.g. 3d,sensors and laser technology on the techniques used in this work for investigating the geometrical (e.g. 2D photographic analysis) and petrographic properties of the muck could also be done onsite e.g. it can be installed or mounted above the exit of the conveyor belt of the machine for a direct collection of the data related to the properties of the excavated materials , as well as for classifying the muck for several constructional use. A similar approach was adopted in the TELT tunnel of Saint Martin La Porte; several challenges still need to be faced; such as, the data collection need to be performed at the same speed with the conveyor belt speed.

The mechanical requirements based on the investigations carried out showed that the muck exhibits some good mechanical properties. In any case, to have an overall picture about the mechanical properties; all the tests referring to the strength and durability of the muck in accordance with the dedicated standards have to be performed to evaluate whether the muck meets all the mechanical requirements for a possible reuse as concrete aggregate.

With regard to all the results obtained, the investigations carried out, as well as the suggestions mentioned above, it emerges that this study certainly deserves further investigation in the future, being the subject of great relevance and interest for a sustainable development of rock excavations.

References

Abu Bakar, M.Z., Gertsch, L., Rostami, J., 2014. Evaluation of fragments from disc cutting of dry and saturated sandstone. *Rock Mechanics and Rock Engineering*, 47(5): 1891-1903.

Alecci, C. 2018. Analisi fotogrammetrica dei terreni: applicazione, limiti e differenze con la granulometria classica. Università degli studi di Padova: pp. 66-94.

Balci, C., 2009. Correlation of rock cutting tests with field performance of a TBM in a highly fractured rock formation: a case study in Kozyatagi-Kadikoy Metro Tunnel, Turkey. *Tunn Undergr Space Technol*, 24: 423-435.

Bellopede, R., Brusco, F., Oreste,P., Pepino,M.,2011. Main Aspects of Tunnel Muck Recycling. American Journal of Environmental Sciences 7 (4): 338-347, Torino, Italy.

Bilgin, N., Copur, H., Balci, C., 2014. *Mechanical excavation in mining and civil industries*. CRC Press, Taylor and Francis Group, Boca Raton.

Bieniawski, Z., T., 1973. Geomechanics classification of jointed rock masses. J S Afr Inst Civ Eng Dec: 382–398.

Bruland, A., 1998. Hard Rock Tunnel Boring. PhD Thesis. Norwegian University of Science and Technology (NTNU), Trondheim, Norway.

Biichi, E. and Thalmann, C. 1994. Reuse of TBM muck versus cutter spacing. TBM Symposium LUCIA 1994, Stockholm,December 13 1994,lO p.

BS 812-105.2, 1990. Methods for determination the particle shape — Section 105.2 referring to the Elongation index of coarse aggregate).

Cardu, M., Rispoli, A., Iabichino, G., Oreste, P., Vagnon, F.,2021 Theoretical and Experimental Results from Laboratory Tests by ILCM . *Rock Mechanics and Rock Engineering* 39:3573–3597.

Cho, J.W., Jeon, S., Yu, S.H., Chang, S.H., 2010. Optimum spacing of TBM disc cutters: a numerical simulation using the three-dimensional dynamic fracturing method. *Tunnelling and Underground Space Technology*, 25 (3): 230-244.

D'Aloia Schwartzentruber, L., Robert, F., 2019. Management and use of materials excavated during underground works. Tunnels and Underground Cities: Engineering and Innovation meet Archaeology, Architecture and Art. In *Proceedings of the WTC 2019 ITA-AITES World Tunnel Congress*, Naples, Italy, 3–9 May, pp. 284-293.

Detert, M. & Weitbrecht, V. 2012. Automatic object detection to analyze the geometry of gravel grains–a free stand-alone tool. River flow, Taylor & Francis Group London: 595-600.

Detert, M. & Weitbrecht, V. 2013. User guide to gravelometric image analysis by BASEGRAIN. Advances in science and research: 1789-1795.

EN 1992-1-1, 2004 *Eurocode 2. Design of concrete structures–Part 1–1: General rules and rules for Buildings*.

EN 206, 2021 *Concrete - Specification, performance, production and conformity*.

EN 932-2 Standard. Tests for general properties of aggregates. Methods for reducing laboratory samples.

Gertsch, L., Fjeld, A., Nilsen, B., Gertsch, R., 2000. Use of TBM muck as construction material. *Tunnelling and Underground Space Technology*, 15(4): 379-402.

Google Company: www. googlemaps.com

Herrenknecht Company: www.herrenknecht.com

Hevdari S., Hamidi J.K., Moniezi M., Eftekhari A., 2019. An investigation of the relationship between muck geometry, TBM performance, and operational parameters: A case study in Golab II water transfer tunnel. *Tunnelling and Underground Space Technology*, 88: 73-86.

Hoek, E., 1994.Strength of rock and rock masses. ISRM News J 2: 4–16

Hoek, E., Carter.,G., Diederichs ,M.,S.,2013.Quantification of the Geological Strength Index Chart Rock Mechanics/Geomechanics Symposium,June San Francisco, California, ARMA-2013-672.

Hugot, E., Burdin, J., Brino, L., Schriqui, P., Parisi, M.E., 2019. Use and management of sulphated excavation material from the Montcenis Base Tunnel. Tunnels and Underground Cities: Engineering and Innovation meet Archaeology, Architecture and Art. In *Proceedings of the WTC 2019 ITA-AITES World Tunnel Congress*, Naples, Italy, 3–9 May, pp. 386-395.

Lin, Q., Cao, P., Cao, R., 2018.Experimental investigation of jointed rock breaking under a disc cutter with different confining stresses. Comptes Rendus Mécanique Volume 346, Issue 9, September Pages 833-843

Maidl, B., Schmid L., Ritz, W., M. Herrenknecht, 2008. Hardrock Tunnel Boring Machines, Ersnt & Sohn, Wiley Company, Berlin.

Ozdemir, L., 1992. Mechanical excavation techniques in underground construction. Short course notebook, vol 1. Istanbul Technical University, Istanbul, pp 1-49.

Olbrecht,H., Studer,W.,1998. Use of TBM chips as concrete aggregate. Materials and Structures/Materiaux et Constructions, Vol. 31, April, pp 184-187, CH-8600 Diibendotf, Switzerland.

Parisi ME, Farinetti A, Gilli P, Brino L (2015) First results from the excavation of the Lyon—Turin Maddalena exploratory tunnel.In: ITA WTC congress and 41st general assembly; proceedings of international symposium, May 22–28, Dubrovnik, ,Croatia pp 0–11 .

Peccerillo A., Perugini D., 2003. Introduzione alla Petrografia ottica. *Morlacchi Ed., Perugia*, 200 p.

Rispoli, A., 2018. Hard Rock TBM excavation: performance analysis and prediction. PhD Thesis, University of Turin, Department of Earth Sciences, Chapters 8 -9.

Rispoli, A., Ferrero, A. M., Cardu, M., 2020. From Exploratory Tunnel to Base Tunnel: Hard Rock TBM Performance Prediction by Means of a Stochastic Approach. Rock Mechanics and Rock Engineering 53:5473–5487.

Rispoli, A., Ferrero, A.M., Cardu, M., Farinetti, A., 2017. Determining the Particle Size of Debris from a Tunnel Boring Machine Through Photographic Analysis and Comparison Between Excavation Performance and Rock Mass Properties. *Rock Mechanics and Rock Engineering*, 50 (10): 2805-2816.

Riviera, P.P., Bellopede,R., Marini,P., Bassani,M.,2013. Performance-based re-use of tunnel muck as granular material forsubgrade and sub-base formation in road construction. Tunnelling and Underground Space Technology 40 (2014) 160–173.

Robbins Company: www.robbinscompany

Rosin, P., Rammler, E.,1993.The laws governing the fineness of powdered coal. J. Inst. Fuel, 7 pp. 29-36.

Rostami. J.. 1997. Development of a force estimation model for rock fragmentation with disc cutters through theoretical modeling and physical measurement of the crushed zone pressure. PhD Thesis, Colorado School of Mines, Golden, Colorado, USA.

Rostami. J.. Ozdemir. L.. 1993. A new model for performance prediction of hard rock TBMs. In: *Rapid Excavation and Tunneling Conference*, June 13–17, Boston, pp. 793-809.

Somodi, G., Krupa, Á, Kovács, L., Vásárhelyi, B., 2021 Comparison of different calculation methods of Geological Strength Index (GSI) is a specific underground site. Eng. Geol. 2018, 243, 50–58.

The Euralpin Lyon Turin (TELT) Company: www.telt-sas.com

Tuncdemir. H.. Bilgin. N.. Copur. H.. Balci. C.. 2008. Control of rock cutting efficiency by muck size. Int J Rock Mech Min Sci, 45: 278-288.

UNI EN 933-1, 2012 Part 1. Tests for geometrical properties of aggregates. Determination of particle size distribution. Sieving method.

UNI EN 933-3, 2012 Part 3. Tests for geometrical properties of aggregates. Determination of particle shape. Flakiness index.

UNI EN 933-4, 2008 Part 4. Tests for geometrical properties of aggregates Determination of particle shape. Shape index.

UNI EN 12620.2013. Aggregates for concrete.

Vásárhelyi, B.; Somodi, G.; Krupa, Á.; Kovács, L. Determining the Geological Strength Index, GSI using different methods. In Proceedings of the 2016 ISRM International Symposium (EUROCK2016), Ürgüp, Turkey, 29–31 August 2016; pp. 1049–1054.

Villeneuve, M.C., 2017. Hard rock tunnel boring machine penetration test as an indicatorof chipping process efficiency. J. Rock Mech. Geotech. Eng. 9 (4), 611–622.Wentworth, C.K., 1922. A scale of grade and class terms for clastic sediments. J. Geol. 30(5), 377–392.

Voit. K.. Zimmermann. T.. 2015. Characteristics of selected concrete with tunnel excavation material. *Constr. Build. Mater.*, 101: 217–226.

Xia Y.. Shi Y.. Lin L.. Zhang Y.. Tan Q.. Yang Y.. 2018. Experimental Evaluation of Fragments from TBM Disc Cutting under Different Load Cases. *Periodica Polytechnica Civil Engineering*, paper 11961, Creative Commons Attribution.

Zhao, L., Zhang, S., Huang, D., Wang, X., & Zhang, Y. 2020. 3D shape quantification and random packing simulation of rock aggregates using photogrammetry-based reconstruction and discrete element method. Construction and Building Materials, 262, 119986.

Zou, D., 2017. Theory and Technology of Rock Excavation for Civil Engineering. Springer, Singapore.